Roles of Protocadherins in Mammalian Cells

by

Mohammad Haroon Qureshi

A dissertation submitted to
Graduate School of Sciences and Engineering
in Partial fulfilment of the requirements of
the Degree of

Doctor of Philosophy in

Biomedical Sciences and Engineering

KOÇ
UNIVERSITY

October 2018

Roles of Protocadherins in Mammalian Cells

Koç University
Graduate School of Sciences and Engineering

This is to certify that I have examined this copy of a doctoral dissertation by

Mohammad Haroon Qureshi

and have found that it is complete and satisfactory in all respects,
and that any and all revisions required by the final
examining committee have been made.

Committee Members:

Assoc. Prof. Nurhan Özlü (Advisor, Koç University)

Assoc. Prof. Tuğba Bağcı Önder (Koç Unıversity)

Asst. Prof. Elif Nur Fırat Karalar (Koç Unıversity)

Asst. Prof. Halil Bayraktar (Istanbul Technical University)

Assoc. Prof. Umut Şahin (Boğaziçi Unıversity)

Date:

ABSTRACT

Cancer is one of the leading causes of morbidity and mortality around the globe. It is a complex disease characterized by hyperproliferation, genetic instability causing cumulative mutations, and at advanced stages spread to secondary sites, through a process known as metastasis. Metastasis is directly dependent on cancer cells' ability to migrate and, for an intervention in metastasis, it is pertinent to understand the molecular details of cell migration. In the current thesis, we attempted to understand the roles of a cell surface protein protocadherin-7 (PCDH7) in cell migration.

Previous work from our group has shown PCDH7 as a cell-cycle regulated membrane protein. In current thesis, we characterized the effects of perturbation of PCDH7 expression on cell migration of mammalian cells in culture, and its role in the cortical migration of neuronal progenitors during embryonic development using *in-utero* electrophoresis. We also characterized its sub-cellular localization using fixed sample imaging and live-cell imaging, which highlighted its association with cellular compartments directly involved in cell migration dynamics.

To further characterize molecular mechanisms behind PCDH7's role in cell migration, we used a quantitative proteomics approach to compare global changes upon PCDH7's knockout which outlines a plethora of upregulated and downregulated proteins. Many of these proteins have previously been shown to be associated with cellular compartments involved in cell migration or have a molecular function characterized in the regulation of cell migration.

Taken together, our work outlines a critical role of PCDH7 in cell migration, association with migration-associated subcellular compartments, and possible molecular players in its role. Our work is a step towards recognizing PCDH7 as a promising therapeutic target for control of cancer metastasis.

ÖZET

Kanser dünya üzerinde en yüksek ölüm oranına sahip hastalıklardan biridir. Kanser kompleks bir hastalık olup kontrolsüz büyüme, zamanla biriken mutasyonların sebep olduğu genetik dengesizlik ve metastaz olarak da bilinen kanserli dokunun sağlıklı bölgelere yayılması olarak tanımlanmaktadır. Metastaz hücrelerin göç edebilme yeteneği ile ilgili olup, metastaz ile alakalı tedavi çalışmaları için bu mekanizmanın detaylı bir şekilde aydınlatılması gerekmektedir. Bu tezde, hücre yüzeyi proteini olan protocadherin-7 (PCDH7)'nin hücre göçü sırasında oynadığı moleküler rolünü anlamayı amaçladık.

Grubumuz daha önce yapmış olduğu çalışmalarda, PCDH7'nin hücre döngüsünde kontrol edilen bir zar proteini olduğunu göstermiştik. Bu tezde, PCDH7 ifadesindeki değişimin memeli hücrelerinin hücre göçüne etkisini ve embriyonun gelişimi sırasında sinir hücrelerinin korteks içerisindeki göçüne etkisini araştırdık. Aynı zamanda fikse edilmiş örnekler ve canlı görüntüleme metotlarını kullanarak PCDH7'nin hücre içerisindeki bulunduğu bölgeleri araştırarak, hücre göçü sırasındaki yapmış olduğu dinamik ilişkileri ortaya koyduk.

PCDH7'nin hücre göçü sırasındaki rolünü daha detaylı anlayabilmek için, kantitatif proteomiks metodunu kullanarak PCDH7 ifadesinin susturulduğu durumlarda hücre içerisinde ifadesi artan ve azalan proteinlerin tamamını araştırdık. Sonuçlarımızda gördüğümüz proteinleri çoğunun ya direk hücre göçü ile ilgili oldukları ya da hücre göçünün kontrolünü sağlayan mekanizmalarda görev almış oldukları geçmiş çalışmalarda gösterilmiştir.

Sonuç olarak bu çalışma PCDH7'nin hücre göçü sırasında önemli bir rolü olduğunu, hücre içerisinde göç ile ilgili diğer organel ve proteinlerle ilişkisinin olduğunu göstermektedir. Bu çalışmanın sonuçları ışığında PCDH7'nin metastazın kontrolü için önemli bir terapatik hedef olabileceğini öngörüyoruz.

Acknowledgements

At the outset, I would like to express my gratitude to my thesis advisor, Dr. Nurhan Özlü for her guidance, and an a highly open-minded approach towards the project. Her support, encouragement and optimism acted as catalysts to take the project towards completion. Her words, "*I have a feeling, we can do it*", often did wonders for the project.

Next, I would like to express a sincere appreciation for the entire thesis monitoring committee. Dr. Elif N. Fırat Karalar and Dr. Tuğba Bağci Önder have always provided good counsel to troubleshoot experiments or for an adjustment to the graduate life. Their insights into the field of cell migration and cytoskeleton often brought easy solutions to seemingly complex problems. I highly appreciate Dr. Umut Sahin and Dr. Gulayse Ince Dunn for their constructive support during committee meetings.

I would like to extend special thanks to Dr. Halil Bayraktar who has been associated with the project since its conception, and has helped us in the data analysis. Dr.Bayraktar has always been just a call or an email away. He has always been willing to help analyse data from any perspective that I proposed. This thesis would not be where it is today without his help. I would like to thank Dr. Ibrahim Bariş for his expert advice in cloning at a very critical time of the project. I thank our collaborator Dr. Ozgur Sahin for help in directed migration assays and to Cansu Kagiali for handling the cells during this experiment. I extend sincere appreciation to Cansu Akkaya for help with *in-utero* electroporation experiments. I thank our technician Busra Akarlar for help with proteomics experiments and to Erdem for help with analysis of proteomics data. I appreciate the help of Dr. Serçin Karahuseyinoğlu for help with live imaging experiments at KUTTAM and Dr. Ihsan Solaroğlu and Dr. Yasemin Özdemir to facilitate my visits. I extend special appreciatıon for the technical support of KUTTAM technicians Nesligul Şenturk, Tayfun Barlas, and Şimal Laçin.

I dedicate this thesis exclusively to my family, my parents Kausar Jamal and Mohammad Naseem Qureshi, my brothers Dr. Akif and Hafez Jawad, sister in law, Munazza and my sweet niece Safoora. Bearing my absence from their lives, they

always extended an untiring support to me. They personify the qualities of persistence and selfless love in my conscience. I hope to be reunited with them soon.

Transition into a new country and culture is often challenging, and graduate studies bring its own complications. Ibrahim Kurt helped me to adjust with life in Istanbul. I have absolutely no reservations for extending my gratitude and wishes for his great career in brewing. Ömer Faruk Ağca always diffused difficult times with his optimistic attitude. Ismail Yorulmaz, Mustafa Eryurek, Abdullah Muti, and Abdullah Bilgin always opened their home, 'the Maden Palace' and were always there for me. Thanks to Isa Ozdemir, Shihab Alabab and Obadah Albahra for their constant support.

Heartily appreciation goes to my former mentors Dr. Hamza Balcı and Dr. Rajiv Bhat for developing my scientific attitude and facilitating my progress. Their kind and graceful personalities would always remind me of their great mentorship.

Members of the Ozlu research group deserves special mention. Especially Dr. Zeynep Sabahat Yunt, Mehmet Akdag, Aydanur Senturk, Busra Harmanda, Esra Unsal and Dr. Elif Kaga. Whenever I needed it, they were more than willing to help in every possible way. My interns Erdem Bozluolcay, Harun Kulak, Ceren Yuce, Fatih Aygenli, Enis Hisarli, and Canelif Yilmaz were of great assistance for experiments. They gave me opportunities to engage in mentoring while tolerating my unorthodox methods.

I thank Dr. Nathan Lack for welcoming me in his group's journal club. All members of Lack lab and their characteristic polite smile and welcoming warmth provided a second home for me.

I thank Koç Üniversity Graduate School of Science and Engineering for provıdıng fınancıal assıstance for throughout. Deserving special mention are people in administration especıally Ms. Elif Tuysuz, and Ms. Emine Buyukdurmus who always extended a guiding hand.

Table of Contents

ABSTRACT iii
ÖZET iv
Acknowledgements v
Table of Contents vii
List of Figures xi
List of Tables xii
Chapter 1 1
Introduction 1
1.1 Mechanisms of cell migration 2
1.2 Literature review 3
Chapter 2 18
Materials and Methods 18
2.1 Cloning of PCDH7 Isoforms 18
PCDH7-isoform b 18
PCDH7-isoform c 19
2.2 Stable cell lines generation 19
PCDH7 expression through transient transfection 19
2.3 Lentiviral constructs of PCDH7 isoforms 20
pLenti-PCDH7-GFP constructs 20
pLenti PCDH7-mCherry plasmids 20
2.4 RNAi mediated knockdown of PCDH7 21
2.5 shRNA resistant plasmid synthesis 22
2.6 CRISPR mediated Knockout generation 23
Reagents for CRISPR/Cas9 mediated knockouts 23
Generation of knockouts 24
Genotyping for monoclonal populations 24
2.7 Generation of stable cell lines expressing PCDH7 for recovery experiment 25
2.8 Single Cell tracking for phenotype assessment 25

Data analysis for single cell tracking 26
2.9 Xcellegance RTCA migration analysis for PCDH7 knockout in HeLa S3 26
2.10 SILAC based Proteomics analysis for PCDH7 knockout in Hela S3 27
SILAC labeling 27
In-solution digest of cell proteome 27
Iso-Electric Focusing (IEF) fractionation of peptides 28
Statistical analysis 29
2.11 *In-vivo* assessment of PCDH7s role in migration 29
In-utero Electroporation 29
2.12 Immunofluorescence 30
2.13 Western Blotting for PCDH7 31
Chapter 3 34
Results and Discussion – Part I 34
Cell Migration Phenotype Assessment 34
3.1 Overview 34
3.2 shRNA mediated knockdown of PCDH7 in RPE cells 36
Migration data 37
3.3 RPE1 CRISPR knockout 40
Generation of PCDH7 knockout in RPE1 cells 40
Live cell imaging for migratory phenotype assessment 41
3.4. Real Time Cell Migration of HelaS3 cells 45
3.5 *In-utero* electroporation. 46
in-utero electroporation for PCDH7 phenotype assessment 46
3.6 Conclusion 49
Chapter 4 51
Results and Discussion – Part II 51
Subcellular localization of Protocadherin-7 51
4.1 Overview 51
4.2 PCDH7 localization - confocal imaging 52
4.3 PCDH7's correlation with Cortactin 54
4.4 PCDH7 correlation with Myosin IIb 55

4.5 Dynamics of subcellular localization of PCDH7 in a migrating cell 57
Confocal Live Imaging 57
Z-section dependent localization changes of PCDH7 60
3-Dimensional reconstruction of confocal imaging sections 62
F-actin perturbation 63
4.6 STED imaging of PCDH7-GFP 64
Chapter 5 67
Quantitative proteomics analysis of PCDH7 knockouts 67
5.1 Overview 67
5.2 PCDH7 knockouts in HelaS3 cells 69
5.3 GO Annotation Clustering 70
5.4 Enlisting roles in Migration/Metastasis of representative proteins 77
Actin cytoskeleton associated proteins 77
Myosin motor proteins 79
Negative regulation of Cell migration 79
Focal Adhesion related proteins 80
5.5 OmicsIntegrator for functional clustering 81
5.6 Conclusion 86
Chapter 6 88
Discussion and Conclusion 88
Working Model 90
References 93
Appendix A 102
Cell Culture 102
Appendix – B 103
Optimization for transfection 103
Lipofectamine 3000 103
Polyetheleneimine preparation (PEI) 103
HelaS3 and Hek293T transfection 104
Appendix C 105
Live imaging 105

Appendix D 106
Oligonucleotide Sequences 106

List of Figures

	Page
Figure 1-1 : Evolution of Protocadherins	5
Figure 1-2: Cell cycle dependent localization of PCDH7	7
Figure 1-3: PCDH7 Structure Prediction	9
Figure 1-4: PCDH7 Isoforms	10
Figure 3-1: Persistence and Angular Displacement	35
Figure 3-2: RNAi mediated PCDH7 knockdown in RPE	36
Figure 3-3: Migration phenotype with shRNA in RPE cell	37
Figure 3-4: Persistence assessment upon shRNA treatment	39
Figure 3-5: RPE1 CRISPR cells and Recovery cell generation	40
Figure 3-6: Phenotype of RPE1 PCDH7 knockout cells-I	41
Figure 3-7: Phenotype of RPE1 PCDH7 knockout cells-II	43
Figure 3-8: RPE1 Angular Displacement:	44
Figure 3-9: RTCA/Xcellegence directed migration for PCDH7 knockout in Hela S3	45
Figure 3-10:In-utero electroporation Immunofluorescence	47
Figure 3-11:In-utero electroporation quantification	49
Figure 4-1: RPE1 PCDH7 immunofluorescence	53
Figure 4-2: PCDH7 and cortactin	55
Figure 4-3: PCDH7 and Myosin IIB	56
Figure 4-4: PCDH7 stills from fame 1	58
Figure 4-5: PCDH7 stills from fame 43	59
Figure 4-6 : PCDH7 stills from fame 68	61
Figure 4-7: PCDH7 stills from fame 75	62
Figure 4-8:3-Dimensional Reconstruction of PCDH7 signal	63
Figure 4-9:STED imaging of Cell Front:	65
Figure 5-1:Outline of SILAC experiment	68
Figure 5-2 :SILAC data correlation of two knockout colonies	70
Figure 5-3 :Cellular compartment based GO clustering	71
Figure 5-4 :Biological Process based GO clustering	72
Figure 5-5 :Molecular Function based GO Clustering	74
Figure 5-6 :KEGG pathway based GO clustering	75
Figure 5-7: Functional Correlation of Protein hits	76
Figure 5-8 :Interaction with Actin cytoskeleton	78
Figure 5-9:Predicted interaction networks within upregulated set using OmicsIntegrator	82
Figure 5-10:Predicted interaction networks within downregulated set using OmicsIntegrator.	83
Figure 5-11:Subnetwork with EMT proteins	84
Figure 6-1: Model of Control Migration	91

Figure 6-2 : Model of Knockout migration	91
Figure B-1:Transfection Optimization	Appendix B

List of Tables

	Table	Page
1	Table 2-1- shRNA constructs and sequences targeted	21
2	Table 2-2 - List of antibodies for Immunofluorescence and Immunoblotting	32
3	Table 5-1 EMT proteins in down network 6	85
4	Table D-1: Oligonucleotide Sequences	106

Chapter 1

Introduction

With ever emerging novel aspects related to cell's physiology and pathological state, cell surface has emerged as an important interface between the cell and its environment. The proteome of the cell surface plays a critical role in maneuvering a cell's behaviour in a complex environment, its response to stimuli, its survival during normal growth and neoplastic evolution. During a pathological state like that of cancer, cell surface adapts to face new challenges stemming from a rapid uncontrolled proliferation. Its interactions and competition with its normally dividing neighbours of the same tissue and cells of the stromal tissue would be mediated through a new set of adaptive changes on its surface. These cell surface modifications have interested cancer biologists as a platform for therapeutic interventions to counter the cancerous growth [1,2]. Contributing to even higher morbidity and mortality is the transformation of cancerous growth into the metastatic state. During metastasis again, it is the cell membrane that encounters new territories that an invading cell must pervade through before it reaches the would-be invaded site. Signal transduction pathways alter cell-cell junctions and cell-matrix interactions, as well as modulation of cytoskeletal dynamics. It is through these changes a static, localized cancerous cell can invade systemically through engaging with blood and lymph vessels, and endothelial walls' penetration.

Mechanisms of cell migration and invasion have been an active area of research for many decades and resulted in the elucidation of pathways involved in the regulation of cytoskeletal dynamics and cell-matrix interactions [3-6]. It is of active interest in the field of cancer biology to find a common, converging pathway for cancer cell metastasis. Migrating cancer cells, however, display a 'plastic' behaviour in

responding to the immediate microenvironment through adaptive changes in cell-adhesion, mechanotransduction and cytoskeletal dynamics [7,8].

1.1 Mechanisms of cell migration

For the process of migration, a seemingly non-polarised cell undergoes changes during which, a cell's shape alteration creates planar asymmetry (Front and rear polarization) followed by cell body translocation. For this thesis, we will focus on single cell migration and not on collective cell migration which is a migration behaviour of multiple cells still connected through cell-cell interactions. Normal cells and cancer cells arguably employ the same migration machinery. Cell migration machinery employs a series of molecular steps which can be summarized as follows: Step 1 sees the polarization of the cell because of differential actin cytoskeleton assembly. On cell's migration front, the F-actin network forms protrusive structures. In step 1, a crucial biochemical process is the activation of GTPases Rac or cdc42. Rac GTPases mediate filopodia or pseudopodia generation. On the other end of the polarised cell, there a pre-uropod region marks cell rear. Step 2 involves the engagement of leading edge with extracellular matrix/substrate. This engagement involves cell surface receptor recruitment and clustering that mediates adhesion to the substrate. This interaction results in the generation of traction forces in the direction of migration. In order to move forward, the cell needs to pervade through the extracellular matrix, many components of which undergo controlled proteolysis. This proteolysis, which marks the step 3 of cellular migration, is performed by cell surface proteases a process that makes room for the advancing cell body. Next, step 4 involves generation of forces mediated through actomyosin contraction. A process involved in this mediation is the activity of Rho GTPase that interacts with myosin II. Actomyosin contraction takes towards later part of the cell. As a result of the contraction, cell rear undergoes a turnover of adhesion interaction with the substrate. This allows the cell rear to move forward, in coordination with the cell front. This marks the step 5 of cell migration.

For cell body to make a persistent migration, these processes are executed by the migrating cell's machinery in a synchronous manner [4]. A migrating cell's engagement with the substrate and ECM components leave a micro track, as a reminiscent of recent activity. This micro track provides an easier path for the other cells pursuing a migration in that very direction and subsequent cells widen this track into a macro track [9,10] through enhanced proteolysis of ECM.

1.2 Literature review

Discovery of Protocadherins

Protocadherins were originally identified as a large group of proteins encoded in rat, human, mouse, Xenopus, *c. elegans* and Drosophila using degenerate PCR [11]. Two human protocadherins were cloned in this work, which were later on characterized as Protocadherin-1 and protocadherin-γC3. Having N-terminal domains similar to cadherin domains of classical cadherins, but very different cytosolic region, these members of protocadherin subfamily have gained increasing attention.

Protocadherin subfamily is divided into clustered (α, β, ϒ as being encoded by clustered gene groups *pcdha*, *pcdhb,* and *pcdhg*) and non-clustered (δ) and a few other minor groups. Delta protocadherins constitute non-clustered protocadherins and fall into two groups termed as δ1 and δ2. δ1 contains 7 EC cadherin domains, while δ2 contains 6 EC cadherin domains. δ1 consists of PCDH1, 7, 9, and 11 and δ2 consists of PCDH8,10, 17, 18 and 19. Many of δ-protocadherin members are highly expressed in the nervous system.

Evolution of Protocadherins

A recent work explored the origins and evolution of protocadherins in Metazoa [12]. Cephalochordate *B. floridae* contains two related proteins termed as AmphiPCDH1

and AmphiPCDH2. One protocadherin has also been identified in Sea Anemone *N. vectensis*, (NvPCDH) and one in *Aplasia californica* (AcPCDH). Comparative analysis of these four protocadherins (AmphiPCDH1, AmphiPCDH2, NvPCDH, and AcPCDH indicates seven EC domains and conserved CM domains in the cytoplasm (figure 1-1 A). These conserved domains are very similar to those observed in long isoforms of δ protocadherins [13]. A profound expansion of the protocadherin family took place among chordates. Mammals, fishes, and reptiles, for example, contain between 60 and 80 different protocadherins [14-16]. Chordates evolved a highly complex nervous system. Data from rodents and zebrafish show expression of δ-protocadherins in major parts of the developing brain [13,17]. An ability for homophilic interactions and expression during neuronal development advocate their being high probability candidates for neuronal architecture and connectivity. A concomitant expression and expansion of protocadherin family among chordates and the fact that most protocadherins are highly expressed in the nervous system may have orchestrated complex chordate nervous system. Understandably, mutations among a group of key genes to neuronal developmental would reflect in terms of developmental, and neural disorders [18,19]. A phylogenetic study analyzing the cytosolic domains of protocadherins classified them into sub-clusters 1) CELSR-PCDHs, 2) FAT-like PCDHs, 3) clustered α,β,γ groups 4) non-clustered δ group and some solitary members [20].

The premise of the project

Cancer is a complex disease defined by hyperproliferation, enhanced genetic instability, and metastasis to secondary sites. It remains as one of the leading causes of morbidity and mortality globally. Main treatments at hand still rely heavily on cytotoxic treatments like chemotherapy and radiotherapy which targets proliferative

cells, killing in process bystander cells and causing unintended damages. Additionally, often these treatments fail to completely root out cancer cells and different cancer types

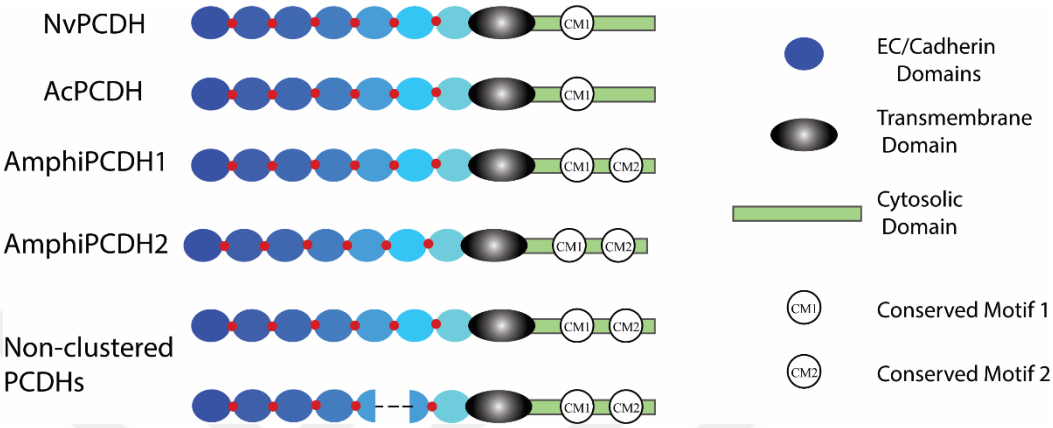

Figure 1-1: Evolution of ProtocadherinsA) Comparison of invertebrate protocadherins and non-clustered protocadherins (Figure redrawn and adapted from (12)).

respond differently to these treatments. Targeted oncological treatments have given much hope to reduce cancer based mortality. There has been an increased interest in finding molecular markers to differentiate between neoplastic tissues from those following normal physiology, for selective therapy and reduced toxicity. Metastatic cells are often resistant to chemotherapy, so targeted therapy also holds great potential to curb metastasis. Proteins are the most attractive candidates for these targeted therapies, owing to their 3-dimensional structure presenting a good number of potential binding sites for small molecules. The subset of proteins present on the cell surface is at the interface of the cell and their external environment, and neighbouring cells. These cell surface proteins are involved in the cell signaling, transport of metabolites, ions, and cells interaction with its extracellular matrix.

Cell surface Proteome of distinctly differentiated cells differs, owing to their distinct functions. There has been a growing interest in deciphering cell surface proteome distinctions across different tissues as well as between cancer and normal tissue. Cancer cells affect the normal expression pattern of the surface proteome. Since excessive proliferation is a hallmark of cancer cells, finding differential interface vs mitotic proteome of cancer cells presents a promising niche for detecting effective biomarkers. With this goal in mind, a previous study from our research group focussed on proteomics screening to find enriched proteins on the cell surface in HelaS3 cells during mitosis and interphase. We performed SILAC based metabolic labelling of light and heavy cells and differentially synchronized them into interphase and mitosis. This was followed by cell surface labelling of NHS-SS-biotin, streptavidin pulldown, release of proteins with DTT and identification of enriched proteins using LC-MS/MS [21]. Data from other protocadherins also indicate that major pools of these proteins lies within intracellular organelles with only a small proportion existing on cell membrane. This disproportionate distribution between internal organelles and cell surface indicates

A

Gene	Protein	Enrichment Phase
PCDH7	Protocadherin-7	Mitosis
PCDH1	Protocadherin-1	Mitosis
ITGB1	Integrin Beta 1	N
EGFR	EGF Receptor	N
GPR56	G-Protein Coupled Receptor	Interphase
TFRC	Transferrin Receptor	Interphase

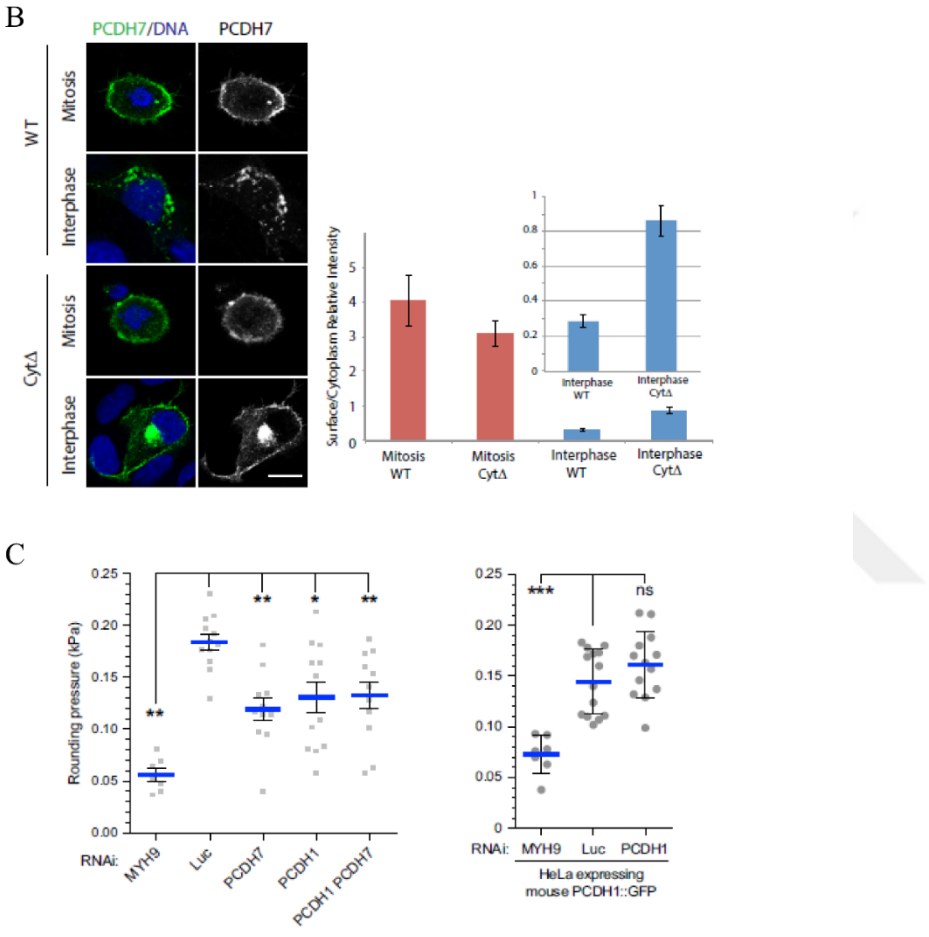

Figure 1-2 : Cell cycle dependent localization of PCDH7 A) Representative proteins cell cycle specific enrichment on cell surface. B) PCDH7 wild type and cyt-del mutant cell surface enrichment profiles C) Cell rounding pressure upon PCDH7 and PCDH1 manipulation. Adapted from [21]

controlled trafficking and internalization of protocadherins. Our work showed that deleting the cytosolic domains of PCDH7 enhanced membrane localization of PCDH7 during interphase, indicating loss of controlled internalization at the commencement of mitosis (figure 1-2 B). Reports from clustered protocadherins, γ-PCDHs also show that deleted cytosolic elements mediate an increase in their cell surface proportion [22,23]. siRNA mediated perturbation of PCDH7 and PCDH1's expression causes reduction of cellular turgidity as measured through rounding pressure (figure 1-2 C) [21]. Cytoskeletal elements play an important role in maintaining cellular architecture and shape, including rounding pressure. Actomyosin elements are responsible for maintenance of cell's cortex and our previous results pointed towards a functional relationship between δ-PCDHs and the actin cytoskeleton. Phylogenetic analysis of cytosolic sequences of δ protocadherins clusters them into two groups, δ1 and δ2 [13]. δ1 subgroup is unique for the presence of CM3 motif in its cytosolic domain. CM3 is not present in δ2 members. δ1 member proteins contain seven cadherin domains as opposed to six in δ2. CM1 and CM2 are conserved domains in the δ subgroup.

To find other roles played by PCDH7, we performed a literature survey. PCDH7 was initially named BH-protocadherin owing to its high expression in brain and heart tissue. [24]. There are 4 splice variants of PCDH7, isoform a, b,c and d. Preceded by a signal peptide (28 amino acid residue), all isoforms contain the same EC region (29-879 residue) containing seven cadherin domains, and a transmembrane region (880-900 amino acid residues). Structure prediction based on sequence similarity using i-TASSER predicted seven cadherin domains in the extracellular (EC) region (figure 1-3 B). Variants show differences in the cytosolic domains. There are three cytosolic domains reported in

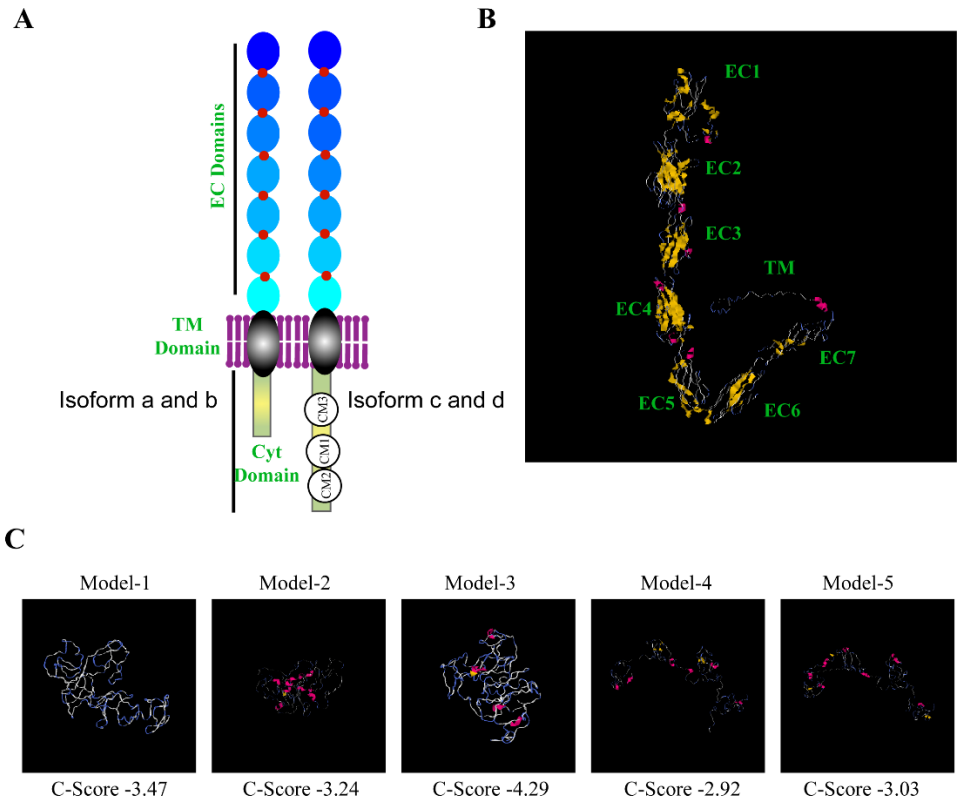

Figure 1-3 PCDH7 structure prediction A) Cartoon representation of PCDH7 isoforms. B) Predictive modelling of EC and TM domain of PCDH7 using i-TASSER predicting seven cadherin domains, EC- extracellular, TM- transmembrane, Cyt- cytosolic

PCDH7, CM1, CM2, and CM3 (figure 1-3 A). Isoform b is the intron-less isoform with 172 amino acid residues in cytosolic part. Isoform a is expressed as a result of alternative splicing and contains 169 amino acids that are different at the c-terminal (figure 1-4 A). Isoform a and b are shorter isoforms whereas isoform c and d are longer isoforms. Isoform c and d contains 347 and 355 residues respectively, with isoform d having an additional patch of 8 residues (GEAEHMEN) in the middle of the cytosolic domain (residues 223-230) (figure 1-4 B). Shorter isoforms lack CM3 domain which

contains a motif RRVTF that interacts with phosphoprotein phosphatase 1 α (PP1α). Another

Figure 1-4: PCDH7 Isoforms: PCDH7 isoform alignment for cytosolic domains. Shorter Isoforms (A) and longer Isoforms (B). Alignment performed using CLUSTAL Omega.

phosphatase PP2A was shown to be functionally associated with PCDH7 to potentiate EGFR and KRAS mediated MAPK signalling [25]. Cytosolic domain structural information, however, is unknown. Protocadherins cytosolic domains are very

different from those of classical cadherins. We user i-TASSER to generate the cytosolic secondary and tertiary structure prediction based on any known sequence similar to PCDH7 Isoform c. i-TASSER could not find any other known template with enough similarity to generate a high confidence structure. i-Tasser predicted a high prevalence of random coil rather than helical of sheathed structures. This could have resulted either in the absence of any known similar sequence with an established secondary and tertiary structure or a tendency of the natively unfolded structure. Natively unfolded domains are fluid structures which may acquire a more rigid conformation upon interaction with other proteins.

An expression study that intended to outline expression differences between brain-specific metastasizing and their parental breast cancer cell lines (MDA-MB-231 and CN34) indicated that PCDH7 is dramatically upregulated in brain metastasizing versions [26]. Functional importance of this upregulation was shown in a later study. PCDH7 and gap junction connexin-43 mediated interactions between invading cancer cell and astrocytes mediated a cross-cell signaling mechanism [27]. In cancer cells, STING signaling is upregulated leading to the production of cGAMP second messengers. cGAMP travels across gap junctions into astrocytes, and mediating secretion of IFN-α and TNF which in a paracrine manner imparts proliferation advantages and chemoresistance to the invading cancer cells. Another study focusing on the effects of PCDH-7 on bone metastasis showed a direct correlation between PCDH7 and bone metastasis of breast cancer cells [28]. Upregulation of PCDH7 in breast cancer cells mediated high bone metastasis. Metastasis is inversely correlated with survival in cancer. A genome-wide association study tabulating SNP's associated with survival in non-small cell lung carcinoma showed some of the top SNP's associated with PCDH7 [29]. A resonating theme among these published works outlines the role of PCDH7 in cancer cell metastasis. We found it pertinent to explore the role of PCDH7 in mammalian cell migration and molecular mechanisms involved in that role. Another

observation from Xenopus ortholog of PCDH7, the NF-PCDH has shown its involvement in axonogenesis and axon guidance, through its interaction with template-activating factor (TAF-1) [30,31].

Role of Cadherin family members in migration and invasion

Classical cadherins have long been known to play roles in calcium-dependent cell-cell adhesions [32-34] and more complex roles including cell signalling [35,36]. Presence of at least two extracellular cadherin repeats defines cadherin family members; most members possess a transmembrane domain and a cytoplasmic domain. Structural similarity in EC domains has facilitated identification of over 100 members in human alone with EC cadherin repeats reaching as many as 34 [37]. Classical cadherins, E-cadherin and N-cadherins are the most studied proteins of the family. They interact in a homophilic fashion with trans molecule from a neighbouring cell and indulge in cis-homophilic interactions within the same cell. There are increasing reports of some members of cadherin superfamily to be involved in heterophilic interactions with other members of the superfamily [38]. Many intracellular proteins have been shown to be associated with the cytosolic domains of classical cadherins that mediate their functions. including cell-cell adhesion and cell signalling [36].

Cadherin Switching in EMT

During development, cells undergo epithelial to mesenchymal transition (EMT). This transition mediates cellular dissemination and migration to other locations where they give rise to subsequent derivative tissues. Neural crest (NC) cells, for example, switch from an epithelial behavior to a mesenchymal one during development. This transition helps NC cells invade other parts of developing embryo and establish diverse lineages across tissues. A hallmark of EMT is the cadherin switching. Epithelial cells exhibit high levels of E-cadherin expression. As cells undergo EMT, they exhibit

downregulation of E-cadherin expression and upregulation of N-cadherin. This cadherin switching is also what is responsible for a differential contact inhibition of locomotion (CIL) profile of cells [39,40]. CIL is a behavior of migratory cells wherein cells' protruding ends upon contacting another cell make cell-cell contacts. After the formation of cell-cell contacts, cells tend to recreate an alternative protrusive end, changes their direction of migration, and detach from the interacting cells. However, this behavior is divergent between epithelial and mesenchymal cells. Epithelial cells, upon contact formation with other cells, do not make an alternative protrusive end. Rater, they lose their motility and do not pull away from one another. A recent work describes this dichotomy of migratory behavior in pre-migratory and migratory NC cells [41]. Pre-migratory NC cells are more epithelial in character with E-cadherin expression [41] and migratory cells are more mesenchymal with N-cadherin expression [42]. Pre-migratory cells do not pull away from neighbouring cells once they establish cell contacts, in contrast to post-migratory cells. In migratory NC-cells overexpression of E-cadherin prevents CIL, despite the presence of N-cadherin whereas in pre-migratory cells, downregulation of E-cadherin mediated CIL. Differential E-cadherin expression thus seemed more deterministic for the behavior of NC lineage. Rac GTPase mediated signaling is responsible for the formation of protrusive cell fronts. In fact, in migratory NC cells, during CIL, Rac signaling gradient changes and establishes alternative protrusive end. This Rac signaling re-orientation away from point of contacts is absent in E-cadherin dominant pre-migratory NC cells. Traction forces patterns on the substrate are also different between the two groups. During CIL traction forces get redirected towards the new protrusive end, but in pre-migratory-NC cells, these forces are randomly distributed upon cell-cell contact establishment.

Fat Protocadherins

Some distantly related member of non-clustered PCDHs termed as fat protocadherins have been shown to play a role in cell polarity maintenance and motility. Fat1 has been

shown to be located on cell's leading edge where it coincides with filopodial extensions as well as associated with F-actin for directed cell motility[43]. Fat1 has direct interactions with Ena/WASP proteins and its cytosolic domain can recruit actin, even when ectopically expressed and directed to mitochondria. Fat1 downregulation affects cell's polarity and motility. Fat1 possesses proline-rich EVS1 domains in its cytosolic domain that interacts with Ena/Vasp and recruits actin. A similar domain is however not present in PCDH7's cytosolic domain indicating that a similar mechanism of actin recruitment may not be relevant for PCDH7.

Mechanotransduction mediated by cadherins

Mechanotransduction is the conversion of cues generated by perturbation in tension into biochemical changes. Cytoplasmic domains of cadherins mediate most of the signalling mechanisms associated with cadherins. Cytoplasmic domains interact with catenin complexes which act as links to the cytoskeletal elements, like actin. β-catenin interacts with the cytoplasmic domains of cadherin molecules. Protein β-catenin interacts with α-catenin which in turn links it to the actin cytoskeleton. Cells require an adaptive mechanism to withstand mechanical forces, from within and from outside. Adhesive interactions mediated by cadherins help cells withstand, and even signal the mechanical changes to other cells within the tissue. E-cadherin, N-cadherin and VE-cadherin are classical cadherins that are F-actin associated and have been shown to mediate mechanotransduction in different experimental settings. In mechanotransduction actomyosin based contraction system acts a key player. As cell migrates, it undergoes dynamic and synchronous shape alterations. Coordinated alterations in cellular morphology and dynamic association with ECM are required for cell migration. Cellular morphology is intricately associated with F-actin driven cytoskeleton and mediation of substrate adhesion through focal adhesions (FA).

Actin Cytoskeleton

Actin has been at the centerstage of muscle contraction and cell motility for a long time. Discovery of actin and its characterization is attributed to Straub but it was first reported almost half a century earlier than Straub's work. It was Halliburton, who first reported actin by naming it 'myosin ferment' in 1887 [44]. Myosin ferment was named so, because a dried muscle extract (actin) when brought in contact with muscle-plasma (containing active myosin) or myosin extract, exhibited coagulation (actomyosin association and precipitation of complex). F-actin dynamics and their impact on cell migration are spatiotemporally controlled through cell signalling pathways. F-actin network can be divided into two distinct networks, protrusive front end lamellipodia or filopodia and an actomyosin assembly based contractile network. A coordination of protrusive and contractile network, regulated by activities of actin regulatory proteins, drives directional migration. Arp2/3 and cofilin drive rapid polymerization of actin on the protrusive edge of the cell [45-47]. Lamellipodial actin mesh is exclusive of other cytoskeletal elements like microtubules and intermediate filaments [48]. Rapid actin polymerization at the leading edge generates a push in the forward direction [49], and as a reaction pushes the actin networks backwards. This backwards flow of actin is referred to as retrograde actin flow[47,50]. Proximal actin fibres depolymerize and produce a treadmilling of F-actin [51]. These coordinated changes where actin polymerization surpasses retrograde movement associated depolymerization produces forward push at the leading edge [52,53]. The contractile module of F-actin lies behind and towards the cell body. It has a complex composition; myosin II and tropomyosin are chief proteins mediating in its contractile functions [50,54,55]. Stress fibres are bundles of actomyosin contractile assemblies. There are three types of contractile bundles: a) dorsal and ventral stress fibres; (b) transverse arcs (c) graded polarity bundles. Relative prevalence of these bundles differs among different motile cells. Composition wise, stress fibres and transverse arcs display a periodic, length-wise, uniform pattern of

association with α-actinin/Myosin II but have different relative orientations [56]. Stress fibres are directed towards the direction of cell migration whereas transverse arcs are perpendicular to the direction of migration. Graded polarity bundles have a non-uniform association with α-actinin/Myosin II, and have an orientation in the direction of migration [57]. Contractile F-actin network and its dynamic nature drives the later steps of synchronized cell migration. Rac and Cdc42 are GTPases that regulate F-actin dependent protrusive front organizations [58]. Rho GTPases organize F-actin network that mediates traction on the substrate, and consequent alterations in FA constitution and morphology [59].

Non-muscle myosin II

Myosins are a class of actin-binding proteins possessing ATPase activity and motor domains. Skeletal muscle myosin was the first myosin to be characterized and it was named myosin II. Since then, many non-muscle myosins have been discovered and myosin family was divided into class I containing small monomeric myosins and class II with dimeric myosins similar in structure to muscle myosin. Based on phylogenetic analysis of motor domains, myosins are classified into 12 different classes [60]. A different nomenclature of conventional and non-conventional myosin is also used. Class II myosins are described as conventional myosins whereas all other 11 classes are classified as unconventional myosins [61]. Non-muscle myosin II (NMII) is a component of actomyosin cytoskeletal system. It has actin binding and contractile properties. NMII possesses two 230 KDa heavy chains, two 20 KDa regulatory light chains, and two 17 KDa essential light chains. NMII has 3 different isoforms differing in their heavy chains subtypes. NMII plays a core role in cell adhesion and migration as well as cell division. At their core these processes require dynamic shape alteration of the cell which in turn requires force generation. NMII majorly accomplishes these processes through its actin binding, ATPase and contractile properties. Heavy chains of different isoforms are coded by three separate genes. MYH9, MYH10, and MYH14

codes for NMII heavy chains A, B and C respectively. NMIIA and NMIB display different localizations in a polarized cell [62]. NMIIA is localized to the protrusion front of the cell, and mediates adhesion maturation; NMII-B localizes differently, behind the localization of NMIIA, usually to large stress fibres and to the cell rear [62]. Recently a serine-rich motif (SFSSSRS) in the c-terminus of NMIIB has been identified as being responsible for NMIIB's rear localization, and cellular polarity. Three residues were phosphorylated within this motif, and S1935 was described as crucial for cell polarity and canonical stress fibre and rear localization of NMIIB [63].

Chapter 2

Materials and Methods

2.1 Cloning of PCDH7 Isoforms

PCDH7-isoform b

PCDH7 isoform b was cloned as an improvement on an existing truncated version present in Dr. Ozlu's repository. This construct lacked 30-240 amino acids on the extracellular domain of PCDH7. To repair the missing part, we synthesized missing portion using gene synthesis service from Genewiz (order # 10-317626515). Synthesized sequence corresponded to first 747 base pairs of the coding sequence, with an additional 5'sequence of 25 bp corresponding to a portion of eGFP-N1 plasmid (after eGFP-N1 has been digested with HindIII enzyme). A PCR was performed to amplify the synthesized sequence using primers #296, #297. A second PCR was performed for the rest of the sequence corresponding to PCDH7 using primers #298, #299. eGFP-N1 plasmid was digested with HindIII and BamHI. PCR products and digested plasmid were gel purified using MN kit following the recommended protocol. A Gibson's assembly was performed using three fragments and an in-house cocktail of enzyme and reagents as previously described [64]. Resulting reaction product was transformed into Stbl3 competent E. coli cells. Resulting colonies were used for plasmid extraction, and plasmids were transfected into HeLa S3 cells, to observe eGFP signal localization. Colonies showing the membranous location of GFP signal were further checked for correct size using PCR corresponding to extracellular EC region. Correct size colonies were selected for sequence confirmation. All PCR reactions were performed using Phusion polymerase with 98 ^{0}C denaturation temperature and 72 ^{0}C extension temperature, and extension span of 30 seconds per kb of DNA.

PCDH7-isoform c

There is a difference in the cytosolic domain of isoform b and c. Isoform has a longer cytosolic domain, and additional characteristic motifs including PP1α binding motif RRVTF. We used RPE1 cells cDNA library to amplify PCDH7-isoform c sequence. Primer # 198, #16. A modified PCR protocol was used for amplification. We used a **dual touchdown** PCR protocol in the same amplification reaction. An initial denaturation was done at 95 ^{0}C for 30s. The initial set of touch down employed 71 ^{0}C with -0.5 ^{0}C step wise for 10 cycles and an elongation temperature of 68 ^{0}C for 1:45 min. Secondly, 66 ^{0}C with -0.5 ^{0}C step wise for 10 cycles annealing with same denaturation and annealing parameters as the first step. Final step included 63 ^{0}C annealing for 15 cycles with the same denaturation and annealing parameters as the first step. The expected band at 3.7 kb was seen. The remaining product was digested with Hind III and BamHI, gel excised and ligated into the eGFP-N1 backbone. The ligation product was transformed into Stbl3 cells, and colonies were transfected into HeLa S3 cells to check for characteristic membrane localization of the GFP signal. Promising colonies were sent for sequencing.

2.2 Stable cell lines generation

PCDH7 expression through transient transfection

PCDH7b-eGFPN1 and PCDH7c-eGFPN1 were transiently transfected in RPE1 cells using lipofectamine 3000. Transfected cells were selected with 700 ug/ml G418 for a period of 14 days, followed by sub-culturing surviving cells. During selection During selection, parallel non-transfected cells were used as a control to monitor cell. Passaging of cells during the selection is important to dispose of the sick and dying cells regularly. This way, the resistant cells do not get affected from the overload of cell debris from sick cells. Surviving cells were sorted using FACS sorter (SONY

SH8000S, benchtop sorter) for GFP expression. Sorted cells were expanded and processed for immunofluorescence using anti-GFP antibody (Hayman lab, goat GFP).

2.3 Lentiviral constructs of PCDH7 isoforms

pLenti-PCDH7-GFP constructs

pLenti CMV GFP Puro (658-5), (Addgene 17448) was used for creating lentiviral constructs of PCDH7 isoforms. Backbone plasmid was digested with XbaI and BamHI and treated with Antarctic Phosphatase for dephosphorylation. Two PCR reactions were performed; first for isoform PCDH7b using primer #250 as forward and #14 as reverse, and second for PCDH7c using primer #250 as forward and #16 as reverse. Plasmids eGFPN1-PCDH7b and eGFPN1-PCDH7c were used as templates. Touch down PCR was employed, with 95 ^{o}C denaturation for 30s, annealing 72-62 ^{o}C within 15 cycles, and extension at 68 ^{o}C for 1:45 minutes. In next phase, 95 ^{o}C denaturation for 30s, followed by 62 ^{o}C annealing and 68 ^{o}C extension for 20 cycles. We observed faint bands with the expected molecular weights. PCR product was PCR purified, digested with XBAI and BamHI-HF and PCR purified again. Backbone plasmid was digested with XBAI and BamHI-HF, treated with Antarctic phosphatase and ligated with T4 ligation reaction (NEB buffer and enzyme) for 16 hours. Reaction products were transformed into Stbl3 cells. Colonies were picked, amplified, and plasmids thus obtained were transfected into HeLa S3 cells to screen for membrane localization (tentative PCDH7 colonies), vs cytoplasmic localization (free GFP). PCDH7-C1 and PCDH7-C4 were positive colonies for PCDH7c isoform. PCDH7-B9 and PCDH7-B13 were positive colonies for PCDH7b isoform.

pLenti PCDH7-mCherry plasmids

Addgene plasmid pLV-mCherry (#36084) was digested with XbaI and BamHI-HF enzymes. Plasmid backbone was treated with Antarctic Phosphatase. PCDH7 Isoform

B and Isoform C were amplified as follows: PCDH7b – primer #249, #209, PCDH7c – primer #249, #203. Restriction enzyme digested plasmid and PCR products were ligated to generate pLenti PCDH7 B and C mCherry fusion constructs. Touchdown PCR was employed, with 95 ^{o}C denaturation for 30s, annealing 72-62 ^{o}C within 15 cycles, and extension at 68 ^{o}C for 1:45 minutes. In next phase, 95 ^{o}C denaturation for 30s, followed by 62 ^{o}C annealing and 68 ^{o}C extension for 20 cycles. PCR products of appropriate molecular weights were digested with XbaI and BamHI-HF, and PCR purified. PCR products and digested backbones were ligated with T4 ligation reaction (NEB buffer and enzyme) for 16 hours. Reactions were transformed into Stbl3 cells and colonies were amplified for plasmid isolation. Plasmids were transfected into HeLa S3 cells for screening purpose. Fluorescence signal from membranes were considered as positive colonies for PCDH7.

2.4 RNAi mediated knockdown of PCDH7

Three separate vectors expressing shRNA targeting PCDH7 and a non-silencing shRNA vector were purchased as shown in the table 2-1. These are part of GIPZ shRNA library from Thermo Fisher Scientific.

Table 2-1:shRNA constructs and sequences targeted

	pGIPZ ID	Lab ID	Target Sequence
1	V3LHS_375966	shRNA C	TGAAAGTGTTTCTAATGCA
2	V3LHS_375967	shRNA D	CAGATGATCTTCGACGAGA
3	V3LHS_152964	shRNA H	TGAAAGTGTTTCTAATGCA
4	Non-Silencing	shRNA NS	CTTACTCTCGCCCAAGCGAGAG

shRNA constructs were packaged into lentiviral particles using pMD2.G and psPax2 packaging plasmids. For packaging, Hek293T cells were transfected using PEI as transfection reagent. Culture media were changed after overnight incubation and particles were collected 48 hours after transfection and a second harvest at 72 hours after transfection. Culture supernatants were filtered through 0.45 μm syringe filters. For infection of cells, viral suspensions were added to cells in culture and cells were monitored between 48-72 hours for GFP expression. RPE cells were selected using 7 μg/ml of puromycin for 48 hours and were processed for western blotting to observe PCDH7 expression.

2.5 shRNA resistant plasmid synthesis

shRNA-D targets CAGATGATCTTCGACGAGA sequence in human PCDH7 sequence. Forward primer was designed with a 5' overhang having sequence 5'-CA**A**ATGAT**T**TT**T**GA**T**GA**A**A-3' with total five point mutations in the sequence targeted by shRNA-D. Change of codons were optimized for human to control codon bias.Forward primer #267, and reverse primer # 265 were used for the amplification of the whole plasmids PCDH7 eGFPN1. For optimization purpose, a touchdown-temperature gradient combination was used. Part I – 95 ^{o}C for denaturation, 30s, touchdown annealing temperature 72 ^{o}C – 62 ^{o}C for 10 cycles with 1 ^{o}C per cycle, extension 68 ^{o}C for 4 minutes. Part II – employed a temperature gradient from 55-72 ^{o}C in annealing temperatures keeping denaturation and extension conditions same as part I. Amplification products at 8 kb were observed at all of the eight temperature gradients in a range of 55 – 72 ^{o}C with higher temperatures producing more products. PCR products were pooled and 3 μl DPNI enzyme was added to remove the template eGFPN1-PCDH7b and left at 37 ^{o}C overnight. PCR purification was done using MN kit and Polynucleotide Kinase (T4PNK) was used in T4 buffer to carry out end phosphorylation of PCR product for 1 hour. Resulting mix was ligated at 16 ^{o}C

overnight using T4 DNA ligase. The ligation reaction was transformed into Stbl3 cells and resulting colonies were amplified and transfected into Hek293 cells to test shRNA resistance expression.

2.6 CRISPR mediated Knockout generation

Reagents for CRISPR/Cas9 mediated knockouts

Six different guide sequences were selected based on the recommendation of mit.crispr.edu software. These guides were named as 7-1, 7-2, 7-3, 7-4, 7-5 and 7-6. Top and bottom oligos were named such as PCDH_1_T, and PCDH7_1_B for 7-1 set and so on. gRNA cloning into the pLentriCRISPRV2 was done as recommended by Zhang lab [65,66]. Briefly, 1 µl of the top and bottom oligos (100 µM stock concentration), 1 µl of 10X T4 Ligation Buffer (NEB), 0.5 ul T4 Polynucleotide Kinase (NEB) and 6.5 µl of RNase and DNAse free water. Annealing was done in a thermocycler with first treating at 37 ^{o}C for 30 min, followed by heating the mix to 95 ^{o}C for 5 min, and then cooling of the mix at a rate of 5 ^{o}C per min to 25 ^{o}C. For digestion of pLentiCRISPRv2, 5 µg of plasmid was mixed with 0.5 µl *BsmBI* (NEB R0580S, 10,000 U/ml)), 3.1 buffer (NEB), 20 mM DTT in a final 50 µl reaction. The reaction was incubated at 55 ^{o}C for 1 hour. Digested backbone was dephosphorylated with Antarctic phosphatase (5.5 µl 10X buffer, 1 µl Antarctic phosphatase), at 37 ^{o}C for 30 min. The reaction was run on an agarose gel, and larger band, above 10 kb was extracted. A ligation reaction was performed as follows: 50 ng of digested and dephosphorylated vector was mixed with 1/200X diluted annealed oligos, with 5µl of 2X NEB quick ligase buffer, and ddH_2O to total volume of 10 µl, and 1 µl of NEB Quick Ligase. Reaction was incubated at room temperature for 1 hour, followed by transformation into Stbl3 cells using standard transformation protocol. Multiple colonies were picked for sequencing confirmation.

Generation of knockouts

HeLa S3 and RPE1 cells were transiently transfected with lentiCRISPRv2 plasmid containing our guides and non-targeting control (from Dr. Tamer Onder's lab, targeting sequence : 5'-ACGGAGGCTAAGCGTCGCAA – 3'). For HeLa S3 cells lipofectamine 3000 was used with overnight incubation with transfection mix. For RPE1 cells transfection was done with lipofectamine 3000, using optimized protocol. Optimized protocol (see appendix 2 for details) includes transfection of the cells in the presence of no more than 1% FBS containing Dulbecco's Modified Eagle's Medium (DMEM). Plasmid and reagent mixing was done in optimem medium. 6 hours after transfection, medium was changed with pre-conditioned medium of overnight growth of at least 50% confluent culture. 24 hours after transfection, cells were treated with puromycin (2 ug/ml for HeLa S3 cells, and 7.5 ug for RPE1 cells). After 36 hours incubation, cells were given normal medium and surviving cells were cultured and analyzed for phenotype.

Generation of monoclonal CRISPR populations

Cells that show downregulation of PCDH7 expression in the population were used for preparing single cell dilution. Cells were diluted manually to be 1 cell / well in a 96 well plate. Cells were grown until clear monoclonal populations were apparent within wells having circular colony morphologies. These monoclonal populations were expanded by serially passaging them and were analyzed for the expression using immunoblotting.

Genotyping for monoclonal populations

We performed DNA isolation for the cell lines as follows: Cells were pelleted and washed with PBS. Washed cell pellets were resuspended into 100 µl pbs and heated at

95 ^{o}C for 10 min. Samples were vortexed and centrifuged at 11,000 rpm for 2 min. supernatant was collected and used as DNA template. PCR was performed to amplify the genomic region within which intended insertion/deletion mutations were expected. PCR parameters were as follows: Primers #446, 447, Phusion polymerase, betaine (1M), extension time, 10 s, annealing temperature 57 ^{o}C extension temperature 72 ^{o}C. Expected product 244 bp. Bands were gel extracted and sent for sequencing using primers 446 and 447 for sequencing.

2.7 Generation of stable cell lines expressing PCDH7 for recovery experiment

We intended to prepare cell lines with recovered PCDH7 expression for validation for recovery of phenotype (add-back recovery). For this purpose, we used lentiviral mediated delivery of PCDH7-isoform b and Isoform c (cloned into pLenti CMV GFP Puro backbones, addgene 17448) (figure 5B). Isoform b is shorter than isoform c and lacks the RRVTF motif which is a characteristic motif of δ-1 protocadherins and a binding site for phosphoprotein phosphatase PP1α. The purpose of using both isoforms for recovery of expression was to see relative differences in contribution to cell migration by different isoforms.

2.8 Single Cell tracking for phenotype assessment

RPE cells stably expressing shRNA and RPE1 CRISPR knockout sets were used for single cell tracking to monitor migration phenotype. shRNA set expresses turboGFP and CRISPR set expresses eGFP. We used OlympusPro (widefield) live imaging system for time lapse fluorescence imaging of cells. 10x objective was used for FITC channel. Time between two frames was 10 minutes. Cell positions were recorded for longer periods ranging between 18 – 24 hours.

Data analysis for single cell tracking

To determine the trajectories of cells, custom scripts written in MATLAB (R2017b, The MathWorks) were used to analyse all video clips. Briefly, trajectories of cells in the field of view were determined by single-cell tracking method. To compose the trajectory of each cell, video frames were analysed through several steps. To reduce the white noise, low pass filter was used for each frame. After images were smoothed, centroid points were determined by computing the local maximum for each cell. Positions were assigned for a given frame. After each frame was analysed, the Euclidian distance between centroids were computed to associate each cell between frames and register their positions. A list of coordinates for each cell was prepared to compute the cell motility parameters. Persistence ratio was analysed by computing the ratio of direct distance (D) to total distance (T). The turning angle of cell centroids between the consecutive two were computed to demonstrate the directional changes (angular displacement).

2.9 Xcellegance RTCA migration analysis for PCDH7 knockout in HeLa S3

160 µl of 10% FBS containing DMEM was added to the bottom chamber, and top chamber containing 50 ul of 1% FBS DMEM was inserted. After one hour of incubation, background measurement was performed in Xcellegance machine. 30,000 cells per cell line were plated on the top chamber in 100 µl of medium and let set for 1 hour for the cells to attach to the surface of top plate. Plates were inserted into Xcellegance for reading. RTCA migration study was performed for 48 hours. 16 well, cell invasion and migration (CIM) plates were used for this experiment. Experiment was performed at Dr. Ozgur Sahin's lab in Bilkent University, and handling of cells was assisted by Cansu U. Kagiali.

2.10 SILAC based Proteomics analysis for PCDH7 knockout in Hela S3

SILAC labeling

HeLa S3 non-targeting guide treated cells and knockout colonies 7-1-2 and 7-5-2 were used for SILAC study. Cells were grown in DMEM without arginine and lysine and dialyzed FBS either in light (12C, 14N) isotope containing lysine and arginine amino acids (for knockout cells) or heavy (13C, 15N) isotope containing lysine and arginine (for non-targeting cells). Lysine was used at 0.146 and arginine at 0.08 g/liter. Metabolic interconversion of amino-acids is a common phenomenon during amino-acid biosynthesis pathways where certain amino-acids play as precursors for others. Arginine is a metabolic precursor of proline. For SILAC experiment, this turns out to be a drawback as peptides containing labelled proline in addition to labelled arginine and lysine give mis-estimated shifts in peptide quantification [67]. A further addition of proline at 200 mg/liter in SILAC media was added to prevent this interconversion as previously reported [68]. Cells were grown in respective heavy and light media for eleven passages to label total proteome. Cells were collected with equal amounts, two culture plates of 150 mm diameter each.

In-solution digest of cell proteome

After removing culture media, cells were washed with PBS once at 37 ^{o}C. Ice cold PBS was added and cells were collected through scrapping and centrifuging at 1200 rpm for 10 min at 4 ^{o}C. Cell pellets were snap frozen at liquid nitrogen. Pellets were lysed (lysis buffer: 50 mM Ammonium Bicarbonate (pH 8.0), 8 M Urea) in the presence of EDTA free protease inhibitors (Pierce # 88666) and phosStop cocktail of phosphatase inhibitors and 1 mM sodium orthovanadate. Concentrations were

measured using BCA method. Equal amounts of samples were mixed as: non-targeting control + knockout 7-1-2 and non-targeting + knockout 7-5-2. DTT added for reduction at 56^{o}C for 45 min. 20 mM IAA added for alkylation, 30 min in dark. Solutions were diluted to 4M urea using 50 mM Ammonium Bicarbonate (1:1 dilution). Lys-C protease was added for 4 hours. Solutions were diluted to 1M urea with 50 mM ammonium bicarbonate and trypsin was added overnight at 37^{o}C. After overnight proteolysis, solutions were acidified using 10% formic acid until it reaches pH 2. For desalting and purification, SepPack column cartridges were employed as column purification. Final eluent was distributed volume wise into 1 mg fractions. Samples were dried in speed vacuum and stored at -20 ^{o}C.

Iso-Electric Focusing (IEF) fractionation of peptides

10 ml of 0.2% IPG buffer (Agilent) pH3-10 was prepared. Tray was cleaned with compressed air to remove dust particles. Gel strip was removed from foil and arranged in the fractionation tray. We added 20 ul of IPG buffer in all 24 slots. Two soaked filter papers were arranged on the side of the tray. Clean lid was placed on the strip and gel was allowed to rehydrate for 1 hour. We added 3.6 ml of 0.2% IPG buffer was added to dehydrated peptides. And samples sonicated for 5 minutes. 150 ul of sample was added to each well and wells were tightly covered with lid. Mineral oil was added at both ends of the strip. Program used for fractionation OG23PE00 Program F8. Samples were left for fractionation for 14 hours. Individual fractions were collected and 200 µl of 0.1% TFA was added to each slot and samples recombined into respective fractions. Samples were processed for desalting using stage tipping. Desalted samples were resuspended and injected for LC-MS/MS analysis.

Statistical analysis

Results from LC-MS/MS were analyzed using MaxQuant analysis package (Max Planck Institute of Biochemistry). Knockouts 7-1-2 and 7-5-2 were taken as biological replicates 1 and 2. Biological replicates 1 and 2 were normalized according to their median values. Each protein ratio is divided by the replicate median and converted to log2 to center median H/L ratios around log2(0). Distribution of protein ratios is normal for both replicates; therefore, we calculated median absolute deviation (MAD) of the normalized ratios by multiplying the median deviation by a correction factor of 1.4826. Deviations of the ratios from the MAD are calculated and 1.645 is used as a cutoff for determining up and down-regulated proteins. 1.645 MAD cutoff corresponds to ratios lower than the 5% quartile and higher than 95% quartile of the distribution. For gene ontology analysis, biological replicates were combined via Maxquant and up and down-regulated proteins GO enrichments were calculated via Enrichr [69,70]. P-value cutoff is set to 0.05.

2.11 *In-vivo* assessment of PCDH7s role in migration

In-utero Electroporation

This part of the project was performed in collaboration with Cansu Akkaya from our research group. Pregnant mice at E14 were anesthetized with isoflurane inside the chamber and were given Bavet-Meloxicam painkillers subcutaneously. Mouse was placed on heating pad throughout the whole procedure. Fur was removed by applying depilatory lotion on the belly and a parafilm with an orifice was placed on top. Using a scalpel, an incision was made to expose uterus which was gently pulled out using ring forceps. Uterus was hydrated periodically using warm ringer solution. Plasmid sets were mixed with pCAGGS_IRES_GFP and fast green. 1 µl of plasmid mixes were injected into the third ventricles as visible through translucent uterine wall. The sequence targeted by shRNA D for PCDH7 is conserved between mouse and human.

That is why we used shRNA D for PCDH7 knockdown. PCDH7b-eGFP-N1 plasmid with modified sequence that is resistant to shRNA D was used in parallel for recovery of the phenotype. Left ventricle was electroporated with settings 0.5 pulses, 30 V, 400 ms intervals. Embryos were reinserted into the mother. Peritoneal membrane was sutured using sterile needle and staple sutures were applied on the skin. Animals were kept under observation for recovery. Three days after electroporation, cortical radial sections of embryonic brains were prepared using cryostat. Sections were stained with anti-turboGFP antibody to look for the pattern of the migration. Radial sections from ventricular layer to cortical planes were divided into 10 equal rectangular sectors and number of GFP positive cells were manually counted within each sector.

2.12 Immunofluorescence

Cells were grown on cover slips overnight in diluted confluency to provide enough room for cells to polarize. After overnight incubation, cells were washed twice with HBSS (not PBS but HBSS contains Ca2+ and Mg2+ ions to stabilize cadherin structures and preserve its physiological location). HBSS was kept warm and was taken out of water bath just prior to use. This was done to prevent a temperature shock to cells. Cells were fixed with 3% paraformaldehyde solution (diluted from 16% stock, using HBSS). 3% PFA vial was also kept in water bath to prevent temperature shock to cells. Samples were left at 37^{o}C for 10 minutes. Post fixation coverslips were washed with PBS – 3 times with 5 minutes interval to remove residual paraformaldehyde. Cells were permeabilized using 0.1% Triton-X in PBS for 5 minutes at 4^{o}C. Detergent containing solution was removed and samples were washed 3 times with PBS. Cells were blocked with 2% BSA in PBS for 30 minutes. All antibodies dilutions were made using 2% BSA in PBS. Washes after primary and secondary antibody incubations were performed using PBS (3 washes at 5min, 10 min and 5 min interval). Coverslips were mounted with Mowiol medium and sealed with transparent nail polish reagents.

2.13 Western Blotting for PCDH7

PCDH7 is a high molecular weight protein which is expressed at a low physiological concentration. An optimized protocol for immunoblotting of PCDH7 included the following steps. Step1. Cell lysis in NP-40 containing lysis buffer which is prepared as follows: 50 mM Tris-HCl, pH-7.4, 250 mM NaCl, 5 mM EDTA, 50 mM NaF, 1 mM Na_3VO_4, 1% NP-40 substitute, 0.02% NaN_3. For ideal lysate extraction, lysis buffer was supplemented with protease inhibitors and cell pellets were resuspended and incubated at ice for 30 min. At every 10 minutes interval lysates were vortexed. Lysates were centrifuged at 13,000 rpm for 5-10 minutes, supernatants were collected and quantified for protein concentration. Generally, BCA method was employed and occasionally Bradford was used. BCA method is not compatible if lysates were supplemented with DTT as DTT reacts with BCA reagent and generates a colored product.

Usually, 50 µg of total lysates were used for loading onto 8% Acrylamide separating gels. PCDH7 has 2 prominent bands corresponding to isoform a and b (~ 116 KDa) and isoform c and d (~135 KDa). Owing to low expression of PCDH7, the only protocol that is useful for transfer is wet transfer with 45V overnight at cold room. Blocking of nitrocellulose membranes were done with 4% non-fat milk for 1 hour. Abcam antibody for PCDH7 (ab139274) at 1:200 concentration with an overnight incubation at 4^{o}C. An HRP labeled secondary antibody concentration of 1:2000 was used. For loading internal control, tubulin is an ideal candidate. For the development of PCDH7 chemiluminescence, ECL – plus (Pierce #32132) or BioRad Clarity western ECL substrate (#1705060) are preferable.

Table 2-2 List of antibodies for Immunofluorescence (IF) and Immunoblotting (IB)

	Reagent	**Source**	**Dilution**
1.	GFP Antibody (IF)	Hyman lab	15,000
2.	Myosin IIb Antibody (IF)	CST (D8H8) XP(R)	1,000
3.	Phalloidin (IF)	Abcam ab176756	1:1000
4.	Anti-rabbit IgG Alexa 555 Fab2	4413S	1:1000
5.	Anti-Goat IgG H&L (Alexa 488)	ab150129	1:1000
6.	PCDH7 (IB)	Abcam ab139274	1:200
7.	α-Tubulin (IB)	CST (DM1A)	1:1000
8.	GAPDH (IB)	CST (14C10)	1:5000

9.	Anti-mouse IgG HRP	CST (70765)	1:2000
10.	Anti-Rabbit IgG HRP	CST (7074S)	1:2000

Chapter 3

Results and Discussion – Part I

Cell Migration Phenotype Assessment

3.1 Overview

Our initial hypothesis was that PCDH7 mediates cell migration and invasion in mammalian cells. Many members of cadherin superfamily has been reported as controlling actors in migration and metastasis. Most notable of these are E-cadherin and N-cadherin which display antagonistic role in metastasis. Metastatic cells lose E-cadherin expression and acquire high N-cadherin expression as they undergo transformation. Some members of protocadherin subfamily have been reported to mediate/control cell migration. Fat protocadherins mediate cell migration through interaction with actin cytoskeleton. Additionally, members of clustered protocadherins, α-PCDH have been shown to control neuronal migration through their interaction with WAVE complex and altering activity of Pyk2, a calcium-dependent adhesion cell-adhesion kinase [71]. To address our hypothesis that PCDH7 plays a role in cell migration, we decided to perturb PCDH7 expression and then perform migration assays. In this chapter we report these experiments and findings.

Choice of mammalian cells for migration

Addressing a migration phenotype requires choice of a cell that is easily polarized, shows distinct front and rear compartments and displays a decent single cell migratory behaviour. RPE cells and its derivative RPE1 cells are immortalized cell lines originally derived from human retinal pigment epithelial cells. Retinal

Pigment Epithelium (RPE) is a layer of neural retina compressed between photoreceptor layer and Bruch's membrane [72]. Inside the tissue, RPE cells are tightly arranged and form a cobblestone-like arrangement of cells. Inside tissue, RPE cells exhibit an 'epitheloid' or polygonal appearance and are polarized with microvilli on the apical surface. Functionally, RPE cells contribute to protecting eyes against photo-oxidative stress through absorption of excess light [73], mediate retinal development regulation [74], VEGF secretion [75], immune response mediation of the organ [76] and removal of old rod and cone cells through phagocytosis [77]. RPE cells, when cultured in low confluency, display remarkable migratory behaviours and distinct front and rear compartments. The advantage of using RPE1 cells over RPE cells is the higher efficiency of chemical transfection. Since RPE/RPE1 cells are immortalized but from a non-cancerous source, we also employed the HelaS3 cancer cell line in our migration experiments, in order to analyse the potential phenotypic changes in the context of cancer as well.

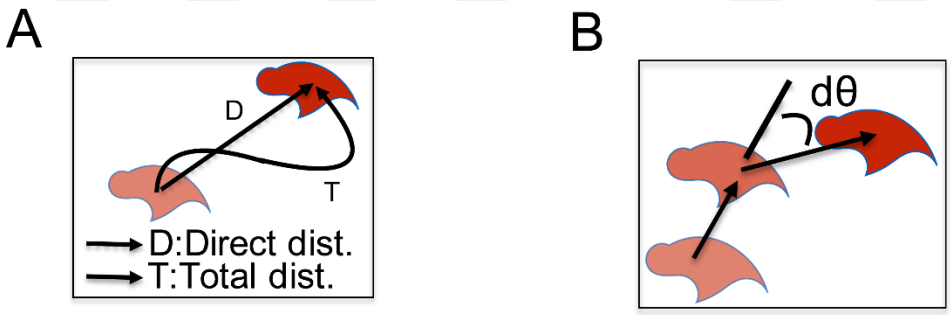

Figure 3-1: Persistence and Angular Displacement: Representation of persistence evaluation as a ratio of direct (Euclidean) distance (D) and total cumulative distance (T). B) A measure of angular displacement during cell migration

3.2 shRNA mediated knockdown of PCDH7 in RPE cells

To investigate the effect of PCDH7 on random migration of single cells, we used RPE cells for stable expression of shRNA (lentiviral-mediated)) targeting human PCDH7 (shRNA C, shRNA D, and shRNA H) as well as a non-silencing shRNA (shRNA NS) with no potential mammalian target (figure 3-2). Immunoblotting results indicate reduced expression of PCDH7 in all three cell lines targeting PCDH7 as compared to non-silencing and control cells. Among these, shRNA H showed the best reduction in expression. The reduction of PCDH7 expression with shRNAC and shRNAD were quite comparable with each other. For further experiments, we chose shRNAD and shRNAH for phenotype assessment.

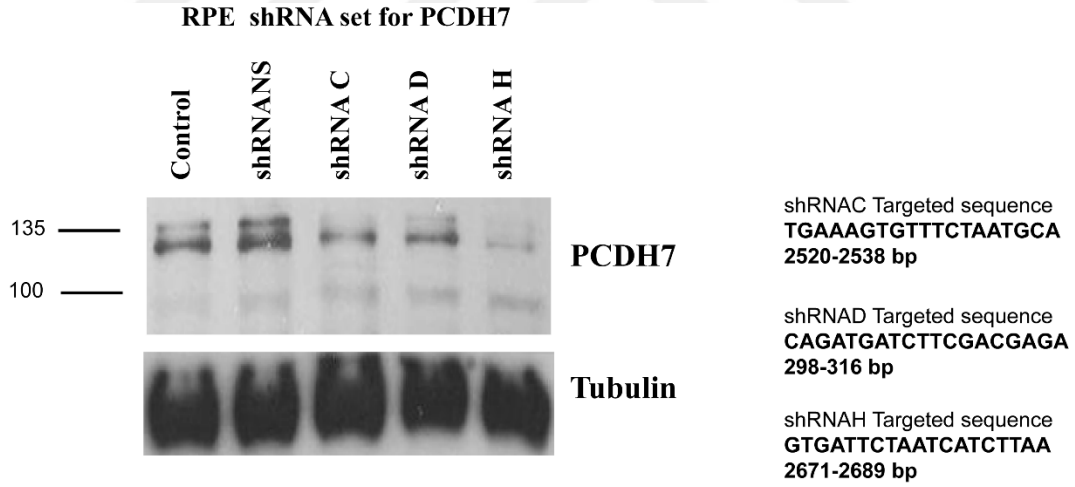

Figure 3-2: **RNAi mediated PCDH7 knockdown in RPE**: Targeted sequences are highlighted on the right.

Migration data

To test the effect of PCDH7 expression on RPE cells, we performed single cell tracking of randomly migrating cells. Time lapse fluorescence live imaging was performed to track the behaviour of cells. Using a custom-built code in MATLAB, we analysed cells migration behaviour and quantified migration parameters. Total distance is the measurement of the distance covered by the cell over the period of imaging.

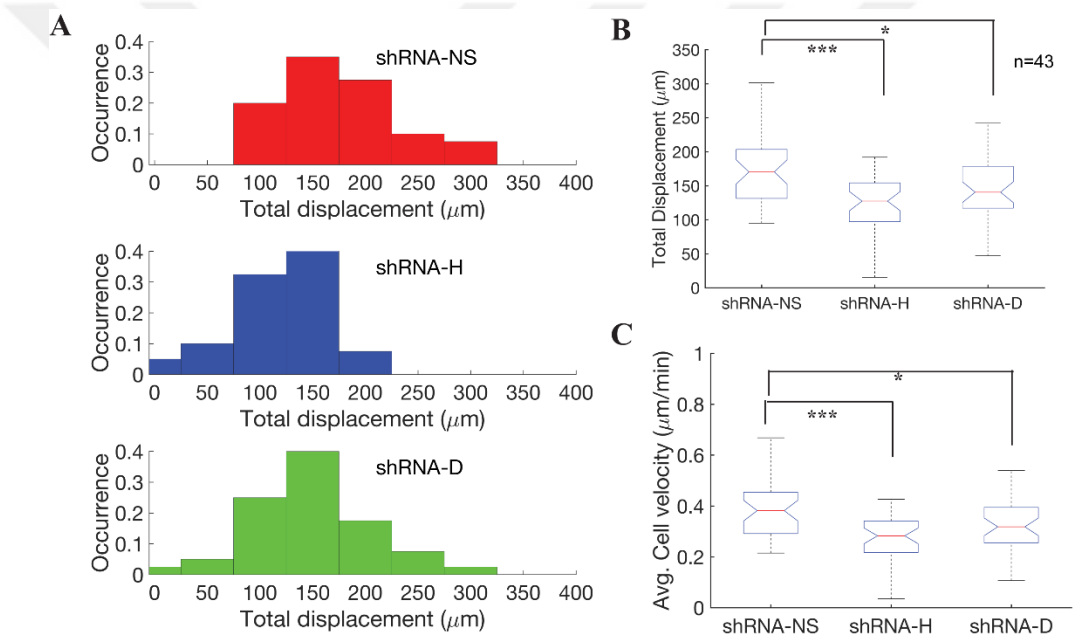

Figure 3-3: Migration phenotype with shRNA in RPE cell: migration upon PCDH7 knockdown. A) and B) Total distance travelled and C) average velocity by RPE cells upon treatment with shRNA

Direct distance is the measurement of Euclidean distance between the initial and final position of the cell over the period of imaging (Figure 3-1). Persistence of migration is the exhibition of directional migration once a cell senses the chemo-attractive cues in its vicinity. Within an observation period, a cell can migrate in a persistent fashion with similar Euclidean (direct distance, D) and actual trajectories (total distance, T) or can exhibit different migratory behaviour where Euclidean trajectories and actual cumulative distance trajectories exhibit a spectrum of variation (Figure 3-1 A). A ratio of D, direct distance and total distance T is a measure of persistence. Similar Euclidean and actual trajectories indicate high persistence whereas different Euclidean and actual trajectories can be interpreted as showing low persistence. We also measured angular displacement of cells. Angular displacement is defined as the angular shift between presumed persistent trajectory and the actual trajectory of the cell (figure 3-1 B). A cell having higher persistence will exhibit prevalence of low angular changes (e.g. 0-15 degree shifts), whereas a cell having low persistence will exhibit a prevalence of higher angular shifts.

Analysing single cell migration pattern of non-silencing shRNA and PCDH7 targeting shRNA D and shRNA H showed different trajectory patterns. Trajectories' length in shRNA D and shRNA H appeared remarkably shorter than the shRNA NS treated cells. Indeed, total distance covered was significantly different between shRNA NS treated cells and shRNA D and shRNA H treated cells (figure 3A and 3B). As a result, velocity of cells was also different, shRNA D and shRNA H treated cells were significantly slower than shRNA NS (figure 3C). A measure of persistence of migration revealed that the shRNA D and shRNA H treated cells were significantly different from the control samples (figure 3-4 (A) and (B)).

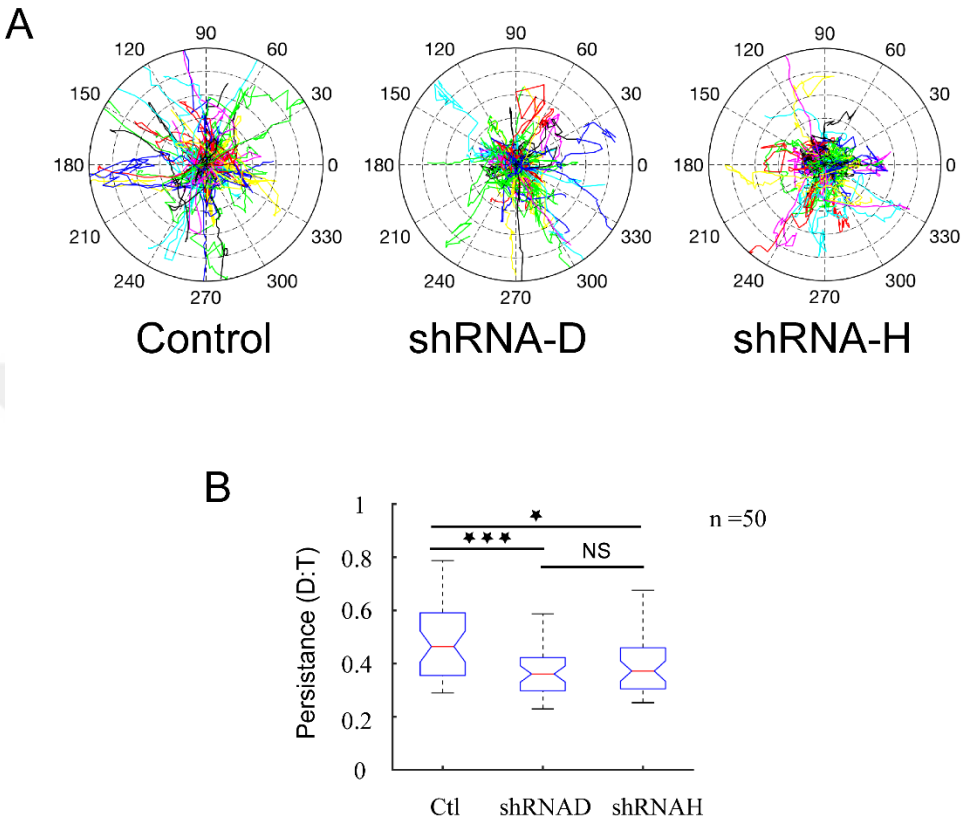

Figure 3-4: Persistence assessment upon shRNA treatment: Rose plots for measurement of persistence upon shRNA mediated downregulation of PCDH7. Each colour represent a separate cell. B) Box plots for persistence calculation.

3.3 RPE1 CRISPR knockout

Generation of PCDH7 knockout in RPE1 cells

We prepared RPE1 knockout cells to study the effect of PCDH7 on cell migration. Although PCDH7 is downregulated in shRNA cell lines, it may well be that a small remaining expression of PCDH7 could mask an otherwise more prominent phenotype. Our results showed a few promising colonies from both 7-1 and 7-2 sets as screened using immunoblotting (figure 3-5A); 7-2-6 and 7-2-11 were the most promising as their immunoblotting results showed the cleanest washout of PCDH7 expression. For recovery experiment, we also prepared stable cells expressing PCDH7isoform b and isoform c (figure 3-5 B).

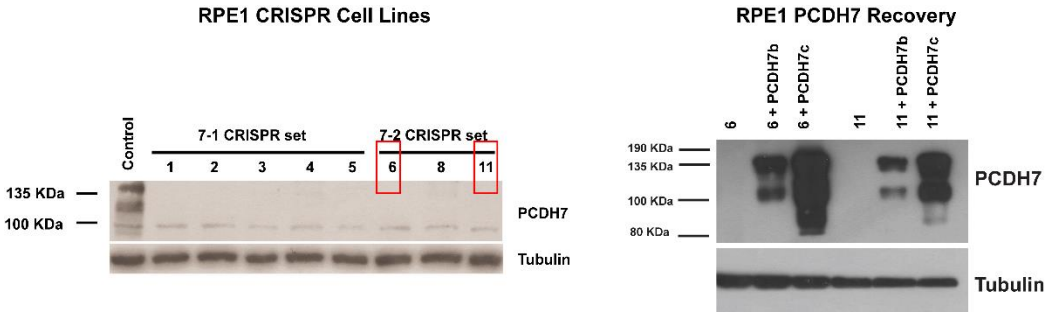

Figure 3-5: RPE1 CRISPR cells and Recovery cell generation :A) RPE 1 CRISPR mediated knockouts. 7-2 colony 6 and 11 were carried for phenotype assessment. B) PCDH7 isoform b and isoform c expression in 7-2 colony 6 and colony 11 for recovery experiment.

Live cell imaging for migratory phenotype assessment

NT1 cells, knockout colonies and expression recovered cell lines were all infected with lentiviral particles carrying GFP cassette. Cells were plated in a non-coated 12-well cell culture plate. Cells were plated at a low confluency (equal number among sets, i.e. 6000 cells per well belonging to specific cell line). The following sets were included in the experiment: **a)** NT, **b)** Knockout 7-2-6 (referred to as 6 henceforth), **c)** knockout 6 expressing PCDH7 isoform b, **d)** knockout 6 expressing PCDH7 isoform c, **e)** Knockout 7-2-11 (referred to as 11 henceforth), **f)** knockout 11 expressing PCDH7 isoform b, **g)** knockout 11 expressing PCDH7 isoform c.

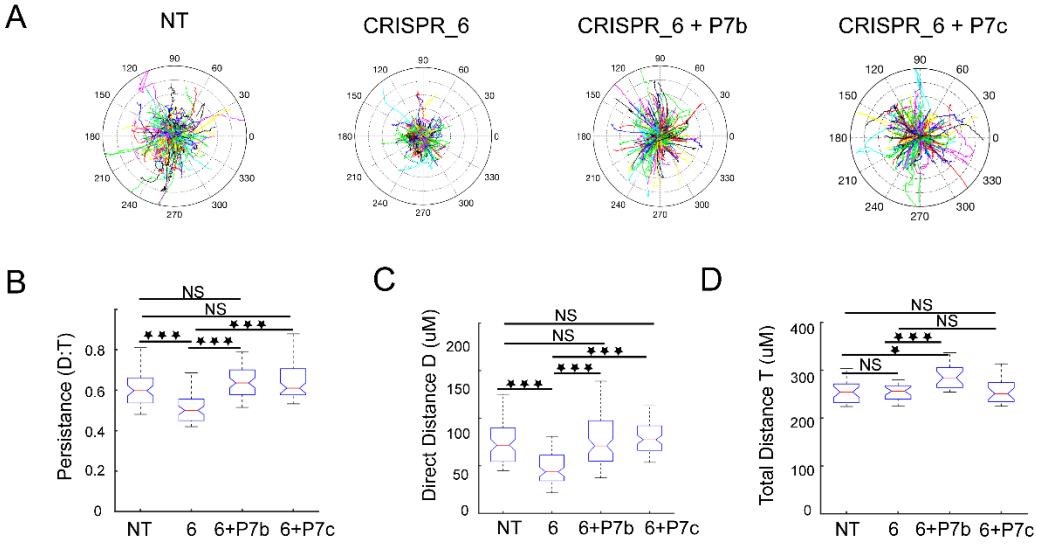

Figure 3-6: Phenotype of RPE1 PCDH7 knockout cells-I. A) Rose plots for persistence measurement of NT, colony 6 and recovery cells. B) box plot for persistence loss and recovery for knockout colony 6. C) Direct distance and D) total distance covered.

Time lapse imaging using FITC channel in live imaging system (Olympus Xcellence Pro) was performed. Individual frames were collected after every 10 minutes using 10X objective. Cells were tracked using MATLAB based custom code. CRISPR knockout cells showed a different pattern of migration trajectories compared with non-targeting cells. Knockout cells showed a reduced persistence in migration and altered their direction frequently as compared to non-targeting control cells which were more persistent in their migration. Rose plots for trajectories outlines the density of trajectories for most cells within first radial sector in knockout cells, whereas in non-targeting cells, these trajectories extend well beyond first sector, many reaching third sector and, in some cases, even boundary of fourth sector (Figure 3-6 (A) and 3-7(A)). Compared to knockout cells, the expression recovered knockout cells shows a recovered persistence in trajectories. Reduction in the persistence of knockout cells in both knockout 6 and 11 was highly significant, (Figure 3-6(B) and 7 (B)). Recovered persistence for both isoform B and isoform C were significantly more than knockout cells. This recovery attributes the facilitation of migration to PCDH7. Both isoforms seem sufficient for recovering the phenotype, which indicates that differences in cytosolic sequences have no significant impact on PCDH7's role in cell migration. An analysis of direct distance as measured by Euclidean length shows significant reduction upon knockout of PCDH7 in both knockout 6 and knockout 11. Direct distance covered improves significantly for both isoforms b and isoforms c.

Although total distance traveled by cells indicate no significant difference between NT and knockout cells (Figure 3-6D), there is a higher 'to and fro' flickering movement in knockout cells. This flickering reflects a disability of knockout cells to persistently migrate in a specific direction. Since our MATLAB code looks for displacement of the centre of fluorescence as a read

for distance covered, a struggle for cells to move is displayed as a frequent shift of cells' centre albeit within a few pixels.

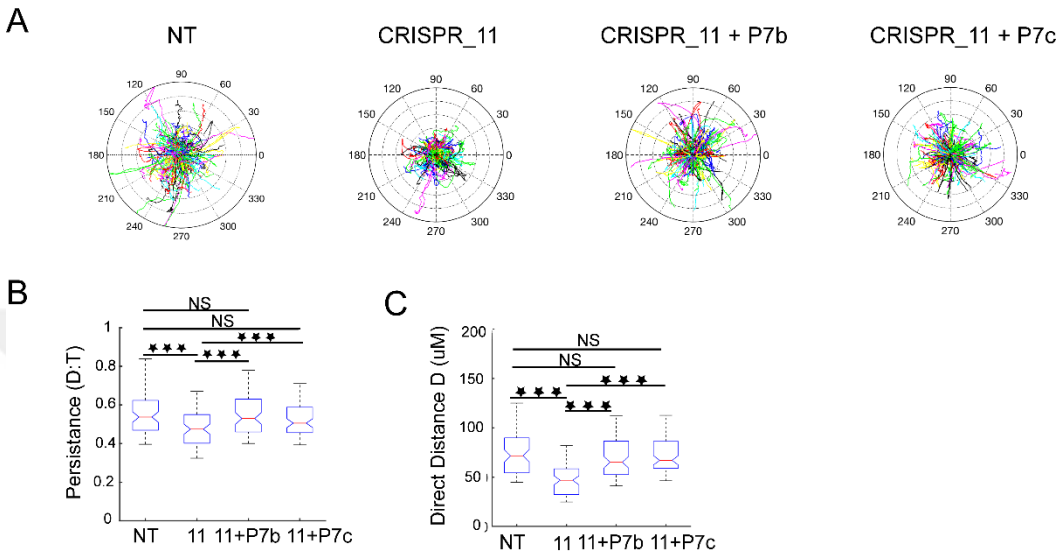

Figure 3-7: Phenotype of RPE1 PCDH7 knockout cells-II. A) Rose plots for persistence measurement. B) box plot for persistence loss and recovery for knockout colony 11. C) Direct distance covered with knockout colony 11 and with recovery

For physiological directional migration and invasion; however, the Euclidian distance, or direct distance covered is more physiologically relevant than the total distance covered (figure 3-6 (C) and 3-7(C)). A closer comparison of recovered trajectories with NT trajectories indicates an improved straightforward directionality, as compared to slightly wavy but still persistently directional trajectories of NT (figure 3-8A). We further analysed the angular displacement of cells which is a measure of cellular directional changes from frame to frame (figure 3-1B). Our analysis shows that there is a significant difference in the angular displacement between NT cells and knockout cells in the lower angle changes (0-15 degree changes) (figure 3-8 B). More proportion

of NT and expression recovery cells showed low angle changes compared to knockout cells.

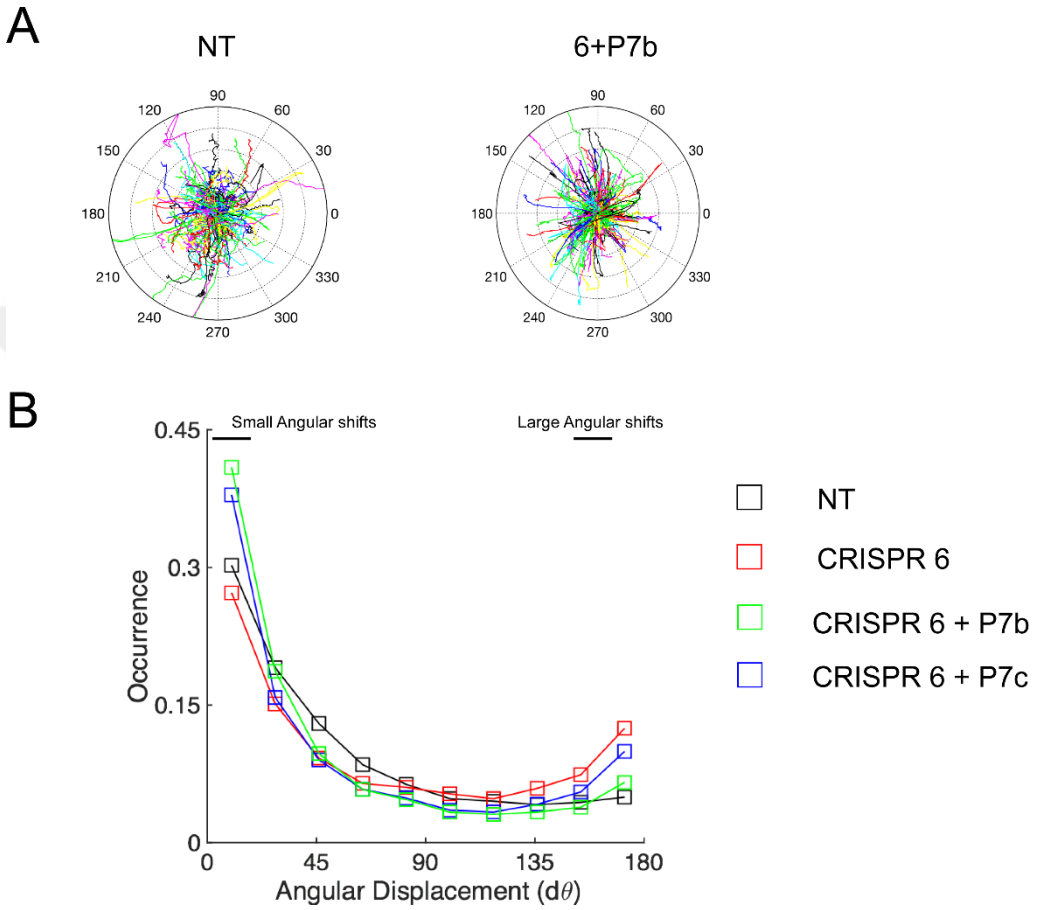

Figure 3-8: RPE1 Angular Displacement: A) Trajectories of NT and recovery expression cells. B) Angular displacement plots

Low angle changes are also occurring more in recovery cells as compared to knockout cells. This explains the observed improvement in straight trajectories of recovered cells compared to slightly wavy trajectories of NT cells (figure 3-8(A)). Of note, NT cells express PCDH7 at physiological concentration whereas in recovered cells,

PCDH7 is overexpressed, above physiological concentration. Quantitative analysis indicates a significant difference in low angle (0-15-degree angular changes), among the groups.

3.4. Real Time Cell Migration of HelaS3 cells

We prepared PCDH7 knockouts in Hela S3 cells (figure 3-9 (A)). We used two of our single cell clones 7-1-2 and 7-5-2 for phenotype assessment in a directed migration assay using RTCA Xcellegence system with an electronically integrated Boyden chamber.

A.

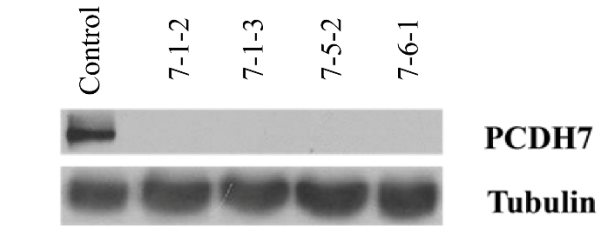

B.

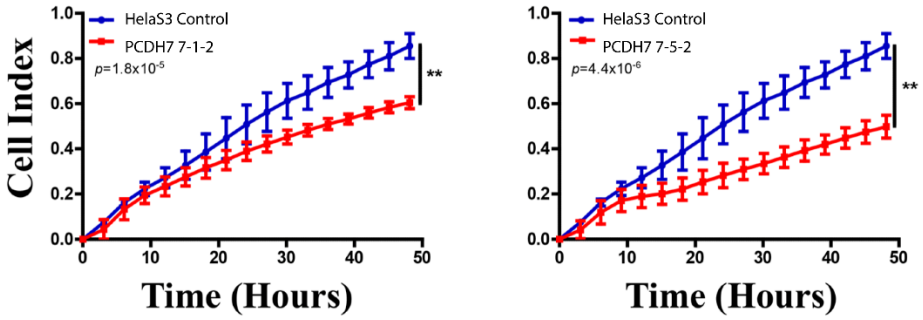

Figure 3-9: RTCA/Xcellegence directed migration for PCDH7 knockout in Hela S3: assessment for HelaS3 knockout colonies. A) HelaS3 knockout cell lines. B) RTCA directed migration

We compared 2 different monoclonal populations (7- 2 and 7-5-2) with control HelaS3 cells. Both cell lines show a significant reduction in cell migration upon depletion (Figure 3-9(B)).

3.5 *In-utero* electroporation.

In-utero electroporation of embryonic lateral ventricle has been used extensively to study mammalian neuronal development including neuronal migration [78-80]. This technique can be used to label developing neurons with fluorescent proteins and to study the roles of specific genes through modulation of expression. The technique employs injection of the plasmid into lateral ventricle and giving cortex electrical impulses which cause the neuronal progenitor cells at the ventricular wall to get electroporated. This electroporation is facilitated through the transient opening of electropores within the membranes of neuronal progenitor cells. These cells would subsequently give rise to neurons which undergo radial migration to specific cortical layers. An altered expression can impart loss-of-function (shRNA, or siRNA) or a gain-of-function (overexpression) to neuronal progenitors. Few days after electroporation, these embryos are surgically removed, fixed with formaldehyde, radially sectioned using cryostat and immunostained to evaluate the phenotype.

in-utero electroporation for PCDH7 phenotype assessment

Our results indicate that shRNA NS electroporated cells are distributed within all 10 sectors, including upper cortical layers. shRNA D electroporated cells, however, were more populated within lower sectors. Remarkably, in the recovery electroporated embryo, most of the GFP expressing cells migrated to the upper cortical layers and were included within the upper sectors. Recovery plasmid overexpresses PCDH7 above physiological levels which may have resulted in enhanced cortical migration (figure 3-10 and 3-11 (A)). Radial cortical migration from ventricular layer to the cortical plane requires persistent directional migration. Treatment with shRNA D affects reduction in directed migration

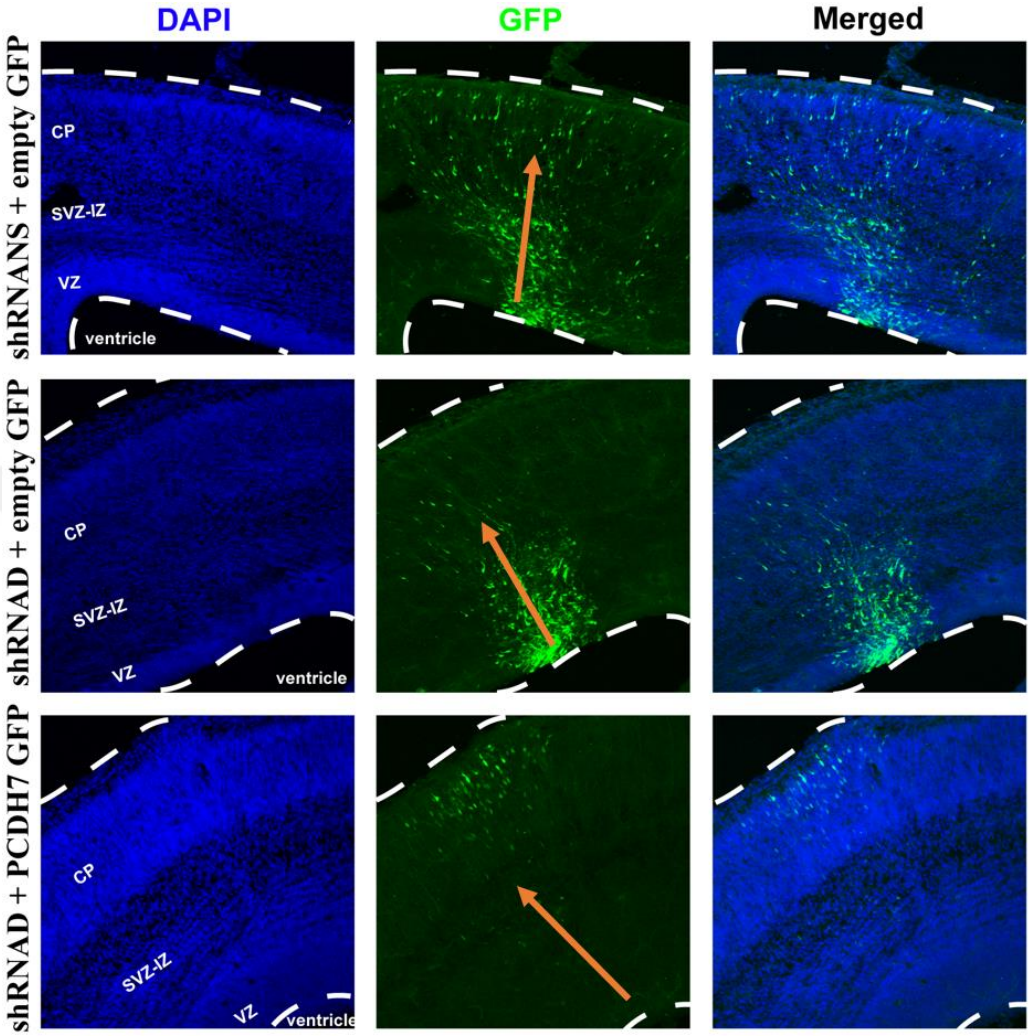

Figure 3-10: *In-utero* electroporation Immunofluorescence: Radial sections embryonic brains immunostained for turboGFP to display the distribution of electroporated cells.

resulting in accumulation of electroporated cells close to ventricular layer than the cortical plane. An enhanced migration with rescue is a result of overexpression of PCDH7b-GFP in neuronal progenitors resulting in enhanced directional

migration. We checked developmental changes expression of PCDH7 in mouse cortex. We dissected cortices at E14, P0, P08, P15 and P30. Immunoblot shows that E14 has very low expression of PCDH7 (Figure 11C). There is a strong expression difference between E14 and P0. P08 onwards PCDH7's expression doesn't change much. Comparing this expression profile with in-utero electroporation study, it seems overexpression at E14 caused a hypermobility of progenitors towards cortical plane. Owing to low expression at E14, these progenitors would traverse their pathway at physiologically relevant velocity. Overexpression of PCDH7 as we expect in recovery experiment, may have made these cells more motile, during radial migration to cortical plane.

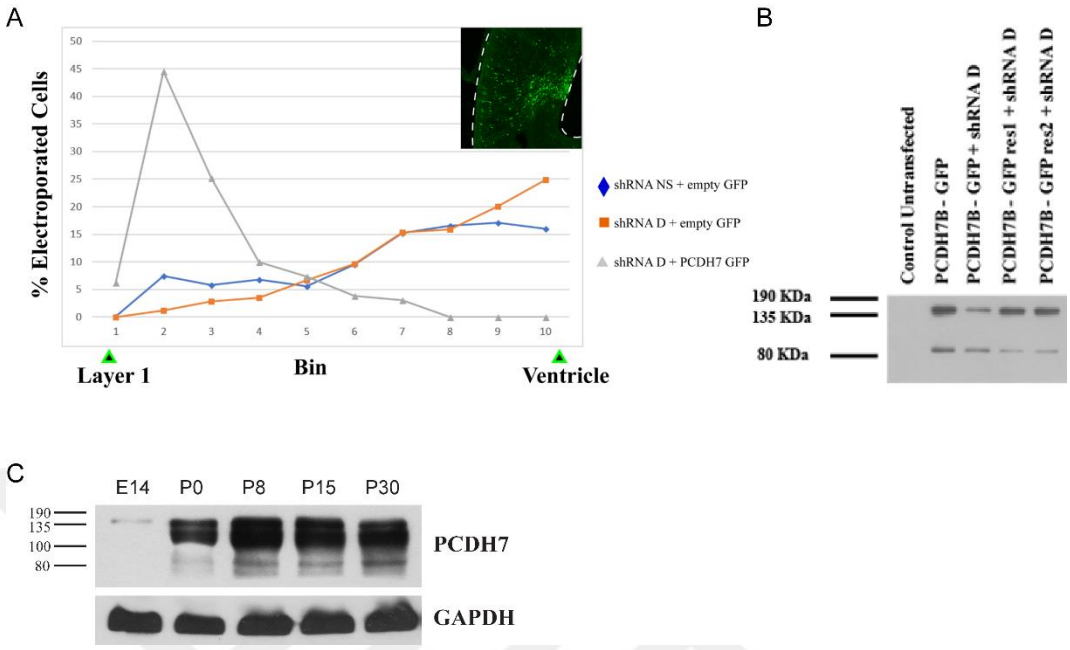

Figure 3-11: A) Line graph for number of electroporated cells in in-utero electroporation. B) GFP immunoblot for PCDH7b-GFP along with shRNA resistant plasmids. C) Immunoblot for cortical PCHD7 expression at different developmental stages. E-Embryonic, P-postnatal

3.6 Conclusion

We performed phenotype assessment for the role of PCDH7 in mammalian cells. Perturbation of PCDH7 expression in RPE and RPE1 cells using shRNA and CRISPR/Cas9 mediated knockout altered migration ability of cells. Upon downregulation of PCDH7 using RNAi, cells show reduced migration, with affected total distance travelled. Upon knockout of PCDH7, RPE1 cells exhibit remarkable loss of persistence and reduced direct/Euclidean distance. This altered migration property was recovered upon addback of PCDH7. Even more remarkable was the observation that overexpression of PCDH7 enhanced cell's persistence. Knockout of PCDH7 in Hela S3 cells significantly reduced their directional migration. This result was consistent with our observation of migration phenotype in RPE1 cells. We performed

in-utero electroporation to explore contribution of PCDH7 in neuronal migration during embryonic development. Our preliminary results indicate a reduction in neuronal migration. Surprisingly, an overexpression of PCDH7 in neurons during recovery remarkably increased the migration of neuronal progenitors towards cortical plane. Although PCDH7 is highly expressed in neurons, E14 cortex showed very low expression, compared to P0 and higher times. An overexpression of PCDH7 may have imparted better mobility profiles to neuronal progenitors.

Chapter 4

Results and Discussion – Part II

Subcellular localization of Protocadherin-7

4.1 Overview

PCDH7 is a transmembrane protein, with a large extracellular part having seven cadherin domains and a short cytoplasmic domain. Its enrichment on cell membrane depends on cell cycle temporal window. It enriches on membrane during mitosis, and most of its reserves lies in ER during interphase [21]. It is likely that PCDH7 is channelled from ER to plasma membrane during mitosis. Its enrichment on cell membrane during mitosis implies its role in cell division. During mitosis, a cell acquires spherical shape with minimal attachments to the extracellular matrix, whereas, during interphase, a migrating cell acquires planar polarity with more cell-ECM adhesions. To play a role on the cell surface during cell migration, it is the interphasic pool that is more critical, as cells migrate during interphase and not during mitosis.

Our hypothesis that PCDH7 mediates cell migration is proven valid as evidenced in chapter 3 from assessing PCDH7 perturbation phenotype. Polarised cells in persistent migration require a decisive push in the forward direction in coordination with the rearward retraction. There are intermediate steps involving focal adhesion turnover, nuclear translocation and extracellular matrix remodelling. A disturbance or alteration in these subcellular compartments, or a mis-coordination in the whole process may result in the migration phenotype. We intended to study the subcellular localization of PCDH7. A possible polarized localization or an association with a sub-compartment involved in cell migration may point at PCDH7's molecular role in cell migration. Cell

migration involves coordinated cell shape alterations, which is mediated by adaptive dynamics of cytoskeleton, chiefly actin cytoskeleton. It was incumbent to explore association of PCDH7 with cytoskeleton, polarized distribution. We explored PCDH7's subcellular localization in fixed samples in RPE cells. We studied PCDH7's localization dynamics using confocal live imaging in a migrating cell. We also performed perturbation experiments to see changes in PCDH7's localization. We employed STED based super-resolution microscopy for finer details of PCDH7's localization.

4.2 PCDH7 localization - confocal imaging

Our interest lies in PCDH7's subcellular localization in a migrating cell. Like many other members of cadherin superfamily, PCDH7 is enriched at cell-cell interaction foci. For exploring PCDH7's subcellular localization, we prepared RPE1 stable cell lines expressing PCDH7-GFP fusion proteins (separate cell lines for Isoform b and c). Our results show PCDH7 enrichment on cell front in polarized RPE1 cells. (Figure 4-1). We observed a faint presence of PCDH7 on lateral sides and another prominent enrichment on cell rear. It is not unusual for a membrane protein with a role in cell migration to show polarization with differential enrichment on cell front and cell rear. Its presence on cell front seemed to highlight lamellipodia like appearance. Lamellipodia is the assembly of F-actin on cell migration front along with other associated proteins which facilitates cells forced forward migration in the intended direction. A co-staining of PCDH7-GFP with Phalloidin attached to alexa-555 indicated a remarkable colocalization of F-actin and PCDH7-GFP both on cell front and cell rear. Another distant member of protocadherin family, Fat1 has been shown to be located in a polarized manner on cell's leading edge where it coincides with filopodial extensions as well as with F-actin for directed cell motility [43]. Fat1 has direct interactions with Ena/WASP proteins and its cytosolic domain can recruit actin, even when ectopically expressed and directed to mitochondrial outer membrane. Fat1

downregulation affects cell's polarity and motility. Fat1 possesses proline rich EVS1 domains in its cytosolic domain that interacts with Ena/Vasp and recruits actin.

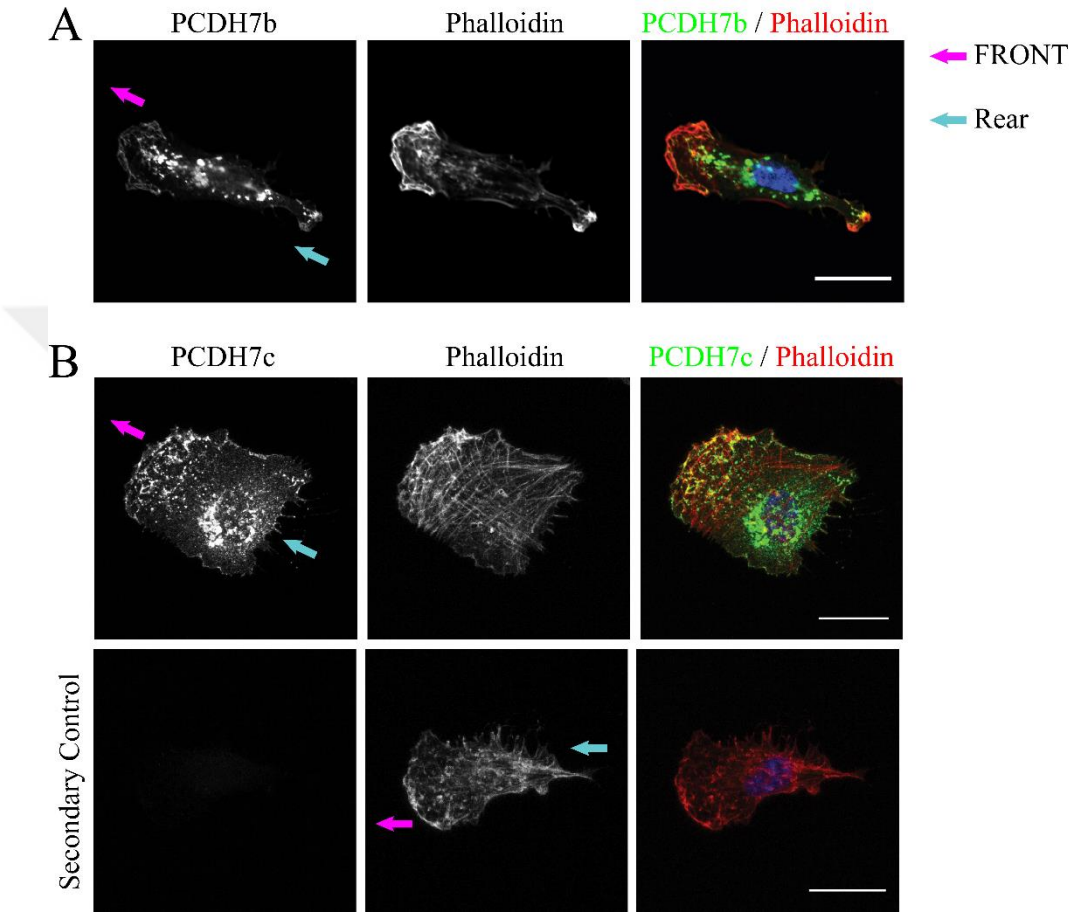

Figure 4-1: RPE1 PCDH7 immunofluorescence: PCDH7 localization in a polarized cell. RPE1 cells expressing PCDH7 isoform b – GFP (A) and Isoform c-GFP. Cells immunostained for GFP expression. Phalloidin-Alexa555 highlights F-actin enrichment.

4.3 PCDH7's correlation with Cortactin

Actin filament is indispensable for cell polarity formation. It focally enriches on the cell front where its assembly is required for the forced extension on cell membrane in the direction of migration. F-actin, co-exists and interacts with several other proteins on cell cortex. Since our initial results showed PCDH7's prominent correlation with F-actin on cell front, it was pertinent to see its correlation with other F-actin interaction proteins on cell front. One of the prominent proteins present on migration cortex is cortactin. Cortactin, as is the name indicates is associated with cortical actin structures. Originally identified as a substrate for Src protein kinase [81], cortactin has been shown to be associated with peripheral actin enriched compartments including lamellipodia and membrane ruffles [82]. Cortactin functions as an actin assembly protein and stabilizes branched actin polymerization through ARP2/3 complex interactions in cellular protrusions like lamellipodia and invadopodia [83,84] . Cortactin also mediates extracellular matrix degrading proteins secretion [85,86]. We prepared stable cell lines expressing cortactin-RFP and PCDH7-GFP. Cortactin and PCDH7 showed a remarkable enrichment and correlation on cell front (figure 4-2). This correlation reinforces our initial result of PCDH7 and F-actin co-existence at the cell cortex. As cortactin plays a critical role in membrane ruffle formation, and lamellipodia, its interaction with another transmembrane protein raises curious questions about functional coordination between PCDH7 and cortactin at these subcellular compartments.

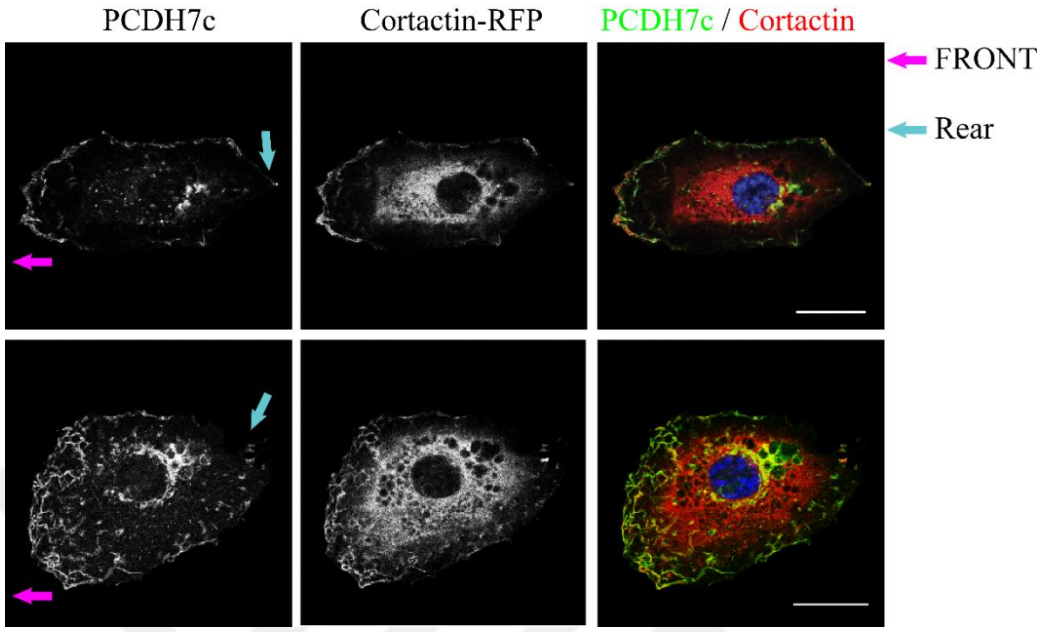

Figure 4-2: PCDH7 and Cortactin: Correlation of PCDH7 and cortical actin interacting protein Cortactin-RFP. Scale bar – 20 µm

4.4 PCDH7 correlation with Myosin IIb

Non-muscle myosin II is an integral part contractile F-actin network in the cell body. Contractile module activity is essential for cell to move in the direction, specified by the protrusive lamellipodial forward push. As PCDH7 is prominently associated with protrusive F-actin network, we were interested in exploring its association with contractile module, and specifically, with NMII. NMII has three isoforms, NMIIA, NMIIB and NMIIC mainly differing in the composing of their heavy chains. Co-staining PCDH7bGFP and PCDH7cGFP with endogenous NMIIB showed a partial colocalization at the cell rear (figure 4-3). This localization seemed to coincide with NMIIB's canonical stress fibres association towards cell rear. This co-localization is interesting for current project. NMIIB mediates retraction of cell rear during the process of cell migration. NMIIB generated pull is central for cell body to move in the

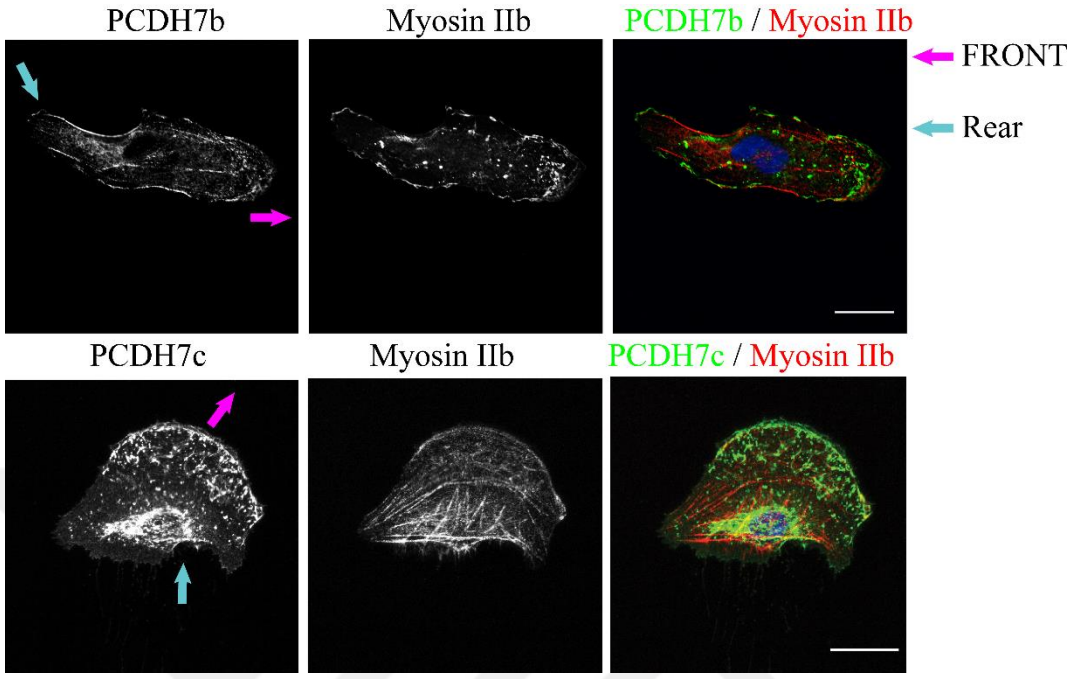

Figure 4-3: **PCDH7 and MyosinIIB**: PCDH7b and PCDH7c correlation with NMIIB. Scale bar – 20 μm

direction of the migration. Correlative presence of a membrane protein like PCDH7 with NMIIB might implicate PCDH7 as a player in rear retraction. During cell migration, cell protrusions are followed by cell body's forward movement and rear edge retraction. Rear edge retraction mechanistically has been attributed to the activity of NMIIB. Rear retraction is a result of acto-myosin mediated contraction. Rear edge membrane compartment also needs a coordinated forward movement. A possible association of PCDH7 with NMIIB may facilitate a co-ordinated forward movement of rear membrane during retraction. As evident from our phenotype assessment, PCDH7 knockout cells lose their persistence during migration. Knockout cells make fewer low angle changes compared to control and expression recovered cells. On a closer look at the time-lapse videos, knockout cells seem to face higher resistance to

retract in the direction the cell intends to move at a given moment. A rear edge retraction inability is a similar phenotype as displayed by NMIIB inhibition/ downregulation.

4.5 Dynamics of subcellular localization of PCDH7 in a migrating cell

Confocal Live Imaging

We observed PCDH7 localization in formaldehyde fixed immunofluorescence experiments where it correlates with F-actin on cell front and on cell. A migrating cell however displays dynamic cytoskeletal assembly. Actin enrichment on cell front, orientation and subsequent retraction of stress fibres, rear edge protrusion and a turnover of focal adhesions are all components of a dynamic migration machinery. Since PCDH7 is required for persistent cell migration (see chapter 3, phenotype assessment of PCDH7) and is associated with F-actin enriched foci and cortactin (figure 4-1 and 4-2), we decided to study dynamics of PCDH7 localization in a migrating cell. To play an important role in cell migration, PCDH7 may also exhibit a dynamic subcellular localization based on momentous decision of cell to alter its position and direction.

We generated a lentiviral construct for PCDH7-eGFP fusion (backbone pLenti CMV GFP Puro (658-5), Addgene 17448). This construct was packaged into lentiviral particles and was used to generate stable cell lines expressing PCDH7-eGFP. Since our preliminary studies showed PCDH7 to be correlated with actin cytoskeleton at cell cortex and stress fibres, we also superinfected PCDH7-eGFP cell lines with lifeact-RFP (a gift from Dr. Michael Way, Francis Crick Institute) for simultaneous imaging

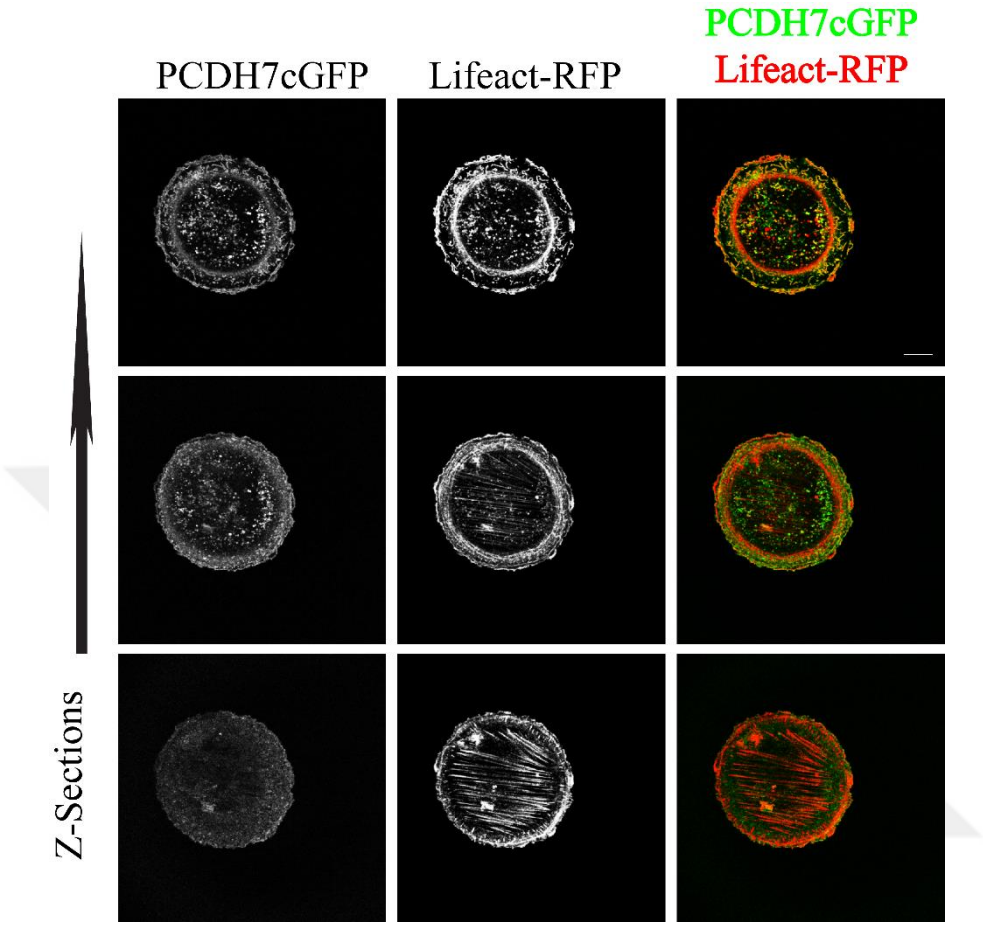

Figure 4-4: **PCDH7 stills from fame 1**: Frame 1 of the confocal live imaging data of PCDH7cGFP and lifeact-RFP. Arrow points in the direction of increasing vertical distance with z-sectioning, lowest panel is closest to the substrate. Scale bar – 20 μM.

of F-actin dynamics. We performed confocal fluorescence time-lapse imaging for PCDH7c-eGFP, and lifeact-RFP in RPE1 cells. In an apparent non-polarized cell, PCDH7 displays a uniform presence on cell surface. (See Video 1). There is an enrichment of PCDH7 on cell membrane and a vesicular enrichment in cell interior. Vesicular signal is most likely PCDH7 residing inside ER during interphase [21]. As cell tries to polarize, PCDH7 signal enriches on cellular migration front. This signal

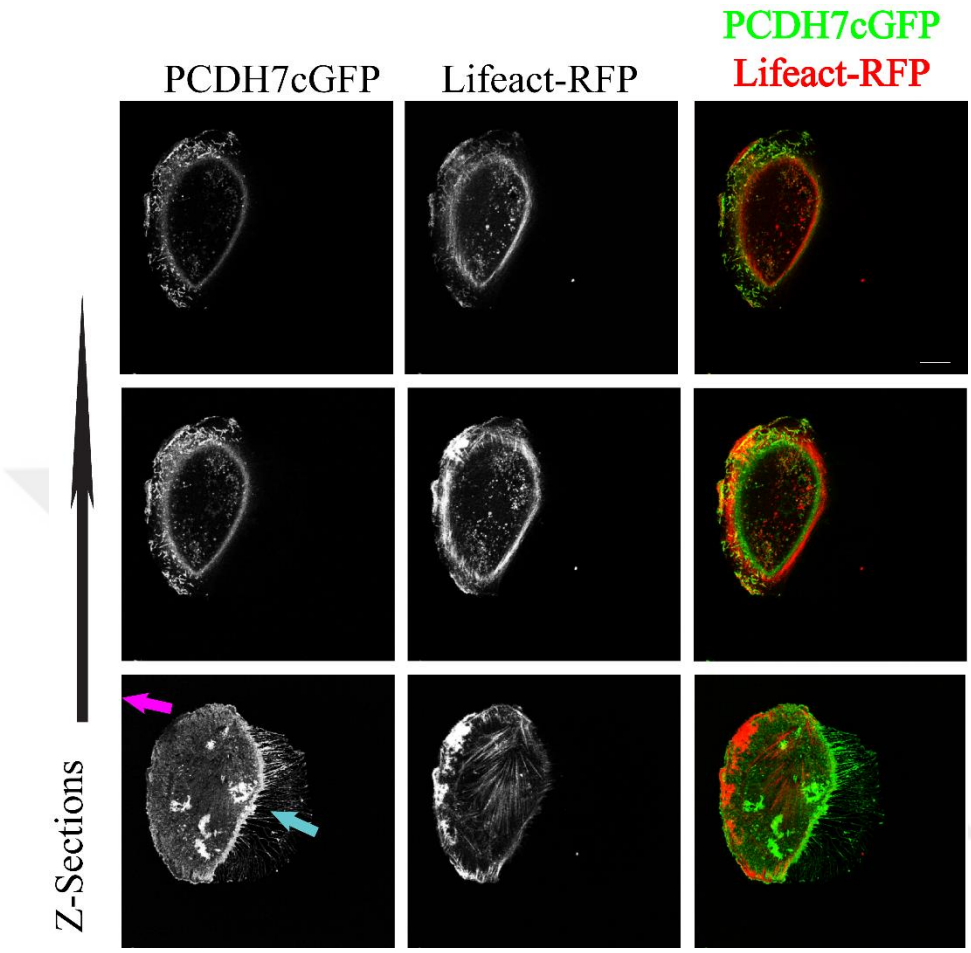

Figure 4-5 : **PCDH7 stills from fame 43**. Frame 43 with separate z-sections. Lowest panel is deepest section. Arrows: magenta, cell migration front and cyan – cell rear. Scale bar – 20 µm.

travels as membrane ruffles towards the cellular front. This enrichment changes as the cell changes its orientation and direction of movement. Another remarkable aspect is pertaining to the cell rear. As cell polarizes itself, there appears a dynamic enrichment of PCDH7-eGFP on cell rear. As cell pushes forth, this rear edge appearance of PCDH7 appears and fades off dynamically over subsequent image acquisition which were 10 minutes apart for our experiment.

Z-section dependent localization changes of PCDH7

Analysis of Z-section still-images from confocal live imaging reveals finer details of PCDH7 localization at subcellular levels. Firstly, when the cell is not polarised as in frame 1, we can see that PCDH7 localization coincides with that of F-actin (Figure 4-4). A disc shaped cell orientation has apparent PCDH7 localization on cell's edges where it may interact with cell-attachment substrate. We separated three Z-sections to closely observe changes in signal and its correlations with F-actin. At lower sections, stress fibres are more apparent, spanning across the cell. At higher z-section, PCDH7 and F-actin co-localizes on cell's periphery with a second inner concentric arrangement. We see significant enrichment of PCDH7 in vesicular structures which appear to be ER vesicles.

We also looked at frames when the cell acquires polarised morphology (Frame 43, frame 68 and frame 75 among others; see figures 4-5 to 4-7). PCDH7 front edge localization is more prominent at higher z-sections (upper panels). In the direction of cell migration (magenta arrow), PCDH7 signal is organized on the membrane and is closely correlated with that of F-actin. In lower z-section (Middle and bottom panels), PCDH7 shows a prominent presence at the rear edge. This localization at the lower z-sections close to the cell attachment substrate displays a continuation of retraction fibres. Retraction fibres are the traces of rear edge of the cell as it migrates forth. This rear edge presence of PCDH7 is more prominent in some frames than others. This can be explained by a dynamic enrichment of PCDH7 on cell rear during cell migration. Lifeact-RFP signal also showed a dynamic enrichment of F-actin in the direction of cell migration. A front edge enrichment of actin in a polarized cell is well characterized. An overlay of the two signals, shows remarkable dynamic colocalization of PCDH7-GFP signal with lifeact-RFP on cell front.

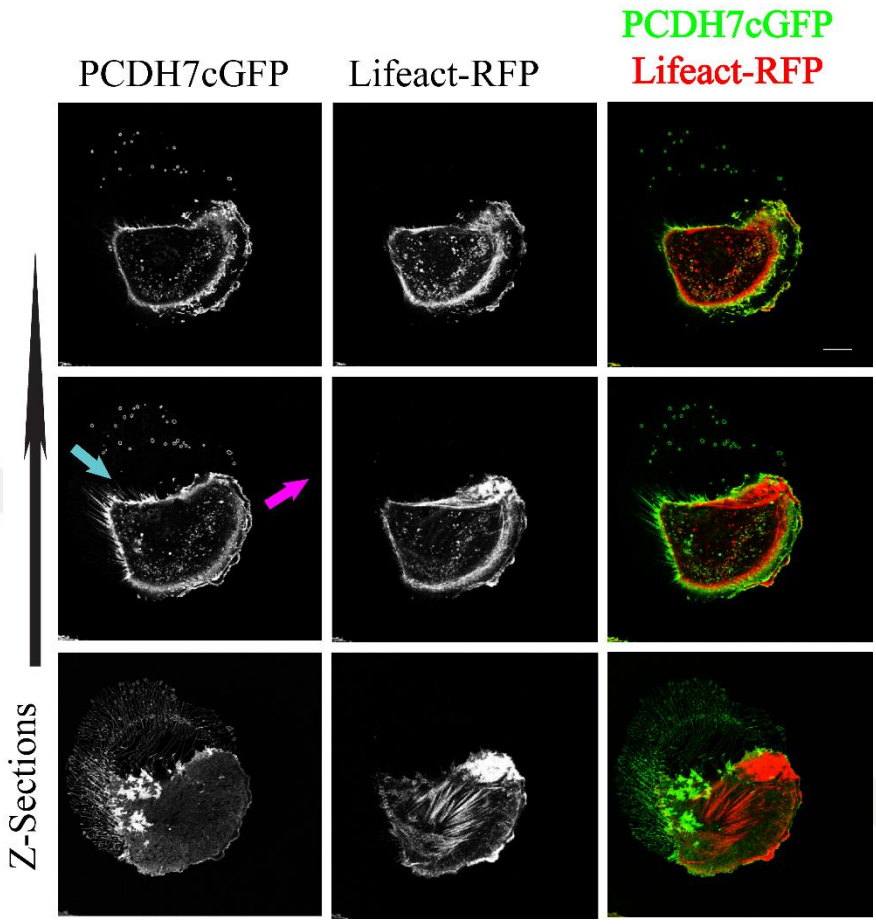

Figure 4-6 : PCDH7 stills from fame 68. Frame 68 with separate z-sections. Lower panel is deepest section. Arrows: magenta, cell migration front and cyan – cell rear. Scale bar – 20 μm

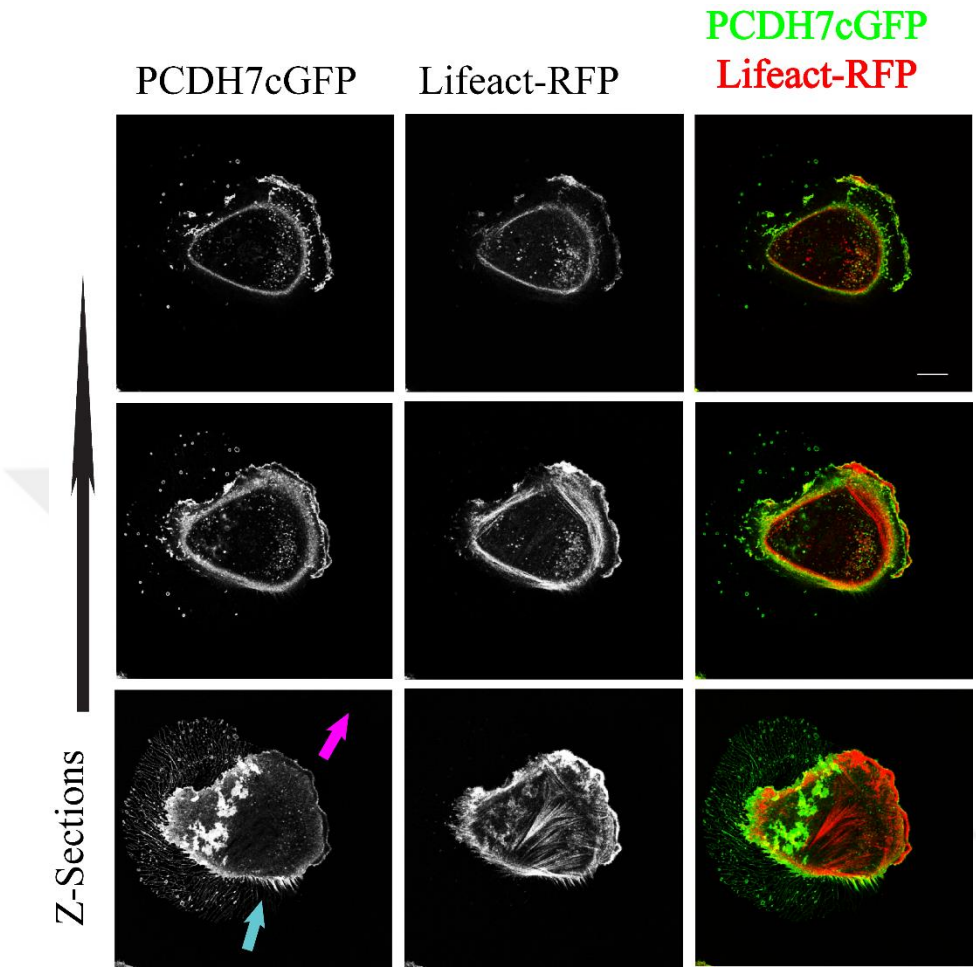

Figure 4-7: PCDH7 stills from fame 43. Frame 43 with separate z-sections. Lower panel is deepest section. Arrows: magenta, cell migration front and cyan – cell rear. Scale bar – 20 μm

3-Dimensional reconstruction of confocal imaging sections

A 3-D reconstruction of the same cell shows PCDH7 dynamic localization on cell front, and cell rear (see video 2). 3-D signal depth coding shows most of the front and all rear signal of PCDH7 to be very close to the attachment surface (blue shade), whereas some perinuclear signal (ER localization) shows higher Z-section localization (Cyan-Yellow shades) from the attachment surface (figure 4-8). Closeness to the

substrate at rear edge is especially intriguing since rear edge membrane retraction from the substrate is an important step in cell migration.

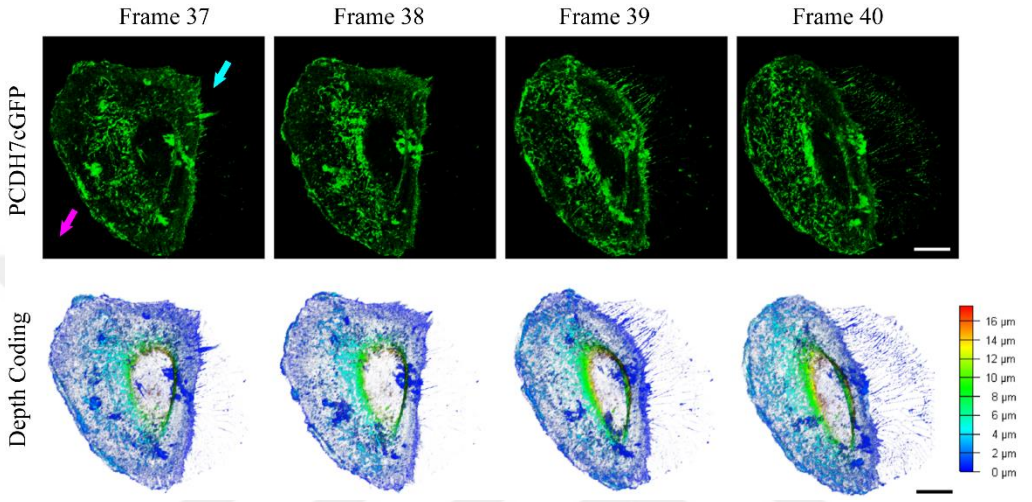

Figure 4-8: 3-Dimensional Reconstruction of PCDH7 signal. PCDH7c-GFP 3D stills from live imaging top panel with depth coding of the 3D stack in lower panel.

F-actin perturbation

Our data indicates a dynamic correlation of between PCDH7-GFP and LA-RFP. This could result due to PCDH7's direct or indirect interaction with F-actin network at migration front and cell rear. We sought to perform actin perturbation assay by incubating polarized RPE1 cells expressing PCDH7 GFP and LA-RFP with latranculinB, a drug that is used for perturbing F-actin. Latranculins bind to the ATP binding pockets of G-actin monomers which prevents their ability to polymerize into F-actin. Latranculins are thus useful drugs to study F-actin associated dynamics and F-actin associated proteins. As F-actin network is very dynamic, a turnover of F-actin into monomers and prevention of new monomers getting incorporated into F-actin

network causes actin cytoskeleton collapse. We chose a polarized cell with PCDH7-GFP expressing polarized dynamic localization. Upon incubation with latranculin b, cell immediately lost its F-actin network as indicated by lifeact-RFP signal (see video set 3). Concomitant with the loss of F-actin network, we clearly see an altered localization of PCDH7c-GFP, which also seems to be dispersed.

4.6 STED imaging of PCDH7-GFP

We were interested to see the organization of PCDH7 in a polarized cell at super-resolution. We employed the STED microscopy to image a live cell expressing PCDH7cGFP. A focus on cell front shows PCDH7c GFP signal organized in fibrous spikes (figure 4-9). This fibrous arrangement appears to delineate the actin cytoskeleton. However, within this fibrous organization there is GFP concentration which appears like beads on a string. It is likely that there is local enrichment of PCDH7 along the length of cytoskeletal fibres. These enriched domains are reminiscent of lipid rafts enriched subdomains of the plasma membrane. Indeed, PCDH7 has featured as a component of lipid rafts from multiple studies. It was enlisted as a lipid raft associated protein in the cerebral cortex of 16-month-old mice [87] along with a few other members of protocadherin subfamily. PCDH7 was also reported to be among the top five flotillin2 (a lipid raft marker) associated protein in nasopharyngeal carcinoma cells [88].

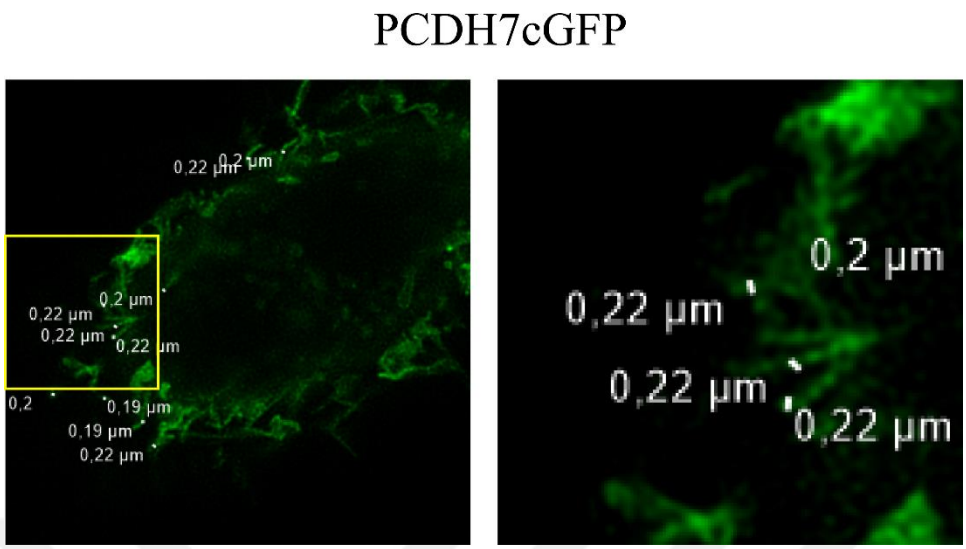

Figure 4-9: STED imaging of Cell Front. PCDH7cGFP expressing cell imaged using STED microscopy. Left panel shows cell front fibrous organization of PCDH7 signal. Inset, enlarged on right shows local enrichment of fibrous organization.

Conclusion

We concluded previously that PCDH7 is required for persistent cell migration (Chapter 3). To further explore PCDH7's role in cell migration, we intended to look for its subcellular localization. We generated stable cells expressing PCDH7isoform b and c. Our data from stable fixed samples indicate PCDH7 having a polarized localization. Signal was concentrated on cell front and cell rear, with a minor presence on lateral edges. Signal was strongly correlated with phalloidin which highlights F-actin structures in cell. There are two separate enrichments of F-actin that control cell migration. F-actin on protrusive ends giving shape to the front end lamellipodia or filopodia and F-actin in cell body and cell rear in the form of stress fibres which are actomyosin assemblies mediating cell's retraction. PCDH7 at cell front and cell rear correlates with F-actin. Myosin IIb enriches in cell body and towards the cell rear but not at protrusive cell front. Our immunostaining with PCDH7 and NMIIB show a

promising colocalization towards the cell rear. Further, we performed live imaging using GFP-fusion of PCDH7 along with lifeact-RFP to highlight F-actin dynamics in real time. As cell intends to acquire a polarized morphology, PCDH7 signal enriches largely on cell front along with enrichment of F-actin on cell front. We also observed a dynamic enrichment of PCDH7 on cell rear edge. This rear edge signal appears to continue as retraction fibres which are remnants left at the cell rear and may contain traces of cell rear edge retraction players. There are enrichments of PCDH7 directed associated with substrate (figure 4-7, lower panel). This enrichment is also dynamic, but doesn't have any directional correlation, although it also displays a colocalization with lifeact, which appears to be attachment of stress fibres to the substrate. Stress fibres attach to the focal adhesion assemblies which mediate a dynamic adhesion of migrating cell. Focal adhesion assemblies undergo turnover as cell migrates. Further assessment of PCDH7 in correlation with other focal adhesion network will be performed in follow up. We also performed super-resolution imaging of PCDH7-GFP expressing RPE1 cells. On cell front, PCDH7 expression appears as enrichment structures, arranged directionally, reminiscent of a fibrous base. These enriched modules had a similar diameter of 0.2 μm and may represent functional units at cell front, such as signalling assemblies, lipid rafts, or substrate attachment structures on cell front.

Chapter 5

Quantitative proteomics analysis of PCDH7 knockouts

5.1 Overview

The central theme for the current project was focusing on delineating PCDH7's role in cell migration. Phenotype assessment has revealed that perturbation of PCDH7's expression affects cell migration as outlined in chapter 3. Looking for subcellular localization of PCDH7 revealed that it is associated with F-actin compartment at cell front and displays a dynamic localization at the cell rear. At the cell rear PCDH7 shows a profile where it correlates with and highlights rear retraction fibres. Our next aim was to outline molecular function of PCDH7. We aimed to study the effect of perturbation of PCDH7 on the function and composition of cells. For this purpose, we performed a quantitative proteomics analysis for global proteomics profiling of PCDH7 knockout cells as a complementary approach. For quantitative proteomics, two different sets of approaches are generally employed. First set exploits isotope labelling of proteins to generate a relative mass shift among the groups of proteomes. Second set, collectively termed as label free approaches, uses either spectral counting or integration of signals from peptides. We generated RPE1 and Hela S3 knockout cell lines. RPE1 cells represent normal cells operating whereas Hela S3 represent cancer cell lines. Knockout versions of both have displayed reduced migration. We performed quantitative analysis of whole cell proteome of Hela S3 cells to ascertain the changes in cellular physiology upon removal of PCDH7.

We performed SILAC (Stable Isotope labelling by amino acids in cell culture) based whole proteome analysis to identify affected subsets of proteins when PCDH7's expression is perturbed. SILAC is a method employed to metabolically label whole proteome of the cell with specific sets of amino acids that have differentially isotope

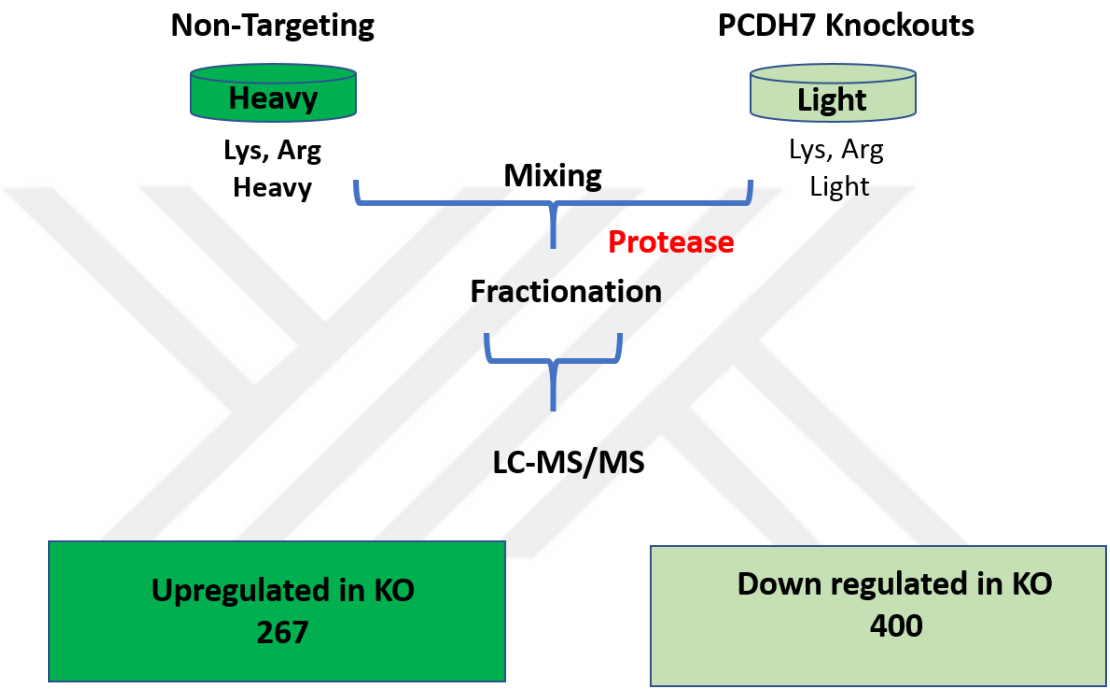

Figure 5-1 : **Outline of SILAC experiment**

constitution. Commonly, Arginine and Lysine amino acids having different carbon and nitrogen isotopes are supplemented in the cell culture media. SILAC cell culture medium lacks arginine and lysine which can be externally supplemented. Heavy, and light labelled arginine and lysine containing cell culture media are used to grow different groups of cells. A relative global analysis of whole cell proteome reveals

subsets of upregulated and downregulated proteins. These subsets can in turn outline the metabolic and signalling pathways that get affected within a subset or upon a specific treatment. An inherent advantage of metabolic labelling is that the outcome of the experiment is usually unaffected by sample handling and processing.

5.2 PCDH7 knockouts in HelaS3 cells

We chose two cell lines 7-1-2 and 7-5-2 that had already showed significant reduction in cell migration as measured using RTCA Xcellegence system (figure 3-9). We labelled 7-1-2 and 7-5-2 colonies of Hela S3 cells with light isotope labelled arginine and lysine and non-targeting guide treated Hela S3 cells with heavy isotope labelled arginine and lysine. Knockout cells and non-targeting cells were cultured in respective labelled media for several generations. For SILAC experiment, equal amount of whole cell lysates from the two sets were mixed and treated with proteases (trypsin and Lys-C). Peptides obtained were fractionated into 24 separate fractions using isoelectric focusing (IEF) based fractionation and analysed using LC-MS/MS. Data obtained was analysed using Maxquant analysis package. Experimental outline is shown in figure 5-1. For each cell line, two technical replicates (TR) were used (TR1, TR2) and a combined analysis was performed using 7-1-2 and 7-5-2 as knockout biological replicates (KO). Figure 5-2 (A) represents intensity comparisons of H/L ratios of 7-1-2 and 7-5-2. A Pearson correlation factor of 0.71 was obtained. 0.71 is a modest correlation of two cell populations. Both colonies are derivative from same population of Hela S3 cells. Hela S3 is a derivative of Hela, a cervical cancer cell line in use since 1951. Owing to divergent and independent evolution of cancer cells within a population, it is possible for two separate colonies to have a modest correlation. Figure 5-2 (B) represents comparative intensity ratios of two TRs of each cell line along with a combined analysis (KO) of two cell lines. Through combined analysis of L/H signals (knockout/Control), we found 267 proteins are upregulated and 400 proteins are downregulated in knockout cell lines.

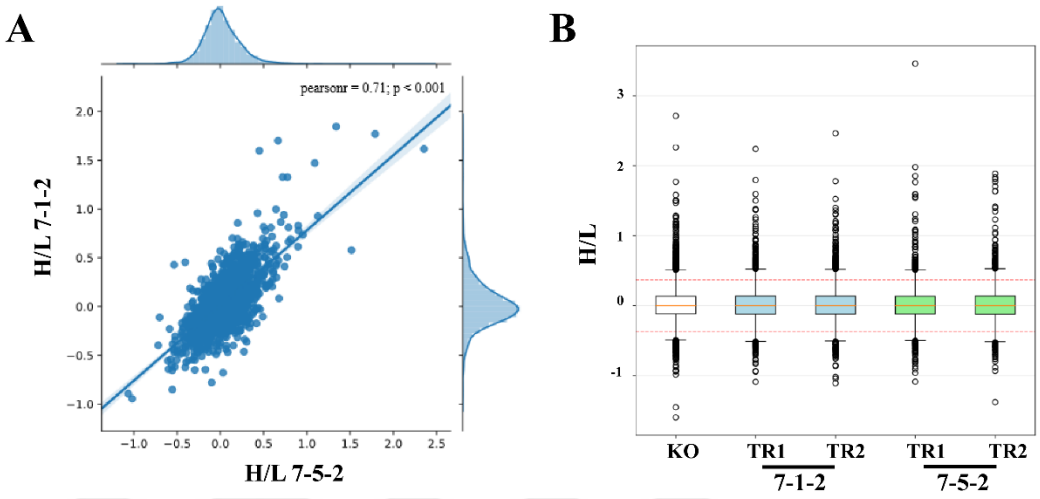

Figure 5-2: SILAC data correlation of two knockout colonies. A), Comparative representation of two colonies and their technical replicates (TR), KO – combined data from two knockouts.

5.3 GO Annotation Clustering

We intended to find a link between our list of proteins with changed expression upon PCDH7 knockout and the phenotypes observed. With an assumption that 90% of proteome is unchanged, we put a cut off corresponding to top 5% upregulated and downregulated proteins. These cut offs correspond to an approximate L/H ratio of ±0.304. Combined sets of upregulated and downregulated proteins were used for GO annotations using ENRICHR software. Following parameters were used to cluster protein sets: ‘Biological Process’, ‘Cell Compartment’, ‘Molecular Function’ and ‘KEGG Pathway’. From a long list of potentially affected parameters, we chose a subset with implication in cell migration and invasion.

Figure 5-3 shows potential cellular compartment related effects upon PCDH7 knockout. Our list of proteins include many proteins associated with various subcellular compartments involved in the cellular migration. Basement membrane

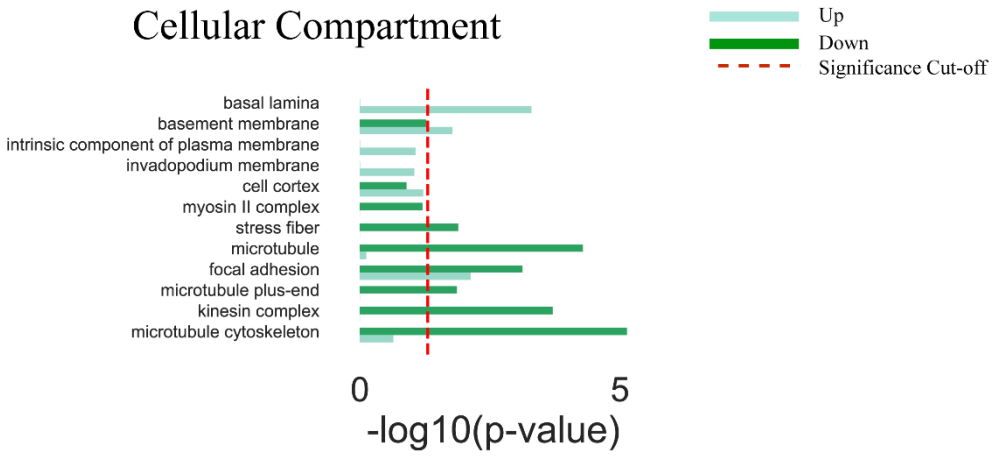

Figure 5-3 Cellular compartment based GO clustering

and basal lamina provide attachment for cells in the tissue and /or for cells to migrate with a dynamic focal adhesion network. A disturbance of basement membrane may alter cells' attachment dynamics and therefore migration abilities. Altered proteins involved in invadopodia membrane can affect the cells migration and invasion. Invadopodia are membranous extensions with dense actin network behind them and concentrated proteases which modify extracellular matrix, helping in turn in cell migration. Cell cortex is the cellular compartment right under plasma membrane. This compartment is rich in actomyosin components and mediates cell shape reformations. In a polarized cell, cortex is also well organized, especially at the cell migration front and rear. Changes in cortical proteins can alter cell shape and may influence the dynamics of cell migration. Stress fibres and myosin II complex are components of contractile compartment of F-actin network towards the cell rear. Stress

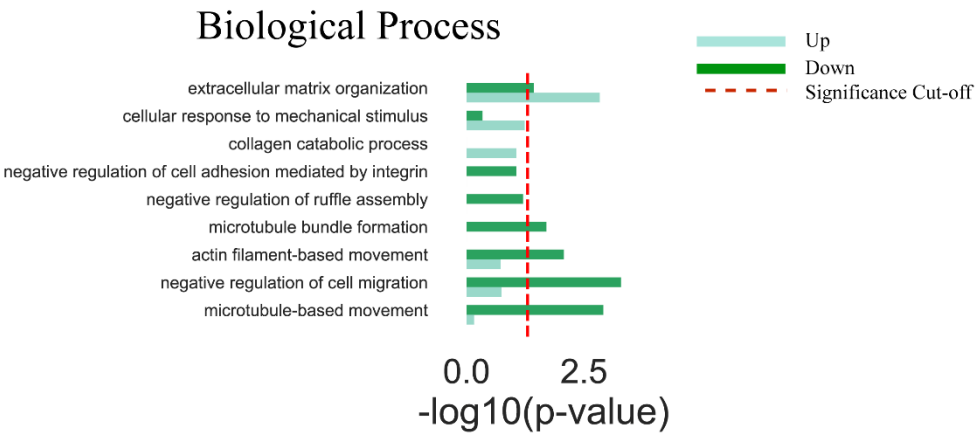

Figure 5-4 : Biological Process based GO clustering

fibres also contact focal adhesions which are attachments points of cell to the extracellular matrix. Actomyosin mediated contraction of stress fibres of what is responsible for the cell body retraction and focal adhesion turnover. Stress fibres also mediate traction forces involved in cells forward migration. A change in focal adhesion compartment will have obvious impact on cell migration. Focal adhesions show maturation, adaptation and a turnover as a cell migrate. An altered composition of focal adhesion and turnover can affect cell migration. Microtubule dynamics are an integral component of cellular migration machinery and kinesins are a group of motor proteins that move along microtubules and act as mediators of cell division and cargo transporters. A significant change in either can impact cell migration.

Figure 5-4 represents a subset of GO annotation clusters (from within our list of proteins) pertaining to biological processes that can impact cell migration. Extracellular matrix components are required for cell membrane proteins' attachment. At migration front, for example, integrin mediated interactions with extracellular matrix provides front attachment of the cells. Also, extracellular matrix components

mediate focal adhesion attachments. Most of the extracellular matrix components are secreted by the cells in culture. Secretion of proteins through extracellular vesicles mediate the process of deposition of proteins. Vesicular secretion is an act of membranous buddings from the cells. Loss of a transmembrane protein may further alter membrane composition and can affect the process of vesicular secretion. Cells respond to mechanical stimulus through mechanotransduction. A series of changes in cell's cytoskeletal machinery and signalling cascades are involved in responding to mechanical stimuli. Cell migration is directly dependent on dynamic changes cytoskeletal machinery, especially actin cytoskeleton. A disparity in mechanotransduction will impact cell migration. Effect on negative regulation of cell migration, actin filament-based movement and microtubule bundling can all deregulate migration related processes.

Figure 5-5 represents subset of GO annotated molecular functions that would be affected upon PCDH7 knockout. Collagen binding involved in cell-matrix adhesion would interfere with the dynamics of cell attachment to the matrix. An unregulated cadherin binding would impact cell-cell interactions, and cell migration, as many cadherins mediate these functions. Cytoskeletal elements dynamics are closely associated with cell shape alteration involved in migration and metastasis. Altered actin filament and intermediate filament binding and microtubule activity can all influence cell migration.

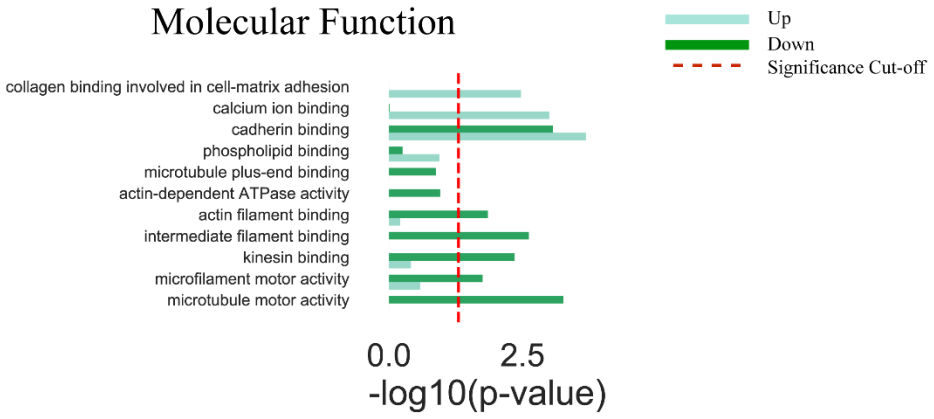

Figure 5-5 Molecular Function based GO Clustering

Figure 5-6 represents altered KEGG pathways upon PCDH7 knockout. Endocytosis of membrane proteins is an essential process integrated within migration dynamics. For directed chemokine migration, internalization of chemical cues after sensing to shape cells response to the gradient, as well as recycling of receptors back to the polarized membrane of the migrating cell are inherently dependent upon an efficient endocytosis [89]. Integrin recycling, its delivery to invadosome foci and focal adhesion turnover are all mediated by endocytosis. Type I matrix metalloproteases are delivered to the cell migration front through endosomal system to reconfigure the extracellular matrix components. Directed migration in response to chemical gradients of chemokine is dependent on receptor availability at the right loci. Chemokine receptors get internalized upon binding to the ligands. This internalization is usually through clathrin-coated vesicular endocytosis [90] but could also be mediated through lipid

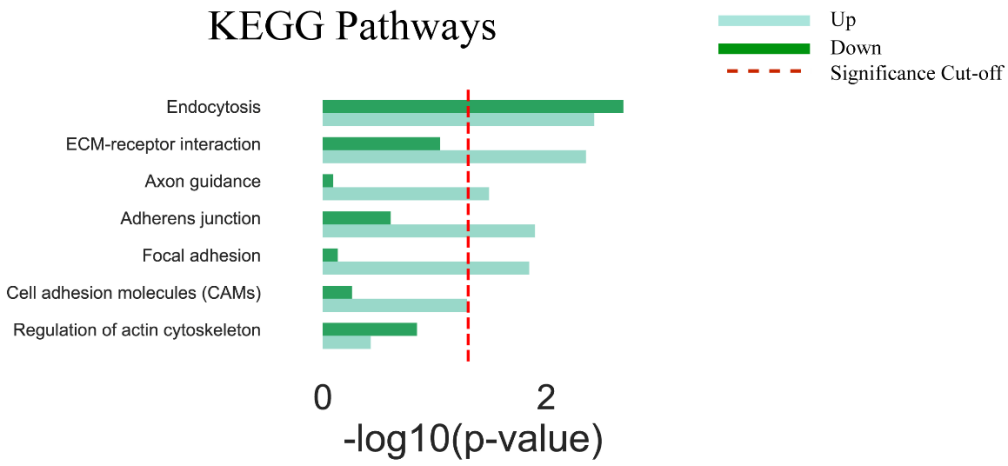

Figure 5-6 : KEGG pathway based GO clustering

rafts and caveolae [90,91]. Axon guidance is an example of directed projection of a cellular appendage, sensing the environmental cues, both attractive and repulsive before reaching target neuron. In a way, axon growth cone is compositionally and physiologically, very similar to the cell migration front. Signalling pathways associated with focal adhesion, and cell adhesion molecules mediate formation, maturation and turnover of cell-substrate attachment dynamics during cell migration. Focal adhesion maturation is also myosin II –mediated, which is an important component of stress fibres, and mediate cell rear retraction.

The sets of proteins clustered for each GO annotation category points at converged functions. We chose some of those categories to scrutinize their involvement in specific migration/ invasion related role they may play in the cell. Figure 5-7 represents histogram for L/H values of the proteins identified in our proteomics screening. A representative subset of proteins associated with a category are displayed in the figure.

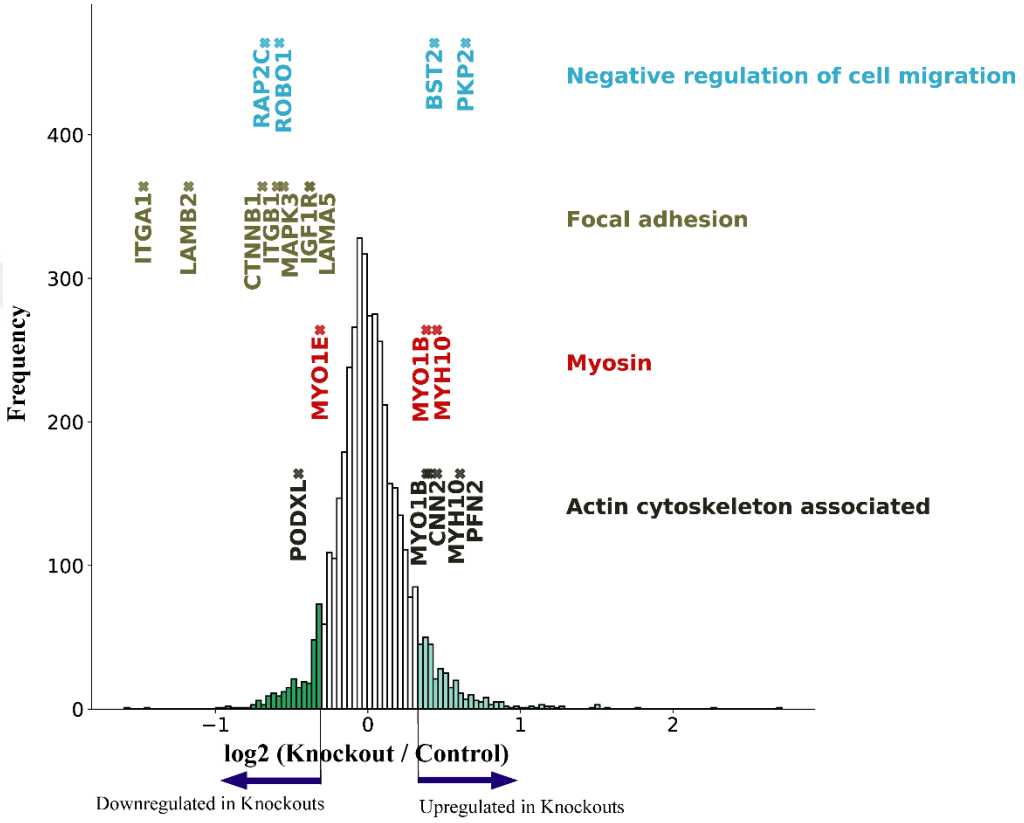

Figure 5-7: Functional Correlation of Protein hits. Histogram showing distribution of proteins in SILAC based proteomics analysis. Representative protein sets that can contribute to cell migration related processes are highlighted.

5.4 Enlisting roles in Migration/Metastasis of representative proteins

Actin cytoskeleton associated proteins

Several actin associated proteins were found to be upregulated or downregulated after knockout of PCDH7. We used Biogrid database to look for known interacting partners of beta-actin (ACTB) and compared that list with our list of proteins. Our expanded list contained at least 21 proteins with known ACTB interactions (figure 5- 8). This group of proteins is intriguing, given the correlation of PCDH7 with actin cytoskeleton (Chapter 4, subcellular localization of PCDH7 is associated with actin network majorly on cell front but also on cell rear. Cell front is associated with lamellipodial F-actin network, and cell rear is associated with stress fibres associated F-actin network. Podocalyxin (PODXL) overexpression is associated with breast cancer metastasis, and invasion and its downregulation affects invadopodia formation. Notable phenotypes upon PODXL downregulation were reduced lamellipodial formation, reduced FAK and F-actin/Cortactin colocalization [92]. Another study showed PODXL's direct involvement in EMT promotion and as a marker of gastric cancer [93]. PODXL levels are reduced in knockout cells which could contribute to our observation of reduced cell migration and persistence. Profilin-2 (PFN2) is a member of profiling group of proteins with known activity in binding to actin monomers and asset negative control on cell migration at high concentration by preventing actin polymerization. A dichotomy in PFN1 and PFN2 function has been described. PFN1 promotes protrusion, cell migration and invasion, whereas PFN2 upregulation suppresses these processes through exertion on actin cytoskeleton [94]. Calponin-2 is an actin binding protein associated with cellular protrusion on migration front, works downstream as a Wnt/Pcp effector and mediated neural crest migration [95]. We also found some members of myosin superfamily to be up-regulated within the set cut-off.

These are MYH10, MYO1B, and MYO1E which are actin based motor proteins described separately below.

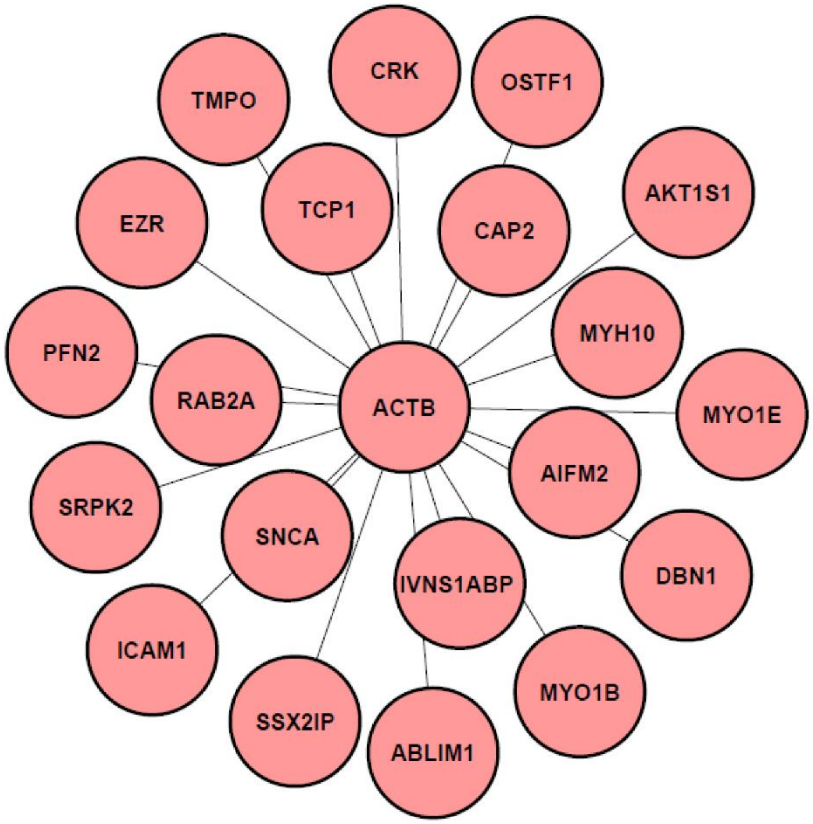

Figure 5-8 : Interaction with Actin cytoskeleton. Beta-Actin interacting proteins with altered expression upon PCDH7 knockout

Myosin motor proteins

As mentioned earlier, we found three members of myosin superfamily in our list of proteins with altered expression upon PCDH7 knockout. MYH10 codes for the heavy chain of NMII, isoform B. NMIIB is a well characterized protein associated with cell migration, focal adhesion dynamics and stress fibre organization. It is associated with the contractile domain of F-actin cytoskeleton and mediates contractile movement of cell body in the direction of migration as well as rear edge retraction. NMIIB is localized towards the cell rear, but in kidney epithelial cell from Xenopus, NMIIB is enriched at the leading edge [96]. In another study, cells with higher metastatic potential were shown to have upregulation of MYO1B along with MYO9B, MYO10B and MYO18A [97]. Correlated expression of these four myosins in PC-3 cells mediate its highly metastatic potential through forging better polarization, and actin cytoskeletal assembly [97].

MYO1B is associated with high metastasis and regulates actin assembly of actin fibres, and membrane remodelling at trans-Golgi network [98]. MYO1E functions downstream of ERK signalling. In the absence of ERK signalling, MYO1E in association with another protein SH3P2 has cytosolic localization. As a result of ERK signalling, SH3P2 is phosphorylated, Myosin-1e translocates to the lamellipodia and interacts with F-actin, where it plays an essential for cell migration [99]. Given a subset of myosins with changed expression PCDH7, it is likely that their coordinated interplay of cytoskeleton mediated manoeuvring is affected, leading to migration and persistence phenotype.

Negative regulation of Cell migration

We also found a subset of proteins that are involved in negative regulation of cell migration in our list. Plakophilin-2 is a desmosomal protein and an epithelial marker

which is directly suppressed by induction of Zeb-2 transcription factors and inducers of EMT [100]. Downregulation of plakophilin-2 in epicardial cells derived from neonatal rats induced enhanced cell migration velocity and cell proliferation [101]. Plakophilin-2 expression is upregulated as a result of Wnt signalling in normal and colon cancer-associated fibroblasts as a feedback intracellular regulator of Wnt signalling [102]. MMPs are cell surface proteases that remodel components of extracellular matrix through proteolysis and their expression mediates invasion and metastasis. Bone marrow Stromal antigen 2 (BST2) has been shown to bind to MT1-MMP (membrane type 1 matrix metalloproteinase) and reduce its proteolysis activity [103]. Another study, however, showed that BST-2 overexpression in tamoxifen-resistant breast cancer cells is associated with enhanced invasiveness [104]. Ras-related protein Rap2c is a GTP-binding protein. Rap2c has recently been shown to enhance migration in osteosarcoma cells through activating MMP2 protein [105]. Roundabout-1 or Robo-1 is a well-known protein involved in growth cone guidance and axon directional projection to target neurons. Earlier work that showed PCDH7 to be upregulated in brain-metastasizing breast cancer cells also shows Robo1 as up to 53 fold upregulated, and falls within top 3 highly upregulated proteins [26]. Therefore, observing Robo1 downregulation in PCDH7 knockout cells is intriguing. Slit/Robo signalling mediates a repulsive signal for migrating axon. The details of Robo1 function in cell migration are yet to be revealed but an intuitive possible is that Robo1 tunes migrating cells directionality through balancing directionality of migration.

Focal Adhesion related proteins

Focal adhesions are crucial subcellular compartments that mediate cell's attachment to the substrate and their dynamic spatial distribution and turnover is essential for cell migration, directionality and persistence. Many components of focal adhesions are regulated during EMT. We found integrin alpha-1, integrin beta-1, to be downregulated. Since integrin molecules mediate nascent attachments at the protrusive

cell front, their suppression can cause significant retardation in cell migration. Components of extracellular matrix like collagen and laminin provide adhesion surfaces for migrating cells. For cells in culture, these proteins are secreted by growing cells to form extracellular matrix on growing substrate upon which cells migration is facilitated. Reduced production of these components (LAMB2 and LAMA5) can alter composition of ECM and migration dynamics of cells. IGF1 induces migration in medulloblastoma cells and IGF1R was reported as a key target for metastatic medulloblastoma therapeutic approaches [106]. Beta-catenin or CTNNB1 is a well-characterized downstream effector of Wnt signalling and has been shown to promote cell migration and invasion, in many cancer types [107,108]. Focal Adhesion kinase (FAK) mediated regulation of beta-catenin signalling has previously been demonstrated [109]. Loss of focal adhesion function due to downregulation of multiple components of focal adhesion assembly can severely hamper cell's migration.

5.5 OmicsIntegrator for functional clustering

Our list of upregulated and downregulated proteins were used to generate networks of proteins that have been previously shown to interact with each other. Omics integrator works on clustering these proteins within subnetworks, and in the process adding additional missing links from literature to provide a comprehensive functionally relevant networks. Omics integrator output provided 14 clusters in upregulated set and 20 networks from among downregulated sets. These sets were further assigned a predicted function using GO. Among the assigned functions to these clusters, two main functions were pertaining to mitochondrial functions, and cell migration. Mitochondrial function related proteins (highlighted as pink circumferences) and those involved in migration (highlighted yellow circumferences) were mapped on to clusters. Mitochondria related proteins as well as migration associated proteins were overly represented in down clusters as compared to the up clusters. Nevertheless, one protein belonging to cytochrome p450 group CYP1B1 was common among

mitochondria related and cell migration related proteins in up clusters and TGM2 was common protein between mitochondrial and cell migration related proteins within down clusters. Possible interface between PCDH7 and mitochondrial function requires further investigation.

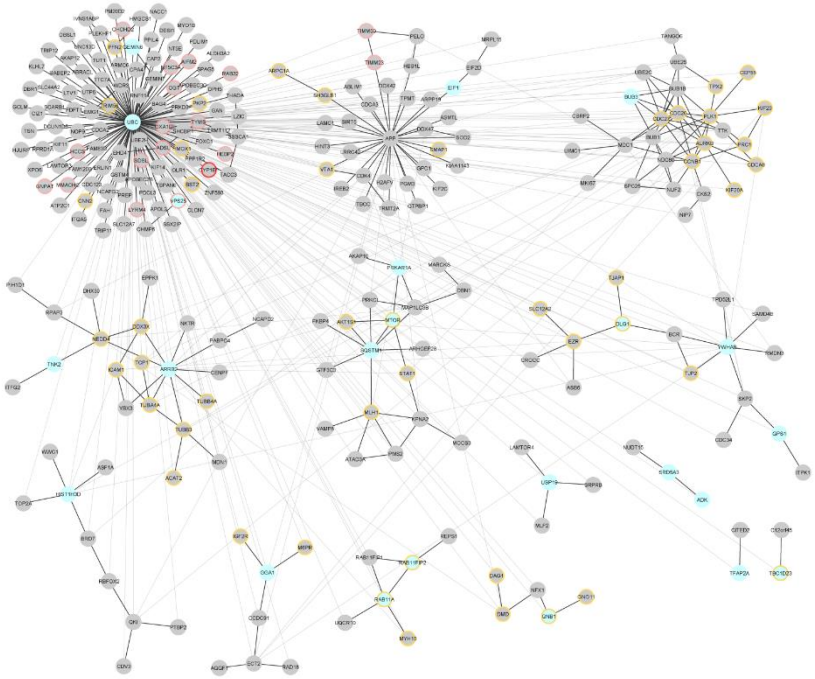

Figure 5-9: Predicted interaction networks within upregulated set using OmicsIntegrator. Grey circles are proteins from our SILAC experiments whereas cyan circles are additional nodes included by OmicsIntegrator to link networks. Yellow circumferences represent individual proteins with role in cell migration related processes and pink circumferences represent proteins with role in mitochondrial functions.

Among down-clusters, we observed one cluster that has an overrepresentation of EMT genes (figure 5-11) and table 5-1. This cluster is relevant for our work which is emphasizing on finding a molecular causal link between PCDH7 perturbation and migration defects.

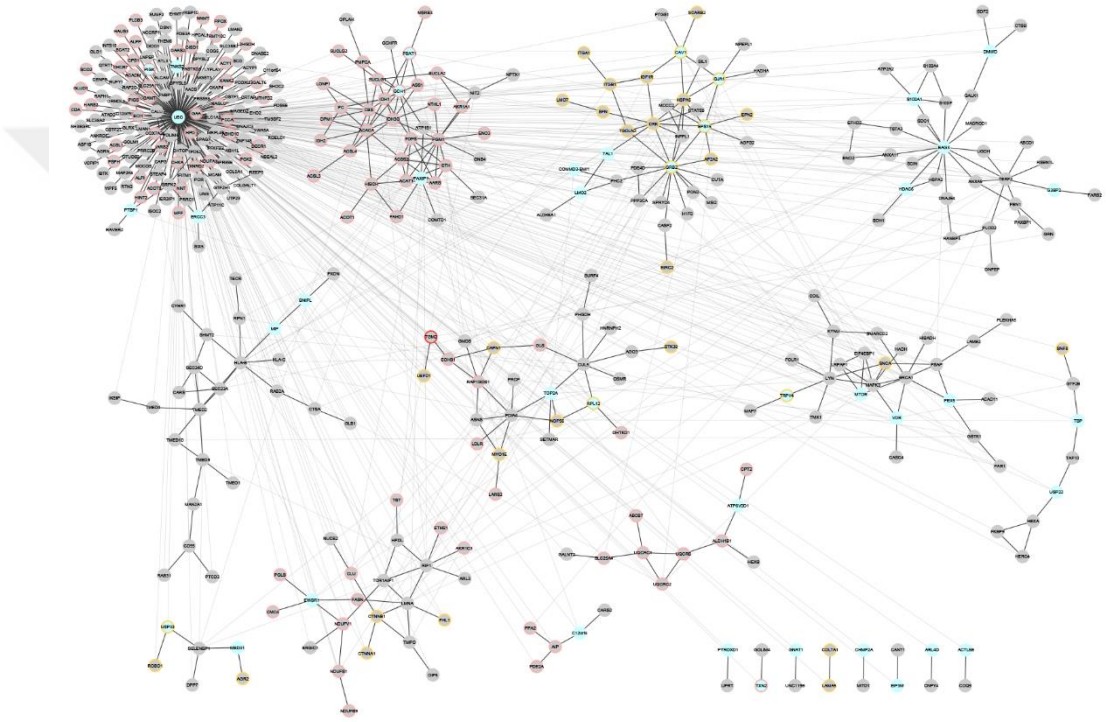

Figure 5-10: Predicted interaction networks within downregulated set using OmicsIntegrator. Grey circles are proteins from our SILAC experiments whereas cyan circles are additional nodes included by OmicsIntegrator to link networks. Yellow circumferences represent individual proteins with role in cell migration related processes and pink circumferences represent proteins with role in mitochondrial functions.

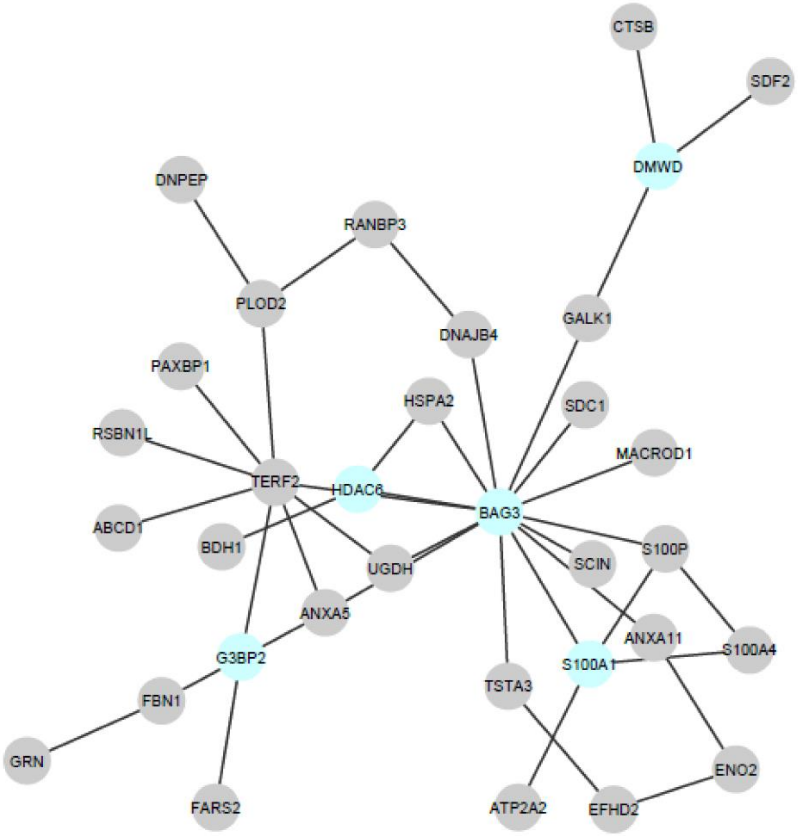

Figure 5-11 Subnetwork with EMT proteins: Down-regulated sub-network 6 with an overrepresentation of EMT related genes in the cluster

	Gene	Protein name	Functional link to EMT
1	FBN1	Fibrillin-1	Promotes Ovarian Cancer Metastasis [110]
2	SCIN	Scinderin	Promotes invasion and metastasis of gastric cancer cells[111]
3	DNAJB4	Heat Shock Protein	Inversely related with Invasiveness [112] but conflicting result from our lab in favor of mesenchymal nature
4	S100A4	p9ka/S100A4 calcium binding protein	Mediator of metastasis [113]
5	BAG3	*Bcl-2* associated athanogene	Activates macrophages to release proliferation factors in pancreatic adenocarcinoma, its suppression reduces metastasis [114]
6	S100A1	S100 calcium binding protein	Lymph node metastasis in Ovarian Cancer [115]
7	HDAC6	Histone Deacetylase	Metastasis in Melanoma cells[116] and enhanced migration in hepatocarcinoma [117]
8	SDC1	Syndecan-1	Enhances migration and metastasis of fibrosarcoma [118]
9	ANXA5	Annexin-A5	Mediates metastasis in hepatocarcinoma cells [119]
10	ABCD1	ATP binding Cassette-D1	Upregulated in ovarian carcinoma metastasis [120]

5.6 Conclusion

In this chapter we described SILAC quantitative proteomics approach to characterize mis-regulated proteins upon PCDH7 knockout. To our surprise, we found a large number of proteins upregulated and downregulated and many of those could be clustered within important cellular compartment and pertaining to molecular functions that are essential for cell migration. We found a large set of actin cytoskeleton associated proteins. A smaller group was that of myosins, including NMIIB, classically associated with cell body and cell rear retraction. Other significant clusters were associated with focal adhesion and regulation of cell migration. Taken together, this huge subset of affected group of proteins that are involved in cell migration and invasion can have an overall deleterious effect on cell's ability to migrate. Thus, our proteomics screening also falls in line with the observed phenotype of reduced cell migration and persistence (chapter 3), and observed association of PCDH7 with actin cytoskeleton and actomyosin contraction (chapter 4). OmicsIntegrator, we clustered upregulated and down-regulated proteins into sub-clusters with potential interactions. Of special interest is a cluster of down-regulated proteins many of which have roles in epithelial-mesenchymal transition. Reduced levels of this cluster of proteins could lead to aberrant migratory phenotype as described in chapter 3. Further proteomics approaches such as BioID based proximity labelling or affinity pull down will be valuable to further delineate PCDH7's molecular function in cell migration.

A pertinent question is why would so many proteins' expression get affected upon PCDH7 knockout. Longer isoforms of PCDH7 has binding sites for phosphoprotein phosphatase -1alpha (PP-1α) on cytosolic domain CM3. This domian may either provide a docking site for PP-1α to be able to have a specific group of substrate proteins, or it may act as a quencher to limit the activity of PP-1α. In either case, a different phosphorylation profile may affect proteins turnover. NF-PC, an orthologue of PCDH7 in xenopus has been shown to interact with TAF-1 transcription factor. This

interaction is essential for efficient axon guidance. An absence of PCDH7 from membrane may alter TAF-10 activity, and can change the rate of transcription of a set of its target proteins.

Chapter 6
Discussion and Conclusion

Cell migration is an essential phenomenon for many physiological processes like embryonic development, and metastasis. Understanding molecular machinery that drives cellular migration, and factors that control migration is therefore one of the central interest for cell and cancer biologists. Famous Croonian lecture of Abercrombie in 1978 revolved around the model of cell migration that he had postulated. Based on separate isolated observations, he outlined four steps in migration; namely: 1) actin polymerization at cell front and protrusion of cells in that direction, 2) formation of new adhesions with the substrate at the cell front, 3) dissolution of adhesions at the cell rear 4) actomyosin-based contraction to move cell body forward. Of special note was the discussion about actomyosin contractility and force generation by 'crawling cells': "*it has been supposed for more than 20 years that non-muscle cells contain the muscle like acto-myosin equipment appropriate for generation of this force*" (an excerpt from the Croonian lecture, 1978). All later models, whether molecular or computational has been built upon Abercrombie's basic postulation model of metazoan crawling, with additional molecular players and finer details.

In this thesis, we explored the role of a cell surface protein, PCDH7 in mammalian cell migration. Our results clearly indicate that manipulation of PCDH7 expression affects cell migration parameters. PCDH7 exists as four different isoforms, longer and shorter versions, due to differences in their cytoplasmic domains. Both shorter and longer isoforms were able to rescue the phenotype; indicating that PCDH7s role in cell migration may not depend on changes in cytosolic domains of different isoforms. *In-utero* electroporation experiment using E14 pregnant mice shows that PCDH7

downregulation using RNAi had a modest effect on neuronal migration but during recovery of the phenotype with overexpression resulted in high directional mobility of neuronal progenitors.

Confocal fixed sample imaging and live imaging to show PCDH7's correlation with actin cytoskeleton on cell migration front (lamellipodial and filopodial F-actin assemblies) and cell rear. This localization was highly dynamic and changed as the cell changed its directed and orientation. On cell rear, PCDH7 showed a modest colocalization with NMIIB. Rear edge dynamic enrichment of PCDH7 observed in live imaging was interesting owing to rear edge retraction being one of the important steps in cell migration. Rear edge retraction and cell body movement in forward direction are actomyosin contractility dependent processes. Largely, myosin motors expend energy for this contraction. STED imaging of cell migration front for PCDH7-GFP shows PCDH7 signal as enriched domains of very similar dimensions hinting at a lipid raft related assembly. Indeed, PCDH7 has previously been enlisted as a lipid raft associated protein [87,88].

Chapter 5 describes our SILAC based quantitative proteomics study to explore altered proteome upon PCDH7 knockout in HelaS3 cells. Among the upregulated and downregulated proteins, many were associated with the cell migration. Our GO annotations clearly indicate multiple possible ways in which cellular migration could be hampered. Many proteins have known actin cytoskeleton association and functions. There were members of myosin superfamily, including MYH10, which is the heavy chain of NMIIB. NMIIB is intricately associated with cell body movement and cell rear retraction. PCDH7's rear edge localization, its smearing along retraction fibres and a colocalization with NMIIB using immunofluorescence, suggest its possible functional interaction with NMIIB. This proposition is also strengthened by our single cell tracking videos of PCDH7 knockout cells that display an inability to detach their rear edges as they tend to make protrusions in an intended direction of migration. We

speculate a strong probability that PCDH7 and NMIIB work together in mediating rear cell retraction. Future work to explore this role will require NMII perturbations and NMII live imaging with PCDH7.

Working Model

For successful migration front and rear of migrating cells adopt a synergistic activity, front edge protrusion and adhesion to the substrate is followed by cell body movement and retraction of rear adhesion points. A miscoordination within this synchrony can lead to impairment of migration, or loss of persistence. Stress fibers mediate forces exerted through NMII activity. Stress fibers are attached to focal adhesions. Proper attachment to these foci are required to effect cell body movement in response to actomyosin contraction. Focal adhesions' size and cell velocity have a bimodal relationship in which cells' velocity is directly related to the size of focal adhesions until a threshold. Above this threshold increase in size of focal adhesions retard the velocity of cell. To elucidate further, lets describe focal adhesion mediated cell motility as a two step process. In step one, stress fiber mediated contraction facillitates cell body contraction, which requires a proper attachment of stress fibers to the focal adhesion points. In next step, focal adhesions are required to undergo a turnover and retraction. As focal adhesion size grows it may enhance contractile forces of stress fiber contraction leading to higher motility, but beyond certain size of focal adhesions, the turnover rate looses synchrony with contraction; as a result the cell velocity is retarded. Our quantitative proteomics results indicate downregulation of a cluster of proteins involved in focal adhesion formation and extracellular matrix organization. Prominent proteins of this cluster belong to integrins, laminins, and collagens among others (figure 5-7). In addition we found a number of actin associated proteins to have different expression levels in knockout (figure 5-8). This repertoire of altered levels may affect F-actin assembly on cell front, as well as stress fibre mediated contraction

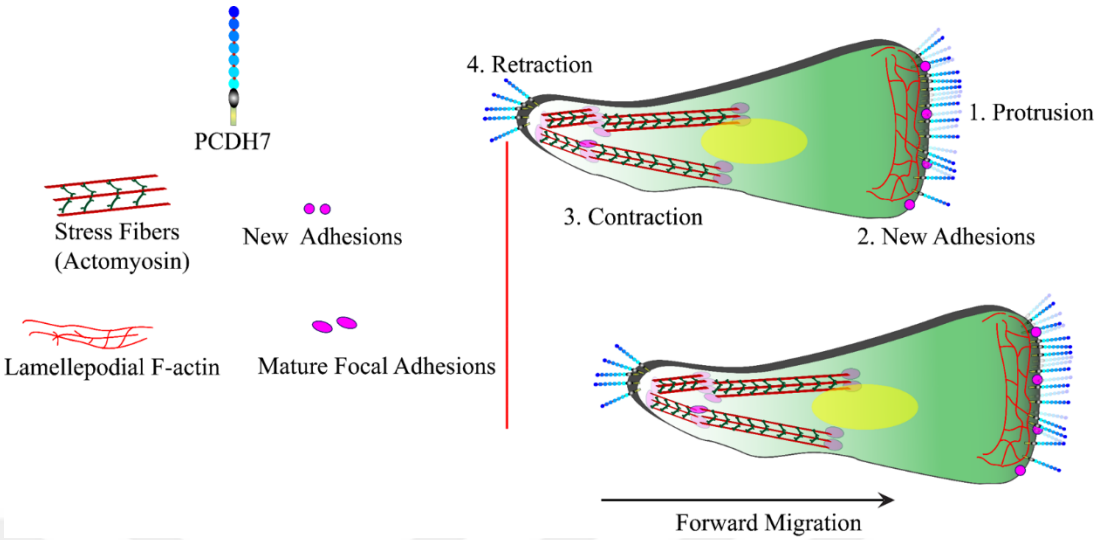

Figure 6-1 : **Control Migration Model**. Cells expressing PCDH7 experience normal parameters of protrusion, new adhesion formation, contraction and rear retraction, resulting in forward migration

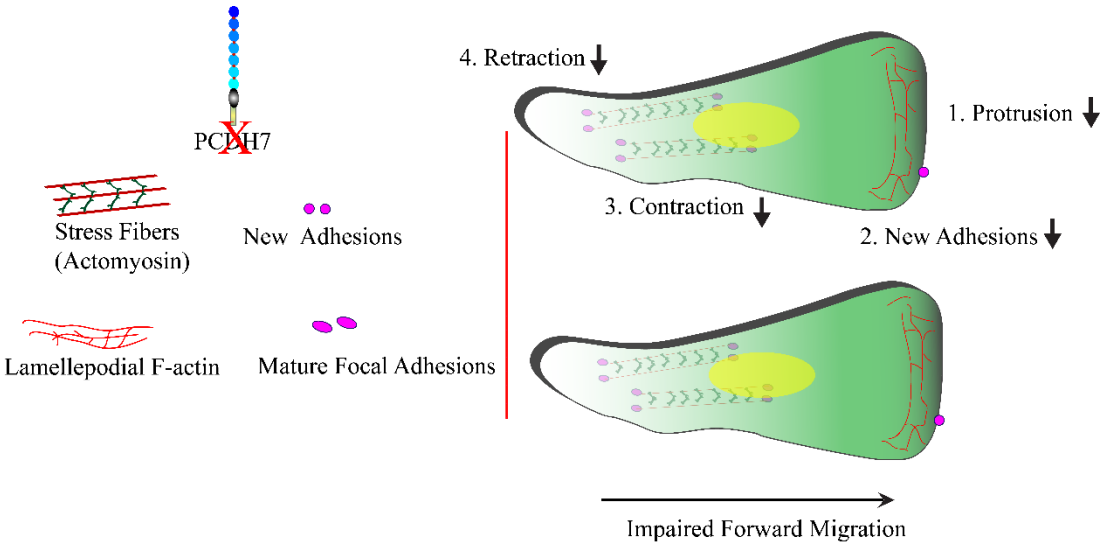

Figure 6-2: **Model of Knockout Migration**. In the absence of PCDH7, protrusion, new adhesion formation, contraction and rear retraction are all affected, contributing to an impaired forward migration phenotype.

of cell body and rear retraction. Such a change can hamper the coordination between different phases involved in cell migration and could present as the leading cause of loss of persistence in migration. We also found a cluster of proteins from within downregulated set, with many proteins in the network having established roles in EMT (Table 5-1). Since retraction of rear edge also requires actomyosin contraction, NMIIB is an important actor in the process. Its altered activity could alter retraction of rear. A combinatorial effect of these could also cause an impaired migration phenotype which requires further investigation. Figure 6-1 represents the model of normal migration in a polarised cell. In the presence of physiological concentrations or overexpression (during recovery) of PCDH7, cell is able to migrate in forward direction. Upon downregulation or knockout of PCDH7, actin assembly on cell front, cell protrusion and actomyosin mediated retraction of cell rear can be potentially affected. Additionally, maturation and dynamics of focal adhesions can be impaired leading to impairment of normal forward cell migration (Figure 6-2).

In summary, we have shown that PCDH7 is required for migration of mammalian cells. Its association with actin cytoskeleton, suggests a fucntional correlation with actin cytoskeleton; an idea further strengthened by altered expression levels of a large number of actin associated proteins upon knockout of PCDH7. These actin interacting proteins include myosins, like NMIIB, myosin-1e and myosin-1B, which can result in miscoordinated cell rear retraction. Further work on finding molecular interactors and pathways involved is required. Our work is a promising step in recognizing PCDH7 as a key player in physiological migration and a therapeutic target for cancer metastasis control.

References

1 Grunicke, H. H. The cell membrane as a target for cancer chemotherapy. *Eur J Cancer* **27**, 281-284 (1991).

2 Kuhlmann, L., Cummins, E., Samudio, I. & Kislinger, T. Cell-surface proteomics for the identification of novel therapeutic targets in cancer. *Expert Rev Proteomics* **15**, 259-275, doi:10.1080/14789450.2018.1429924 (2018).

3 Lauffenburger, D. A. & Horwitz, A. F. Cell migration: a physically integrated molecular process. *Cell* **84**, 359-369 (1996).

4 Ridley, A. J. *et al.* Cell migration: integrating signals from front to back. *Science* **302**, 1704-1709, doi:10.1126/science.1092053 (2003).

5 Sanz-Moreno, V. & Marshall, C. J. The plasticity of cytoskeletal dynamics underlying neoplastic cell migration. *Curr Opin Cell Biol* **22**, 690-696, doi:10.1016/j.ceb.2010.08.020 (2010).

6 Friedl, P. & Alexander, S. Cancer invasion and the microenvironment: plasticity and reciprocity. *Cell* **147**, 992-1009, doi:10.1016/j.cell.2011.11.016 (2011).

7 Sahai, E. Illuminating the metastatic process. *Nat Rev Cancer* **7**, 737-749, doi:10.1038/nrc2229 (2007).

8 Friedl, P. & Wolf, K. Plasticity of cell migration: a multiscale tuning model. *J Cell Biol* **188**, 11-19, doi:10.1083/jcb.200909003 (2010).

9 Ilina, O., Bakker, G. J., Vasaturo, A., Hofmann, R. M. & Friedl, P. Two-photon laser-generated microtracks in 3D collagen lattices: principles of MMP-dependent and -independent collective cancer cell invasion. *Phys Biol* **8**, 015010, doi:10.1088/1478-3975/8/1/015010 (2011).

10 Wolf, K. *et al.* Multi-step pericellular proteolysis controls the transition from individual to collective cancer cell invasion. *Nat Cell Biol* **9**, 893-904, doi:10.1038/ncb1616 (2007).

11 Sano, K. *et al.* Protocadherins: a large family of cadherin-related molecules in central nervous system. *EMBO J* **12**, 2249-2256 (1993).

12 Hulpiau, P. & van Roy, F. New insights into the evolution of metazoan cadherins. *Mol Biol Evol* **28**, 647-657, doi:10.1093/molbev/msq233 (2011).

13 Vanhalst, K., Kools, P., Staes, K., van Roy, F. & Redies, C. delta-Protocadherins: a gene family expressed differentially in the mouse brain. *Cell Mol Life Sci* **62**, 1247-1259, doi:10.1007/s00018-005-5021-7 (2005).

14 Noonan, J. P., Grimwood, J., Schmutz, J., Dickson, M. & Myers, R. M. Gene conversion and the evolution of protocadherin gene cluster diversity. *Genome Res* **14**, 354-366, doi:10.1101/gr.2133704 (2004).

15 Yagi, T. Clustered protocadherin family. *Dev Growth Differ* **50 Suppl 1**, S131-140, doi:10.1111/j.1440-169X.2008.00991.x (2008).

16 Jiang, X. J., Li, S., Ravi, V., Venkatesh, B. & Yu, W. P. Identification and comparative analysis of the protocadherin cluster in a reptile, the green anole lizard. *PLoS One* **4**, e7614, doi:10.1371/journal.pone.0007614 (2009).

17 Blevins, C. J., Emond, M. R., Biswas, S. & Jontes, J. D. Differential expression, alternative splicing, and adhesive properties of the zebrafish delta1-protocadherins. *Neuroscience* **199**, 523-534, doi:10.1016/j.neuroscience.2011.09.061 (2011).

18 Hirano, S. & Takeichi, M. Cadherins in brain morphogenesis and wiring. *Physiol Rev* **92**, 597-634, doi:10.1152/physrev.00014.2011 (2012).

19 Redies, C., Hertel, N. & Hubner, C. A. Cadherins and neuropsychiatric disorders. *Brain Res* **1470**, 130-144, doi:10.1016/j.brainres.2012.06.020 (2012).

20 Redies, C., Vanhalst, K. & Roy, F. delta-Protocadherins: unique structures and functions. *Cell Mol Life Sci* **62**, 2840-2852, doi:10.1007/s00018-005-5320-z (2005).

21 Ozlu, N. *et al.* Quantitative comparison of a human cancer cell surface proteome between interphase and mitosis. *EMBO J* **34**, 251-265, doi:10.15252/embj.201385162 (2015).

22 Fernandez-Monreal, M., Kang, S. & Phillips, G. R. Gamma-protocadherin homophilic interaction and intracellular trafficking is controlled by the cytoplasmic domain in neurons. *Mol Cell Neurosci* **40**, 344-353, doi:10.1016/j.mcn.2008.12.002 (2009).

23 Schreiner, D. & Weiner, J. A. Combinatorial homophilic interaction between gamma-protocadherin multimers greatly expands the molecular diversity of cell adhesion. *Proc Natl Acad Sci U S A* **107**, 14893-14898, doi:10.1073/pnas.1004526107 (2010).

24 Yoshida, K., Yoshitomo-Nakagawa, K., Seki, N., Sasaki, M. & Sugano, S. Cloning, expression analysis, and chromosomal localization of BH-protocadherin (PCDH7), a novel member of the cadherin superfamily. *Genomics* **49**, 458-461, doi:10.1006/geno.1998.5271 (1998).

25 Zhou, X. *et al.* PROTOCADHERIN 7 Acts through SET and PP2A to Potentiate MAPK Signaling by EGFR and KRAS during Lung Tumorigenesis. *Cancer Res* **77**, 187-197, doi:10.1158/0008-5472.CAN-16-1267-T (2017).

26 Bos, P. D. *et al.* Genes that mediate breast cancer metastasis to the brain. *Nature* **459**, 1005-1009, doi:10.1038/nature08021 (2009).

27 Chen, Q. *et al.* Carcinoma-astrocyte gap junctions promote brain metastasis by cGAMP transfer. *Nature* **533**, 493-498, doi:10.1038/nature18268 (2016).

28 Li, A. M. *et al.* Protocadherin-7 induces bone metastasis of breast cancer. *Biochem Biophys Res Commun* **436**, 486-490, doi:10.1016/j.bbrc.2013.05.131 (2013).

29 Huang, Y. T. *et al.* Genome-wide analysis of survival in early-stage non-small-cell lung cancer. *J Clin Oncol* **27**, 2660-2667, doi:10.1200/JCO.2008.18.7906 (2009).
30 Heggem, M. A. & Bradley, R. S. The cytoplasmic domain of Xenopus NF-protocadherin interacts with TAF1/set. *Dev Cell* **4**, 419-429 (2003).
31 Piper, M., Dwivedy, A., Leung, L., Bradley, R. S. & Holt, C. E. NF-protocadherin and TAF1 regulate retinal axon initiation and elongation in vivo. *J Neurosci* **28**, 100-105, doi:10.1523/JNEUROSCI.4490-07.2008 (2008).
32 Takeichi, M. Functional correlation between cell adhesive properties and some cell surface proteins. *The Journal of cell biology* **75**, 464-474 (1977).
33 Hyafil, F., Babinet, C. & Jacob, F. Cell-cell interactions in early embryogenesis: a molecular approach to the role of calcium. *Cell* **26**, 447-454 (1981).
34 Damsky, C. H., Knudsen, K. A., Dorio, R. J. & Buck, C. A. Manipulation of cell-cell and cell-substratum interactions in mouse mammary tumor epithelial cells using broad spectrum antisera. *The Journal of cell biology* **89**, 173-184 (1981).
35 Suzuki, S. T. Structural and functional diversity of cadherin superfamily: are new members of cadherin superfamily involved in signal transduction pathway? *Journal of cellular biochemistry* **61**, 531-542, doi:10.1002/(SICI)1097-4644(19960616)61:4<531::AID-JCB6>3.0.CO;2-P (1996).
36 Wheelock, M. J. & Johnson, K. R. Cadherin-mediated cellular signaling. *Curr Opin Cell Biol* **15**, 509-514 (2003).
37 Nichols, S. A., Roberts, B. W., Richter, D. J., Fairclough, S. R. & King, N. Origin of metazoan cadherin diversity and the antiquity of the classical cadherin/beta-catenin complex. *Proceedings of the National Academy of Sciences of the United States of America* **109**, 13046-13051, doi:10.1073/pnas.1120685109 (2012).
38 Yasuda, S. *et al.* Activity-induced protocadherin arcadlin regulates dendritic spine number by triggering N-cadherin endocytosis via TAO2beta and p38 MAP kinases. *Neuron* **56**, 456-471, doi:10.1016/j.neuron.2007.08.020 (2007).
39 Davis, J. R. *et al.* Inter-cellular forces orchestrate contact inhibition of locomotion. *Cell* **161**, 361-373, doi:10.1016/j.cell.2015.02.015 (2015).
40 Carmona-Fontaine, C. *et al.* Contact inhibition of locomotion in vivo controls neural crest directional migration. *Nature* **456**, 957-961, doi:10.1038/nature07441 (2008).
41 Scarpa, E. *et al.* Cadherin Switch during EMT in Neural Crest Cells Leads to Contact Inhibition of Locomotion via Repolarization of Forces. *Dev Cell* **34**, 421-434, doi:10.1016/j.devcel.2015.06.012 (2015).
42 Theveneau, E. *et al.* Collective chemotaxis requires contact-dependent cell polarity. *Dev Cell* **19**, 39-53, doi:10.1016/j.devcel.2010.06.012 (2010).

43 Moeller, M. J. *et al.* Protocadherin FAT1 binds Ena/VASP proteins and is necessary for actin dynamics and cell polarization. *EMBO J* **23**, 3769-3779, doi:10.1038/sj.emboj.7600380 (2004).

44 Halliburton, W. D. On Muscle-Plasma. *J Physiol* **8**, 133-202 (1887).

45 Arnaout, M. A. Integrin structure: new twists and turns in dynamic cell adhesion. *Immunol Rev* **186**, 125-140 (2002).

46 Bailly, M. *et al.* Relationship between Arp2/3 complex and the barbed ends of actin filaments at the leading edge of carcinoma cells after epidermal growth factor stimulation. *J Cell Biol* **145**, 331-345 (1999).

47 Pollard, T. D. & Borisy, G. G. Cellular motility driven by assembly and disassembly of actin filaments. *Cell* **112**, 453-465 (2003).

48 Abercrombie, M., Heaysman, J. E. & Pegrum, S. M. The locomotion of fibroblasts in culture. IV. Electron microscopy of the leading lamella. *Exp Cell Res* **67**, 359-367 (1971).

49 Alberts, J. B. & Odell, G. M. In silico reconstitution of Listeria propulsion exhibits nano-saltation. *PLoS Biol* **2**, e412, doi:10.1371/journal.pbio.0020412 (2004).

50 Ponti, A., Machacek, M., Gupton, S. L., Waterman-Storer, C. M. & Danuser, G. Two distinct actin networks drive the protrusion of migrating cells. *Science* **305**, 1782-1786, doi:10.1126/science.1100533 (2004).

51 Watanabe, N. & Mitchison, T. J. Single-molecule speckle analysis of actin filament turnover in lamellipodia. *Science* **295**, 1083-1086, doi:10.1126/science.1067470 (2002).

52 Giannone, G. *et al.* Lamellipodial actin mechanically links myosin activity with adhesion-site formation. *Cell* **128**, 561-575, doi:10.1016/j.cell.2006.12.039 (2007).

53 Mallavarapu, A. & Mitchison, T. Regulated actin cytoskeleton assembly at filopodium tips controls their extension and retraction. *J Cell Biol* **146**, 1097-1106 (1999).

54 DesMarais, V., Ichetovkin, I., Condeelis, J. & Hitchcock-DeGregori, S. E. Spatial regulation of actin dynamics: a tropomyosin-free, actin-rich compartment at the leading edge. *J Cell Sci* **115**, 4649-4660 (2002).

55 Gupton, S. L., Eisenmann, K., Alberts, A. S. & Waterman-Storer, C. M. mDia2 regulates actin and focal adhesion dynamics and organization in the lamella for efficient epithelial cell migration. *J Cell Sci* **120**, 3475-3487, doi:10.1242/jcs.006049 (2007).

56 Hotulainen, P. & Lappalainen, P. Stress fibers are generated by two distinct actin assembly mechanisms in motile cells. *J Cell Biol* **173**, 383-394, doi:10.1083/jcb.200511093 (2006).

57 Cramer, L. P., Siebert, M. & Mitchison, T. J. Identification of novel graded polarity actin filament bundles in locomoting heart fibroblasts: implications for the generation of motile force. *J Cell Biol* **136**, 1287-1305 (1997).

58 Raftopoulou, M. & Hall, A. Cell migration: Rho GTPases lead the way. *Dev Biol* **265**, 23-32 (2004).

59 Nobes, C. D. & Hall, A. Rho, rac and cdc42 GTPases: regulators of actin structures, cell adhesion and motility. *Biochem Soc Trans* **23**, 456-459 (1995).

60 Hodge, T. & Cope, M. J. A myosin family tree. *J Cell Sci* **113 Pt 19**, 3353-3354 (2000).

61 Berg, J. S., Powell, B. C. & Cheney, R. E. A millennial myosin census. *Mol Biol Cell* **12**, 780-794, doi:10.1091/mbc.12.4.780 (2001).

62 Vicente-Manzanares, M., Zareno, J., Whitmore, L., Choi, C. K. & Horwitz, A. F. Regulation of protrusion, adhesion dynamics, and polarity by myosins IIA and IIB in migrating cells. *J Cell Biol* **176**, 573-580, doi:10.1083/jcb.200612043 (2007).

63 Juanes-Garcia, A. *et al.* A regulatory motif in nonmuscle myosin II-B regulates its role in migratory front-back polarity. *J Cell Biol* **209**, 23-32, doi:10.1083/jcb.201407059 (2015).

64 Gibson, D. G. *et al.* Enzymatic assembly of DNA molecules up to several hundred kilobases. *Nat Methods* **6**, 343-345, doi:10.1038/nmeth.1318 (2009).

65 Sanjana, N. E., Shalem, O. & Zhang, F. Improved vectors and genome-wide libraries for CRISPR screening. *Nat Methods* **11**, 783-784, doi:10.1038/nmeth.3047 (2014).

66 Shalem, O. *et al.* Genome-scale CRISPR-Cas9 knockout screening in human cells. *Science* **343**, 84-87, doi:10.1126/science.1247005 (2014).

67 Van Hoof, D. *et al.* An experimental correction for arginine-to-proline conversion artifacts in SILAC-based quantitative proteomics. *Nat Methods* **4**, 677-678, doi:10.1038/nmeth0907-677 (2007).

68 Bendall, S. C. *et al.* Prevention of amino acid conversion in SILAC experiments with embryonic stem cells. *Mol Cell Proteomics* **7**, 1587-1597, doi:10.1074/mcp.M800113-MCP200 (2008).

69 Cox, J. & Mann, M. MaxQuant enables high peptide identification rates, individualized p.p.b.-range mass accuracies and proteome-wide protein quantification. *Nat Biotechnol* **26**, 1367-1372, doi:10.1038/nbt.1511 (2008).

70 Kuleshov, M. V. *et al.* Enrichr: a comprehensive gene set enrichment analysis web server 2016 update. *Nucleic Acids Res* **44**, W90-97, doi:10.1093/nar/gkw377 (2016).

71 Fan, L. *et al.* Alpha protocadherins and Pyk2 kinase regulate cortical neuron migration and cytoskeletal dynamics via Rac1 GTPase and WAVE complex in mice. *Elife* **7**, doi:10.7554/eLife.35242 (2018).

72 El-Beltagy Ael, F. Light and electron microscopic studies on the pigmented epithelium and photoreceptors of the retina of common buzzard (Buteo buteo). *Tissue Cell* **47**, 78-85, doi:10.1016/j.tice.2014.11.008 (2015).

73 Simo, R., Villarroel, M., Corraliza, L., Hernandez, C. & Garcia-Ramirez, M. The retinal pigment epithelium: something more than a constituent of the

blood-retinal barrier--implications for the pathogenesis of diabetic retinopathy. *J Biomed Biotechnol* **2010**, 190724, doi:10.1155/2010/190724 (2010).

74 Gamm, D. M. *et al.* Regulation of prenatal human retinal neurosphere growth and cell fate potential by retinal pigment epithelium and Mash1. *Stem Cells* **26**, 3182-3193, doi:10.1634/stemcells.2008-0300 (2008).

75 Kay, P., Yang, Y. C. & Paraoan, L. Directional protein secretion by the retinal pigment epithelium: roles in retinal health and the development of age-related macular degeneration. *J Cell Mol Med* **17**, 833-843, doi:10.1111/jcmm.12070 (2013).

76 Rutar, M., Natoli, R., Chia, R. X., Valter, K. & Provis, J. M. Chemokine-mediated inflammation in the degenerating retina is coordinated by Muller cells, activated microglia, and retinal pigment epithelium. *J Neuroinflammation* **12**, 8, doi:10.1186/s12974-014-0224-1 (2015).

77 Grierson, I. *et al.* Development, repair and regeneration of the retinal pigment epithelium. *Eye (Lond)* **8 (Pt 2)**, 255-262, doi:10.1038/eye.1994.54 (1994).

78 Saito, T. & Nakatsuji, N. Efficient gene transfer into the embryonic mouse brain using in vivo electroporation. *Dev Biol* **240**, 237-246, doi:10.1006/dbio.2001.0439 (2001).

79 Tabata, H. & Nakajima, K. Efficient in utero gene transfer system to the developing mouse brain using electroporation: visualization of neuronal migration in the developing cortex. *Neuroscience* **103**, 865-872 (2001).

80 Chen, G. *et al.* Semaphorin-3A guides radial migration of cortical neurons during development. *Nat Neurosci* **11**, 36-44, doi:10.1038/nn2018 (2008).

81 Wu, H., Reynolds, A. B., Kanner, S. B., Vines, R. R. & Parsons, J. T. Identification and characterization of a novel cytoskeleton-associated pp60src substrate. *Mol Cell Biol* **11**, 5113-5124 (1991).

82 Weed, S. A. & Parsons, J. T. Cortactin: coupling membrane dynamics to cortical actin assembly. *Oncogene* **20**, 6418-6434, doi:10.1038/sj.onc.1204783 (2001).

83 Uruno, T. *et al.* Activation of Arp2/3 complex-mediated actin polymerization by cortactin. *Nat Cell Biol* **3**, 259-266, doi:10.1038/35060051 (2001).

84 Weaver, A. M. *et al.* Cortactin promotes and stabilizes Arp2/3-induced actin filament network formation. *Curr Biol* **11**, 370-374 (2001).

85 Artym, V. V., Zhang, Y., Seillier-Moiseiwitsch, F., Yamada, K. M. & Mueller, S. C. Dynamic interactions of cortactin and membrane type 1 matrix metalloproteinase at invadopodia: defining the stages of invadopodia formation and function. *Cancer Res* **66**, 3034-3043, doi:10.1158/0008-5472.CAN-05-2177 (2006).

86 Pinheiro, J. J. *et al.* Invadopodia proteins, cortactin and membrane type I matrix metalloproteinase (MT1-MMP) are expressed in ameloblastoma. *Histopathology* **59**, 1266-1269, doi:10.1111/j.1365-2559.2011.03995.x (2011).

87 Chadwick, W., Brenneman, R., Martin, B. & Maudsley, S. Complex and multidimensional lipid raft alterations in a murine model of Alzheimer's disease. *Int J Alzheimers Dis* **2010**, 604792, doi:10.4061/2010/604792 (2010).

88 Liu, W. *et al.* PLCD3, a flotillin2-interacting protein, is involved in proliferation, migration and invasion of nasopharyngeal carcinoma cells. *Oncol Rep* **39**, 45-52, doi:10.3892/or.2017.6080 (2018).

89 Boldajipour, B. *et al.* Control of chemokine-guided cell migration by ligand sequestration. *Cell* **132**, 463-473, doi:10.1016/j.cell.2007.12.034 (2008).

90 Neel, N. F., Schutyser, E., Sai, J., Fan, G. H. & Richmond, A. Chemokine receptor internalization and intracellular trafficking. *Cytokine Growth Factor Rev* **16**, 637-658, doi:10.1016/j.cytogfr.2005.05.008 (2005).

91 Borroni, E. M., Mantovani, A., Locati, M. & Bonecchi, R. Chemokine receptors intracellular trafficking. *Pharmacol Ther* **127**, 1-8, doi:10.1016/j.pharmthera.2010.04.006 (2010).

92 Lin, C. W. *et al.* Podocalyxin-like 1 promotes invadopodia formation and metastasis through activation of Rac1/Cdc42/cortactin signaling in breast cancer cells. *Carcinogenesis* **35**, 2425-2435, doi:10.1093/carcin/bgu139 (2014).

93 Zhang, J. *et al.* PODXL, negatively regulated by KLF4, promotes the EMT and metastasis and serves as a novel prognostic indicator of gastric cancer. *Gastric Cancer*, doi:10.1007/s10120-018-0833-y (2018).

94 Mouneimne, G. *et al.* Differential remodeling of actin cytoskeleton architecture by profilin isoforms leads to distinct effects on cell migration and invasion. *Cancer Cell* **22**, 615-630, doi:10.1016/j.ccr.2012.09.027 (2012).

95 Ulmer, B. *et al.* Calponin 2 acts as an effector of noncanonical Wnt-mediated cell polarization during neural crest cell migration. *Cell Rep* **3**, 615-621, doi:10.1016/j.celrep.2013.02.015 (2013).

96 Kelley, C. A. *et al.* Xenopus nonmuscle myosin heavy chain isoforms have different subcellular localizations and enzymatic activities. *J Cell Biol* **134**, 675-687 (1996).

97 Makowska, K. A., Hughes, R. E., White, K. J., Wells, C. M. & Peckham, M. Specific Myosins Control Actin Organization, Cell Morphology, and Migration in Prostate Cancer Cells. *Cell Rep* **13**, 2118-2125, doi:10.1016/j.celrep.2015.11.012 (2015).

98 Almeida, C. G. *et al.* Myosin 1b promotes the formation of post-Golgi carriers by regulating actin assembly and membrane remodelling at the trans-Golgi network. *Nat Cell Biol* **13**, 779-789, doi:10.1038/ncb2262 (2011).

99 Tanimura, S. *et al.* ERK signaling promotes cell motility by inducing the localization of myosin 1E to lamellipodial tips. *J Cell Biol* **214**, 475-489, doi:10.1083/jcb.201503123 (2016).

100 Vandewalle, C. *et al.* SIP1/ZEB2 induces EMT by repressing genes of different epithelial cell-cell junctions. *Nucleic Acids Res* **33**, 6566-6578, doi:10.1093/nar/gki965 (2005).

101 Matthes, S. A., Taffet, S. & Delmar, M. Plakophilin-2 and the migration, differentiation and transformation of cells derived from the epicardium of neonatal rat hearts. *Cell Commun Adhes* **18**, 73-84, doi:10.3109/15419061.2011.621561 (2011).

102 Niell, N. *et al.* The human PKP2/plakophilin-2 gene is induced by Wnt/beta-catenin in normal and colon cancer-associated fibroblasts. *Int J Cancer* **142**, 792-804, doi:10.1002/ijc.31104 (2018).

103 Gu, G., Zhao, D., Yin, Z. & Liu, P. BST-2 binding with cellular MT1-MMP blocks cell growth and migration via decreasing MMP2 activity. *J Cell Biochem* **113**, 1013-1021, doi:10.1002/jcb.23433 (2012).

104 Yi, E. H. *et al.* BST-2 is a potential activator of invasion and migration in tamoxifen-resistant breast cancer cells. *Biochem Biophys Res Commun* **435**, 685-690, doi:10.1016/j.bbrc.2013.05.043 (2013).

105 Wu, J. *et al.* Ras-related protein Rap2c promotes the migration and invasion of human osteosarcoma cells. *Oncol Lett* **15**, 5352-5358, doi:10.3892/ol.2018.7987 (2018).

106 Svalina, M. N. *et al.* IGF1R as a Key Target in High Risk, Metastatic Medulloblastoma. *Sci Rep* **6**, 27012, doi:10.1038/srep27012 (2016).

107 Iwai, S. *et al.* Involvement of the Wnt-beta-catenin pathway in invasion and migration of oral squamous carcinoma cells. *Int J Oncol* **37**, 1095-1103 (2010).

108 He, L. *et al.* Wnt/beta-catenin signaling cascade: A promising target for glioma therapy. *J Cell Physiol*, doi:10.1002/jcp.27186 (2018).

109 Premaraj, S., Souza, I. & Premaraj, T. Focal adhesion kinase mediates beta-catenin signaling in periodontal ligament cells. *Biochem Biophys Res Commun* **439**, 487-492, doi:10.1016/j.bbrc.2013.08.097 (2013).

110 Wang, Z. *et al.* Fibrillin-1, induced by Aurora-A but inhibited by BRCA2, promotes ovarian cancer metastasis. *Oncotarget* **6**, 6670-6683, doi:10.18632/oncotarget.3118 (2015).

111 Liu, J. J. *et al.* Scinderin promotes the invasion and metastasis of gastric cancer cells and predicts the outcome of patients. *Cancer Lett* **376**, 110-117, doi:10.1016/j.canlet.2016.03.035 (2016).

112 Tsai, M. F. *et al.* A new tumor suppressor DnaJ-like heat shock protein, HLJ1, and survival of patients with non-small-cell lung carcinoma. *J Natl Cancer Inst* **98**, 825-838, doi:10.1093/jnci/djj229 (2006).

113 Garrett, S. C., Varney, K. M., Weber, D. J. & Bresnick, A. R. S100A4, a mediator of metastasis. *J Biol Chem* **281**, 677-680, doi:10.1074/jbc.R500017200 (2006).

114 Rosati, A. *et al.* BAG3 promotes pancreatic ductal adenocarcinoma growth by activating stromal macrophages. *Nat Commun* **6**, 8695, doi:10.1038/ncomms9695 (2015).
115 Tian, T. *et al.* S100A1 promotes cell proliferation and migration and is associated with lymph node metastasis in ovarian cancer. *Discov Med* **23**, 235-245 (2017).
116 Liu, J. *et al.* Both HDAC5 and HDAC6 are required for the proliferation and metastasis of melanoma cells. *J Transl Med* **14**, 7, doi:10.1186/s12967-015-0753-0 (2016).
117 Kanno, K. *et al.* Overexpression of histone deacetylase 6 contributes to accelerated migration and invasion activity of hepatocellular carcinoma cells. *Oncol Rep* **28**, 867-873, doi:10.3892/or.2012.1898 (2012).
118 Peterfia, B. *et al.* Syndecan-1 enhances proliferation, migration and metastasis of HT-1080 cells in cooperation with syndecan-2. *PLoS One* **7**, e39474, doi:10.1371/journal.pone.0039474 (2012).
119 Sun, X. *et al.* Annexin A5 regulates hepatocarcinoma malignancy via CRKI/II-DOCK180-RAC1 integrin and MEK-ERK pathways. *Cell Death Dis* **9**, 637, doi:10.1038/s41419-018-0685-8 (2018).
120 Elsnerova, K. *et al.* Gene Expression Profiling Reveals Novel Candidate Markers of Ovarian Carcinoma Intraperitoneal Metastasis. *J Cancer* **8**, 3598-3606, doi:10.7150/jca.20766 (2017).

Appendix A

Cell Culture

HelaS3 cells and Hek-293T

Dulbecco's Modified Eagle's Medium (DMEM), with phenol red supplemented with 10% FBS and 1% Penicillin/ Streptomycin and 2 mM L-glutamine in addition to L-glutamine present in DMEM. Cells were cultured for up to 3 days in the same medium before passaging. For passaging, cells were washed with 37 ºC PBS once and 0.05% trypsin EDTA mix and incubated at 37 ºC until cells can be resuspended into single cell suspensions.

Cryopreservation

70% Complete supplemented DMEM, 20% FBS, and 10% DMSO.

RPE/RPE1 Cells

DMEM and F-12 (1:1), phenol red supplemented with 10% FBS and 1% Penicillin/ Streptomycin and 2 mM L-glutamine. Cells were cultured for up to 3 days in the same medium. For passaging, cells were washed with 37 ºC PBS once and 0.05% trypsin EDTA mix and incubated at 37 ºC until cells can be resuspended into single cell suspensions.

Cryopreservation

90% FBS, and 10% DMSO.

Appendix – B

Optimization for transfection

Lipofectamine 3000

1. Day 0 – plate cells targeting 70% confluency on Day 1
2. Day 1 – One hour prior to transfection, remove conditioned culture medium and store at 4 ^{o}C. Add transfection enhancement medium (DMEM or any regular cell specific culture medium with 1% FBS and no antibiotics) to the cells. Keep cells at 37 ^{o}C for one hour.
   Volume of the medium should be minimal, just so all cells are covered with a thin layer of medium.
3. Prepare transfection mix in lipofectamine medium.
   ***Mixing of reagent from yellow tube with DNA in optimem and reagent from red tube with optimem should be incubated separately for 5 minutes before putting these two mixes together*.**
4. Incubate transfection mix at RT for 15-20 minutes.
5. Add the transfection mix to your cultures.
6. Keep the cells in incubator for 4-6 hours.
7. Remove the transfection medium and add conditioned medium to the cells.
8. Incubate overnight and check transfection efficiency next day.
9. Refresh medium if you see some dead cells.

Polyetheleneimine preparation (PEI)

1 mg/ml of stocks were prepared as follows: 50 mg PEI dissolved into H_2O with addition of concentrated HCl dropwise to bring the pH to 2.0 with constant stirring and mild heating at 65 ^{o}C until solution is clear. HEPES pH 7.0 was

added to a final concentration of 50 mM. Concentrated NaOH was added to gradually bring pH to 7.0. PEI solution was sterile filtered and aliquoted.

HelaS3 and Hek293T transfection

Cells cultured to higher than 80% confluency were used for transfection. Before transfection, medium was refreshed. DNA:PEI in a ratio of 1:3 were mixed and vortexed immediately. Mixture was incubated at room temperature for 40 minutes before adding it to the cells. Medium was changed after overnight incubation.

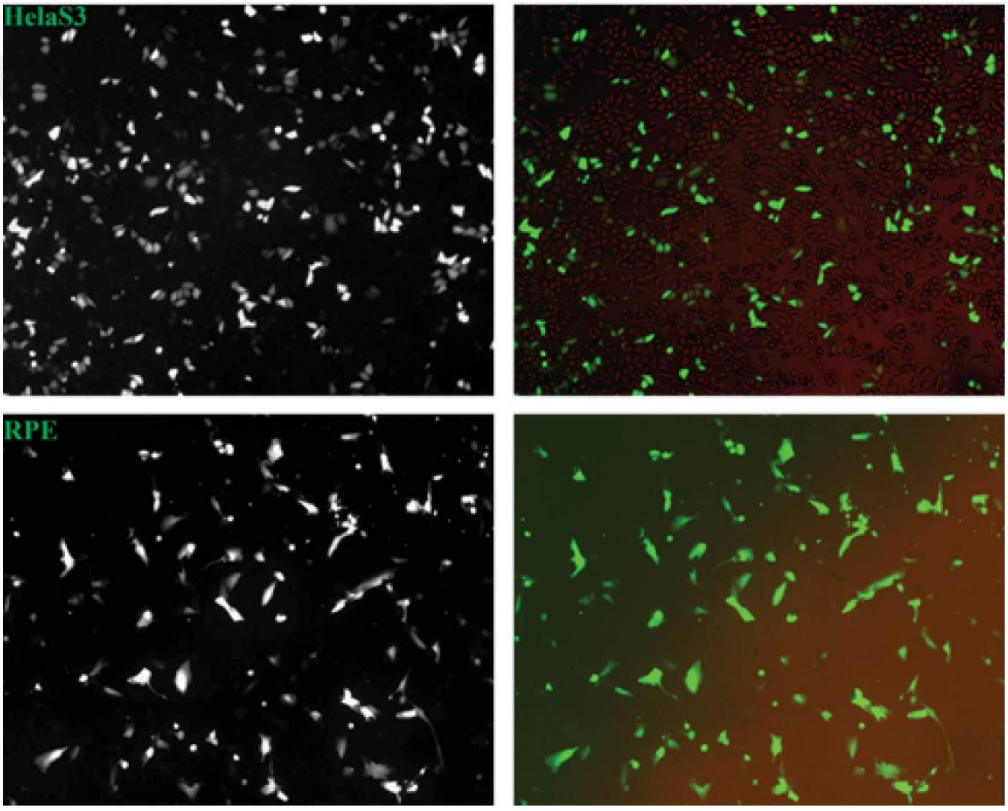

Figure B-1: Transfection Optimization. Transfection of pGIPZ shRNA vector (11.8 kb) into HelaS3 and RPE cells using lipofectamine3000. Left panel GFP expression and right panel overlayed GFP and phase images.

Appendix C

Live imaging

Confocal Live Imaging protocol

Ibidi multi-well µ-slide imaging plates were employed for imaging (Ibidi # 80826). Wells were coated with human collagen 50 µg/ml dissolved in 0.01 N acetic acid. 100 µl of solution added per well and incubated at 4 ºC overnight. Excess solution was removed, and wells washed three times with sterile water. Wells were air dried and exposed to UV inside the cell culture hood for 30 min to sterilize the surface. RPE1 cells were resuspended after trypsinization and added to wells for a low confluency. For optimal migration ability without high neighbouring population, ~2000 cells per well is a good number to start for optimization. Cells were incubated in the medium until they attach well and exhibit polarized morphology. Cell culture medium ~200 ul was added to each well before starting the imaging.

After finding appropriate subject cells, their positions were marked under Mark and Find position set up in LasX. For Z-stacks, cells were imaged with an average of 10 z-sections within the imaging dimension. For time lapse imaging, time difference between two frames was kept approximately at 10 minutes.

Appendix D

Oligonucleotide Sequences

Table D-1: Oligonucleotide Sequences

Reference#	Name	Sequence
14	PCDH7bR	GCGCGGATCCGCGCCCTCCCT GGGATATTTA
16	PCDH7cR	GCGCGGATCCGCCAGGTAAA CTTCTCTTCTAGTGAG
16	PCDH7cR	GCGCGGATCCGCCAGGTAAA CTTCTCTTCTAGTGAG
198	PCDH7-c partI-HindIII For	cagtctAAGCTTATGCTGAGGAT GCGGACCGCGGGAT
198	PCDH7-c partI-HindIII For	cagtctAAGCTTATGCTGAGGAT GCGGACCGCGGGAT

203	PCDH7-C Part III BamHI Rev	cagtctGGATCCCAGGTAAACTTCTCTTCTAGTGAGAGT
209	PCDH7-b Part III BamHI Rev	cagtctGGATCCGCCCTCCCTGGGATATTTAAATATATTTG
249	XbaI_PCDH7_mCHERRY_pLENTY_For	GCGACCTCTAGAATGGACAGCGGGGCGGGC
250	XbaI_PCDH7_mcherry_pLenty_Rev	GCCAGCTCTAGAACTGAGTCTCTGTTTGCTAATTTC
265	Rev modified shRNA	ACACTGGGGCAGCTTCTCG
267	Q5 For modified	CAAATGATTTTTGATGAAAACGAGTGCTTCCTGGACTTCG
268	PCDH7_1_T	caccgCGACGTCCGCATCGGCAACG

269	PCDH7_1_B	aaacCGTTGCCGATGCGGACGTCG
270	PCDH7_2_T	caccgTTGCCGATGCGGACGTCGGC
271	PCDH7_2_B	aaacGCCGACGTCCGCATCGGCAA
272	PCDH7_3_T	caccgCACGTTGCCGATGCGGACGT
273	PCDH7_3_B	aaacACGTCCGCATCGGCAACGTG
274	PCDH7_4_T	caccgGTTGCCGATGCGGACGTCGG
275	PCDH7_4_B	aaacCCGACGTCCGCATCGGCAAC

276	PCDH7_5_T	caccgCATCGTGACCGGATCGGGTG
277	PCDH7_5_B	aaacCACCCGATCCGGTCACGATG
278	PCDH7_6_T	caccgGGCCCCGCCGACGTCCGCAT
279	PCDH7_6_B	aaacATGCGGACGTCGGCGGGGCC
296	repair_seq1_F	GGACTCAGATCTCGAGCTCAAGCTT
297	repair_seq1_R	CGCCACCTGCAGCTCGAAC
298	repair_seq2_F	AGCGTGTTCGAGCTGCAGGTGGCG

299	repair_seq2_R	CACCATGGTGGCGACCGGTGGATCC
446	P7-Sur-For2	CTGTGGTTAGAAGGAGCAGT
447	P7-Sur-Rev2	CAGGCTGAAAGTCACCTCA